European Journal of Medicinal Chemistry

Methylsulfanylpyridine based diheteroaryl isocombretastatin analogs as potent anti-proliferative agents.

--Manuscript Draft--

Manuscript Number:	EJMECH-D-20-01733R1
Article Type:	Full Paper
Keywords:	Isocombretastatins and phenstatin oximes; Pyridine analogs; Solubility improvement; Tubulin polymerization inhibition; G2/M arrest and apoptosis; Docking
Corresponding Author:	Rafael Pelaez, Ph. D. Universidad de Salamanca Salamanca, Salamanca SPAIN
First Author:	Raquel Álvarez, Dr
Order of Authors:	Raquel Álvarez, Dr
	Laura Aramburu, Dr
	Consuelo Gajate, Dr
	Alba Vicente, Bsc
	Faustino Mollinedo, Professor
	Manuel Medarde, Professor
	Rafael Pelaez, Ph. D.
Abstract:	Isocombretastatins are the not isomerizable 1,1-diarylethene isomers of combretastatins. Both families of antimitotics are poorly soluble and new analogs with improved water solubility are needed. The ubiquitous 3,4,5-trimethoxyphenyl ring and most of its replacements contribute to the solubility problem. 39 new compounds belonging to two series of isocombretastatin analogs with 2-chloro-6-methylsulfanyl-4-pyridinyl or 2,6-bis(methylsulfanyl)-4-pyridinyl moieties replacing the 3,4,5-trimethoxyphenyl have been synthesized and their antimitotic activity and aqueous solubility have been studied. We show here that 2-chloro-6-methylsulfanylpyridines are more successful replacements than 2,6-bis(methylsulfanyl)pyridines, giving highly potent tubulin inhibitors and cytotoxic compounds with improved water solubilities. The optimal combination is with indole rings carrying polar substitutions at the three position. The resulting diheteroaryl isocombretastatin analogs showed potent cytotoxic activity against human cancer cell lines caused by tubulin inhibition, as shown by in vitro tubulin polymerization inhibitory assays, cell cycle analysis, and confocal microscopy studies. Cell cycle analysis also showed apoptotic responses following G 2 /M arrest after treatment. Conformational analysis and docking studies were applied to propose binding modes of the compounds at the colchicine site of tubulin and were in good agreement with the observed SAR. 2-Chloro-6-methylsulfanylpyridines represent a new and successful trimethoxyphenyl ring substitution for the development of improved colchicine site ligands.
Suggested Reviewers:	Pedro Miguel Cardá Usó, Professor Catedràtic d'Universitat, Universitat Jaume I mcarda@uji.es Recent corresponding author in Eur J Med Chem. Works in tubulin agents and other antitumor compounds
	Ahmed Kamal, Professor Professor, Indian Institute of Chemical Technology ahmedkamal@iict.res.in Recent corresponding author in Eur J Med Chem. Works in antitumor compounds and tubulin ligands

Graphical abstract

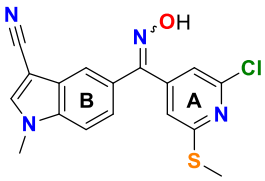

Tubulin inhibition

G_2/M arrest

Apoptosis

Binding to colchicine site

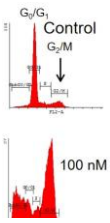

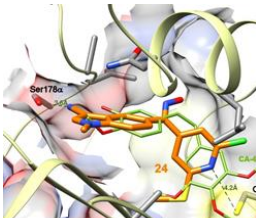

Highlights

- 2-Chloro-6-methylsulfanyl-4-pyridyl isocombretastatins are potent antimitotics
- Indole substitution increases potency
- Solubility improvements
- Disruption of microtubules in cells, G_2/M cell cycle arrest, and induction of apoptosis.
- Binding at the colchicine site of tubulin

Methylsulfanylpyridine based diheteroaryl isocombretastatin analogs as potent anti-proliferative agents.

Raquel Álvarez,[a,c,d] Laura Aramburu,[a,c,d] Consuelo Gajate,[b] Alba Vicente-Blázquez,[a,b,c,d] Faustino Mollinedo,[b] Manuel Medarde[a,c,d] and Rafael Peláez*[,a,c,d]

[a] Laboratorio de Química Orgánica y Farmacéutica, Departamento de Ciencias Farmacéuticas, Universidad de Salamanca, Campus Miguel de Unamuno, E-37007 Salamanca, Spain.
[b] Laboratory of Cell Death and Cancer Therapy, Department of Molecular Biomedicine, Centro de Investigaciones Biológicas Margarita Salas, Consejo Superior de Investigaciones Científicas (CSIC), E-28040 Madrid, Spain.
[c] Instituto de Investigación Biomédica de Salamanca (IBSAL), Facultad de Farmacia, Universidad de Salamanca, Campus Miguel de Unamuno, E-37007 Salamanca, Spain.
[d] Centro de Investigación de Enfermedades Tropicales de la Universidad de Salamanca (CIETUS). Facultad de Farmacia, Universidad de Salamanca, Campus Miguel de Unamuno, E-37007 Salamanca, Spain.

e-mail addresses:

Laura Aramburu	lauramvil@usal.es
Raquel Álvarez	raquelalvarez@usal.es
Consuelo Gajate	cgajate@cib.csic.es
Alba Vicente Blázquez	avicenteblazquez@usal.es
Faustino Mollinedo	fmollin@cib.csic.es
Manuel Medarde	medarde@usal.es
Rafael Peláez	pelaez@usal.es

* Corresponding author:
Phone: 00 34 923294528; 00 34 677554890. FAX: 00 34 923294515.
e-mail: pelaez@usal.es.
Address: Laboratorio de Química Orgánica y Farmacéutica, Departamento de Ciencias Farmacéuticas, Facultad de Farmacia, Campus Miguel de Unamuno, E-37007 Salamanca, Spain.

Graphical abstract

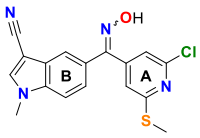

Tubulin inhibition

G_2/M arrest

Apoptosis

Binding to colchicine site

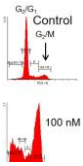

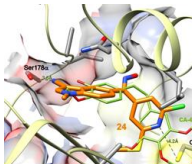

Highlights

- 2-Chloro-6-methylsulfanyl-4-pyridyl isocombretastatins are potent antimitotics
- Indole substitution increases potency
- Solubility improvements
- Disruption of microtubules in cells, G_2/M cell cycle arrest, and induction of apoptosis.
- Binding at the colchicine site of tubulin

Abstract

Isocombretastatins are the not isomerizable 1,1-diarylethene isomers of combretastatins. Both families of antimitotics are poorly soluble and new analogs with improved water solubility are needed. The ubiquitous 3,4,5-trimethoxyphenyl ring and most of its replacements contribute to the solubility problem. 39 new compounds belonging to two series of isocombretastatin analogs with 2-chloro-6-methylsulfanyl-4-pyridinyl or 2,6-bis(methylsulfanyl)-4-pyridinyl moieties replacing the 3,4,5-trimethoxyphenyl have been synthesized and their antimitotic activity and aqueous solubility have been studied. We show here that 2-chloro-6-methylsulfanylpyridines are more successful replacements than 2,6-bis(methylsulfanyl)pyridines, giving highly potent tubulin inhibitors and cytotoxic compounds with improved water solubilities. The optimal combination is with indole rings carrying polar substitutions at the three position. The resulting diheteroaryl isocombretastatin analogs showed potent cytotoxic activity against human cancer cell lines caused by tubulin inhibition, as shown by *in vitro* tubulin polymerization inhibitory assays, cell cycle analysis, and confocal microscopy studies. Cell cycle analysis also showed apoptotic responses following G_2/M arrest after treatment. Conformational analysis and docking studies were applied to propose binding modes of the compounds at the colchicine site of tubulin and were in good agreement with the observed SAR. 2-Chloro-6-methylsulfanylpyridines represent a new and successful trimethoxyphenyl ring substitution for the development of improved colchicine site ligands.

Keywords

Isocombretastatins and phenstatin oximes

Pyridine analogues

Solubility improvement

Tubulin polymerization inhibition

G_2/M arrest and apoptosis

Docking

1. INTRODUCTION

The microtubules of the eukaryotic cells are hollow dynamic tubes formed by polymerization and depolymerization of αβ-tubulin heterodimers, referred to as tubulin. This dynamic equilibrium is essential for their functioning and the aim of microtubule-targeting agents or MTAs, acting as anti-tumor and anti-parasitic drugs.[1] MTAs bind to tubulin in at least seven structurally characterized binding sites, some of them favoring (microtubule-stabilizing agents or MSAs) and some of them opposing polymerization (microtubule destabilizing agents or MDAs).[2] The combretastatins are a family of natural products that bind to the colchicine domain of tubulin, located at the interface between the αβ-tubulin heterodimers. Binding of combretastatins to the colchicine site hampers the curved to straight transition of tubulin dimers necessary for polymerization, and therefore they behave as MDAs.[3] MDAs inhibition of tubulin polymerization is especially patent in the highly dynamic mitotic microtubules and, therefore, they arrest cells at the metaphase to anaphase transition, which results in an enhanced population of cells in the G_2/M phases of the cell cycle, and a late apoptosis onset of cancer cells.[4] Furthermore, combretastatins act as vascular disrupting agents or VDAs, causing a rapid collapse of the tumor neo-vasculature *in vivo* and tumor death.[5] The phosphate prodrug of combretastatin A-4 (CA4P, fosbretabulin) as fosbretabulin tromethamine (Fig. 1) has been granted the orphan drug designation for the treatment of ovarian adenocarcinoma, gastroenteropancreatic and neuroendocrine cancers, and anaplastic thyroid cancer, and the combretastatin A-1 diphosphate prodrug Oxi4503 (Fig. 1) for the treatment of relapsed/refractory Acute Myeloid Leukemia (AML) in combination with cytarabine.[6]

Despite their clinical success, the combretastatins present several properties that limit their therapeutic potential and have therefore been the aim of many medicinal chemistry programs: they are highly hydrophobic compounds with low aqueous solubility, the double bond linking the two aromatic rings is configurationally unstable, they are inactivated *in vivo* by phase I and II

metabolic transformations, and their vascular disrupting activity which causes tumor necrosis leaves a peripheral rim of undamaged cancer cells that rapidly regenerates the tumor mass.[7-15] The solubility problem has been tackled by the formation of highly soluble prodrugs such as phosphates on the hydroxyl groups.[16] However, the hydroxyl group is also involved in phase II metabolic transformations leading to resistance.[17] The double bond isomerization problem has been solved by the inclusion of the bridge in different cycles,[10, 11, 18] by the replacement of the double bond by configurationally stable bridges of different lengths[19] or by bridges preferentially adopting *cisoid* conformations, such as the sulfonamides,[20] and has even been turned into an advantageous feature for photodynamic therapy.[21] A very successful strategy has been the reduction of the two - atom bridge of combretastatins to one - atom bridges as in benzophenones (phenstatins),[22] oximes,[23] diarylamines,[24, 25] 1,1-diarylethanes,[26] and 1,1-diarylethenes (isocombretastatins, the regioisomers of combretastatins).[27-29] Avoidance of the metabolic transformations has been pursued by modifications on the bridge[17] and the aromatic rings,[30] and combination therapy and increased cytotoxic potency have been proposed to escape the resistance to VDAs.[8] However, many of these improvements are often achieved at the expense of others (e.g. replacement of the guaiacol ring to avoid metabolic transformation reduces the solubility).

Formatted: Highlight

The B ring of combretastatins and isocombretastatins has been the subject of multiple replacements showing a permissive SAR requirement in this region.[15] However, few of them have addressed the increase in hydrophobicity associated with its replacement by naphthalene, indole, or differently substituted phenyl rings. The substitution of the hydroxyl group by amino substituents,[31] the replacement of the phenyl by pyridine rings,[25, 32, 33] and the introduction of polar groups on otherwise lipophilic moieties such as the indole rings [34, 35] are representative examples of such attempts. We have shown that the efficiency of these promising modifications is highly dependent on the structural context in which they are introduced,[34-36], and therefore needs to be ascertained in every structural context.

The 3,4,5-trimethoxyphenyl ring of combretastatin A-4 (A ring) due to its large size and hydrophobic nature is the target of metabolic transformations of combretastatins[14] and isocombretastatins,[13] and also represents a highly desirable target for solubility improvements. However, SAR studies have firmly established its importance for high cytotoxic potency.[15] Recently, successful replacements of the trimethoxyphenyl ring by quinolines[37, 38] and quinazolines[39] and related heterocycles have been described.[25, 40, 41] These potent benzo-fused heterocyclic compounds however unwillingly increase the hydrophobic area and the ring count.[42, 43] Successful replacements with smaller pyridine or related heterocycles have been less frequent and require hydrophobic substituents to compensate for the size reduction.[38, 44, 45] We have recently shown that replacement of the trimethoxyphenyl ring by pyridines can be favorably achieved with methylsulfanyl and methoxy substituents and that the encountered difficulties in the direct replacement of the phenyl ring of the trimetoxyphenyl ring by similarly substituted pyridines are due to unfavorable conformational preferences.[46] Furthermore, docking experiments showed optimal adjustment to complexes of tubulin with a chloro-furopyrimidine,[41] thus suggesting a region for further improvement devoid of the mentioned conformational issues. In all these instances, the polar interaction with the sidechain of Cys241of β-tubulin is preserved through the pyridine nitrogen.

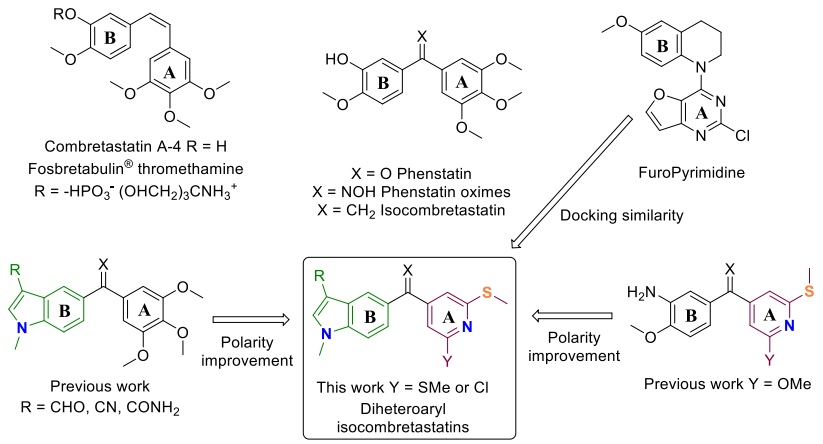

Figure 1. Chemical structure of combretastatins and one-atom bridged analogs, and design rationale for the compounds described in this work.

A long-term goal of the design of new combretastatin and related analogs involves the replacement of the 3,4,5-trimethoxyphenyl ring (A ring) with polar moieties with higher intrinsic water solubility, thus allowing the removal of the troublesome solubilizing hydroxyl substituent of the B ring. The aim is to piece a piece enhance the overall polarity of the compounds in a way tolerated by the highly hydrophobic colchicine domain such that a solubility increase is accompanied by potent tubulin inhibition. We have combined two previous successful strategies of structural modification, the first one affecting and consisting in the replacement of ring A with substituted pyridines and the second involving modifications of ring B that remove the troublesome groups while allowing additional polarity enhancements. On the pyridine A ring we have further explored the methylsulfanyl groups that have less conformational penalties than the methoxy groups to partially compensate for the size reduction associated with the removal of the central methoxy group, and based on previous docking results we have also combined them with chlorine substituents. We have done so in the context of 1,2-ethenylene (combretastatin) and 1,1-ethenylidene (isocombretastatin), carbonyl (phenstatin), and ketoxime bridges that avoid the undesired isomerization of the bridge. Substantial solubility improvements

were accomplished, and highly potent tubulin inhibitors were found. Potencies higher than the reference combretastatin A-4 in tubulin inhibition were attained, along with cytotoxic potencies in the mid nanomolar range in a more consistent way than with previous pyridine-based series against sensitive HeLa human cervix epithelioid carcinoma and HL-60 human acute myeloid leukemia cell lines. Submicromolar antiproliferative activity against the combretastatin A-4-resistant colon adenocarcinoma (HT-29) cell line was also achieved.[12, 17, 30, 47] Treatment with the most potent compounds at concentrations of 100 nM resulted after 24 hours in the accumulation of cells in the G_2/M phases of the cell cycle, followed by significant increases of the sub-G_0/G_1 cell populations 48 hours post-treatment. The effects of the compounds on the cytoskeleton were confirmed by immunofluorescence studies. Conformational analysis combined with docking studies suggest binding at the colchicine site with association energies dependent on the conformational preferences of the pyridine substituents. These results show that pyridine A rings can be a favorable modification in colchicine site ligands with improved water solubility and potent cytotoxic activity through tubulin polymerization inhibition for the development of new antimitotic drugs.

2. RESULTS AND DISCUSSION

2.1. Chemistry

2.1.1. Chemical synthesis

Nucleophilic additions of aryl-lithium derivatives to disubstituted pyridinecarboxylic acids prepared from citrazinic acid (scheme 1) were applied for the synthesis of the key intermediate diarylketones (schemes 2 and 3). Diarylketones were, in turn, converted into the 1,1-diarylethenes by Wittig reactions and into the oximes by treatment with hydroxylamine hydrochloride. The combretastatin analogs were synthesized using Wittig reactions with pyridinemethylphosponium salts.

Citrazinic acid was converted in neat phosphorous oxychloride to 2,6-dichloroisonicotinic acid (**1**),[48] which was the key intermediate for aromatic nucleophilic substitutions with sodium methanethiolate to give the mono- and disubstituted acids **2** and **3** (Scheme 1). Reduction of **3** with LAH to the benzylic alcohol **4**, nucleophilic substitution with HBr to benzylic bromide **5**, and then with triphenylphosphine gave triphenylphosphonium salt **6**, used for the Wittig reactions in the synthesis of the combretastatins (scheme 3).

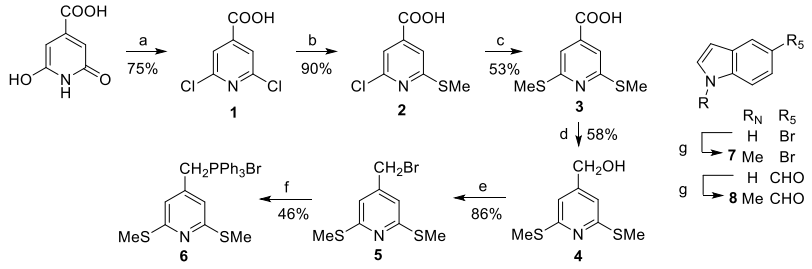

Scheme 1. Reagents and conditions: a) Me_4NBr, $POCl_3$, 90 - 140 ºC, 24 h; b) 1.5 eq NaSMe, DMF, reflux, 24-48 h; c) excess NaSMe, DMF, reflux, 24-48 h; d) LAH, THF, 0 ºC - r.t., 24 h; e) HBr, AcOH, 0 ºC - r.t., 24 h; f) PPh_3, Toluene, 24h, r.t.; g) MeI, NaOH, Bu_4NHSO_4, CH_2Cl_2, r.t., 24 h.

Diarylketones (phenstatins) **9**, **10**, **16**, **17**, **33**, **36**, **39**, and **40** were synthesized (schemes 2 and 3) by nucleophilic additions of aryl-lithium reagents, prepared by treatment of the corresponding aryl bromides with *n*BuLi, to isonicotinic acids **2** and **3**. 1,1-Diarylethenes (isocombretastatins) **11**, **12**, **18**, **19**, **34**, **37**, and **41** were prepared by Wittig reaction of the diarylketones with methyltriphenylphosphonium iodide, while treatment with hydroxylamine rendered the mixtures of *E* and *Z* oximes **13**, **14**, **22**, **23**, **24**, **35**, **38**, and ***42***. Hydrogenation of **12** yielded diarylethane **15**. The introduction of substituents at position 3 of the indole rings to obtain more polar analogs is shown in scheme 2. 3-Formylindoles **20**, **21**, **25**, and **26** were prepared under Vilsmeier – Haack conditions. Formyl indoles were converted into the oximes by treatment with hydroxylamine and then to the 3-cyanoindoles **24**, **29**, and **30** by acetylation followed by thermal elimination. Indoleamides **31** and **32** were prepared from the unsubstituted indoles by reaction

with CSI and indole carboxylic acids **27** and **28** by aromatic electrophilic substitution with phosgene followed by hydrolysis.

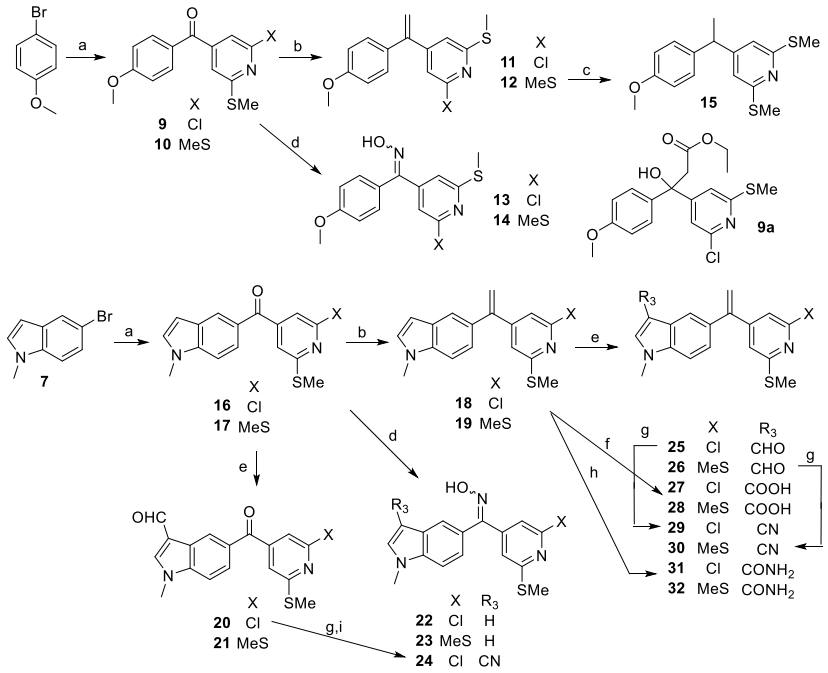

Scheme 2. Synthesis of *p*-methoxyphenyl and *N*-methyl-1*H*-indolyl analogs. Reagents and conditions: (a) i) *n*BuLi, dry THF, -40 ºC, 1 h; ii) **2** or **3**, dry THF, -40 ºC - r.t., 24 h; (b) i) CH_3PPh_3Br, *n*BuLi, dry THF, -40 ºC, 1 h; ii) **9, 10**, **16** or **17**, dry THF, -40 ºC - r.t., 24 h; (c) H_2, Pd(C), r.t., 24-48 h; (d) $NH_2OH{\cdot}HCl$, MeOH, pyridine, reflux, 24 h; (e) i) $POCl_3$, dry DMF, 0 ºC, 30 min; ii) **16** or **17** and heat to 60 ºC 2 h, or **18** or **19** and heat to room temperature 2 h; (f) Phosgene, CH_2Cl_2, room temperature, 24-48 h; (g) i) $NH_2OH{\cdot}HCl$, MeOH, pyridine, reflux, 24 h; ii) Ac_2O, pyridine, 130 ºC, 24-48 h; (h) CSI, 1,2-dichloroethane, r.t., 24 h; (i) 10% NaOH, MeOH, r.t., 72 h.

Wittig reactions between the phosphonium ylide formed by treatment of **6** with *n*BuLi and *N*-methylindole-5-carbaldehyde **11** (scheme 1) or *p*-anisaldehyde gave the combretastatins A (1,2-diarylethenes) **43** and **44** (scheme 3), whose *E* and *Z* isomers were chromatographically separated.

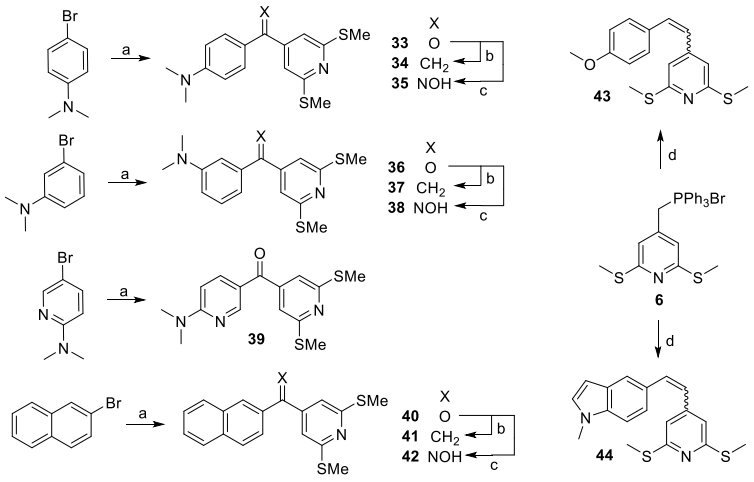

Scheme 3. Synthesis of analogs **33** - **44**. Reagents and conditions: (a) i) ArBr, *n*BuLi, dry THF, -40 ºC, 1 h, then **3**; ii) room temperature, 24 h; (b) i) CH_3-PPh_3I, *n*BuLi, dry THF, -40 ºC, 1 h; ii) **33**, **36** or **40**, r.t., 24 h; (c) NH_2OH·HCl, MeOH, pyridine, reflux, 24 h; (d) i) **6**, dry THF, *n*BuLi, -40 ºC, 1 h; ii) *p*-methoxybenzaldehyde or **8**, dry THF, -40 ºC - r.t., 24 h.

Different B ring modifications and bridges have been combined with methylsulfanylpyridine rings and thus provide a significative sample of the potential of the new pyridine analogs as cytotoxic and tubulin polymerization inhibitory agents, which were subsequently used in the biological assays.

2.1.2. Aqueous solubility

Colchicine site ligands are highly lipophilic due to the mainly hydrophobic nature of the colchicine domain, which results in low water solubilities. The established solution has been the formation of prodrugs that increase the aqueous solubility, but the anchor points are the substrate for metabolism and loss of activity, and alternative strategies are needed. Replacing highly hydrophobic phenyl rings by heterocycles of higher polarity, such as the pyridines here described, should improve water solubility. The solubility of representative compounds (Table 1) was determined by shaking the compounds in phosphate buffer at pH 7.0 until equilibration,

microfiltration, and quantification of the dissolved compound by UV absorbance. Most of the compounds show solubilities higher than the 1 µg/mL of combretastatin A-4, but the increase is in many cases modest although improvements of more than ten-fold are also observed. There is no clear SAR in the solubility values, as evidenced by a comparison of matched pairs. There is not a great difference in solubility between methylsulfanyl groups and chlorine atoms as pyridine substituents (e.g. compare the pairs **11** *vs* **12**, **25** *vs* **26**, but **29** *vs* **30**), or between the bridges, despite their different polarity and hydrogen bonding capabilities (e.g. compare **33**-**35**, **36**-**38**, **11** *vs* **13**, **18** *vs* **22** or **24** *vs* **29**). For the B rings, the *p*-methoxyphenyl seems somewhat more favorable, and in some instances, substitutions at the indole 3 position result in good solubilities (e.g. **21**, **28**, **30**), but unpredictably, possibly due to complex solvation interactions.

Table 1. Solubility of representative compounds in phosphate buffer at pH 7.0

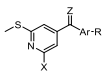

Comp	X	Z	Ar	R	Solubility (µg/mL)	TPSA (Å²)[49]
CA-4	-	-	-	-	1.04[50]	57
10	SMe	O	4-MeO-Ph	H	1.5	90
11	Cl	CH_2	4-MeO-Ph	H	48.9	47
12	SMe	CH_2	4-MeO-Ph	H	35.7	73
13	Cl	NOH	4-MeO-Ph	H	41.7	80
18	Cl	CH_2	*N*MeIND	H	12.3	43
21	SMe	O	*N*MeIND	CHO	230.2	103
22	Cl	NOH	*N*MeIND	H	14.8	76
24	Cl	NOH	*N*MeIND	CN	5.1	125
25	Cl	CH_2	*N*MeIND	CHO	6.3	60
26	SMe	CH_2	*N*MeIND	CHO	7.6	85
28	SMe	CH_2	*N*MeIND	COOH	102.7	106
29	Cl	CH_2	*N*MeIND	CN	3.2	67
30	SMe	CH_2	*N*MeIND	CN	46.3	92
33	SMe	O	4-NMe_2Ph	H	1.0	84
34	SMe	CH_2	4-NMe_2Ph	H	6.9	67
35	SMe	NOH	4-NMe_2Ph	H	1.1	99
36	SMe	O	3-NMe_2Ph	H	1.3	84
37	SMe	CH_2	3-NMe_2Ph	H	2,4	67
38	SMe	NOH	3-NMe_2Ph	H	14.7	99
39	SMe	O	6-NMe_2-pyr-3-yl	H	47.1	103
41	SMe	CH_2	2-Naphthyl	H	1.9	63

2.2. Biology.

2.2.1. Cell proliferation inhibitory activity

The cell proliferation inhibitory activity of the synthesized compounds against three human cancer cell lines has been assayed by measuring cell viability with the XTT method (Table 2).[51] The three selected cell lines show different sensitivities to treatment with combretastatin A-4:[52] HeLa (human cervix epithelioid carcinoma) and HL-60 (human acute myeloid leukemia) are sensitive, whereas HT-29 (human colon adenocarcinoma) are resistant.[12, 17, 30, 47] Most of the synthesized diarylmethane derivatives show anti-proliferative activity against the sensitive cell lines with sub-micromolar potencies, and many also against HT-29, although with reduced potencies. A handful of the compounds inhibit proliferation with IC_{50} values in the double-digit nanomolar range, with values 3−20 times higher than those of combretastatin A-4, but lower than ABT-751 (Table 2), an oral antimitotic drug that binds to the colchicine site and has reached clinical trials. These results confirm that the selected diarylmethane skeleton is a good scaffold for anti-proliferative activity and that the trimethoxyphenyl ring can be successfully substituted by the pyridine moieties here considered. Computational prediction of the sites of metabolism for the most potent compounds suggest that oxidation of the methylsulfanyl is the most likely point of metabolic transformation in this series (Supple~~m~~mentary figure 1).

Concerning the bridges between the two aryl groups, there is no big difference in anti-proliferative activity for ethenes (isocombretastatins) or ketone oximes, with the ketones (phenstatins) showing lower potencies for the methoxyphenyl ring B series (e.g. compare the triplets **9** *vs* **11** *vs* **13**, **10** *vs* **12** *vs* **14**, or **33** *vs* **34** *vs* **35**) and more similar in the indoles (e.g. compare the triplets **16** *vs* **18** *vs* **22**, or **17** *vs* **19** *vs* **23**). The oximes are stable in aqueous solution for more than 72 hours (data not shown) and computational prediction of the sites of metabolism do not point at them as significant transformation points (Supplementary figure 1)

and therefore their potency is not apparently due to hydrolysis to the ketones, which are in fact less potent. The combretastatins **43** and **44** did not consistently reach sub-micromolar potencies.

Among the B rings, which were selected because they had been previously shown to give active analogs, 4-methoxyphenyl,[27, 28] 3-substituted and unsubstituted *N*-methyl-5-indolyl,[34, 35] and 4-dimethylaminophenyl[36] containing analogs led to sub-micromolar inhibitors, whereas 3-dimethylaminophenyl[32] and 2-naphthyl[27, 53] rings were inactive. Similar potencies are observed for the 4-methoxyphenyl, 4-dimethylaminophenyl and the unsubstituted *N*-methylindole series (e.g. compare **12** *vs* **34** *vs* **19** or **14** *vs* **35** *vs* **23** respectively), while the substituted indoles showed slightly improved potencies only when combined with 2-chloro-6-methylsulfanylpyridines as A ring (e.g. compare **18** *vs* **25**, **29**, and **31** for 2-chloro-6-methylsulfanylpyridines and **19** *vs* **26**, **30**, and **32** for 2,6-bis(methylsulfanyl)pyridines).

Table 2. Tubulin Polymerization Inhibitory Activity and Cytotoxic Activity against Human Cancer Cell Lines.

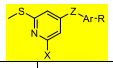

N	X	Z	Ar	R	IC_{50} TPI (μM)[a]	IC_{50} Hela (nM)[b]	IC_{50} HL-60 (nM)[b]	IC_{50} HT-29 (nM)[b]
9	Cl	>C=O	4-MeO-Ph	H	>5	≥10^3	≥10^3	≥10^3
9a	Cl	>C(OH)AcOH	4-MeO-Ph	H	>5	≥10^3	≥10^3	≥10^3
10	SMe	>C=O	4-MeO-Ph	H	>5	≥10^3	≥10^3	≥10^3
11	Cl	>C=CH_2	4-MeO-Ph	H	1.5	628 ± 256	464 ± 142	485 ± 103
12	SMe	>C=CH_2	4-MeO-Ph	H	2.0	399 ± 122	306 ± 114	550 ± 261
13	Cl	>C=NOH	4-MeO-Ph	H	4.6	518 ± 49	613 ± 207	≥10^3
14	SMe	>C=NOH	4-MeO-Ph	H	3.0	457 ± 94	299 ± 106	292 ± 54
15	SMe	>C(H)CH_3	4-MeO-Ph	H	>5	≥10^3	≥10^3	≥10^3
16	Cl	>C=O	*N*MeIND	H	2.4	388 ± 168	490 ± 106	≥10^3
17	SMe	>C=O	*N*MeIND	H	1.7	233 ± 81	222 ± 64	549 ± 79
17b	SMe	>C-OH	(*N*MeIND)$_2$	H	>5	≥10^3	≥10^3	≥10^3
18	Cl	>C=CH_2	*N*MeIND	H	0.3	176 ± 28	416 ±159	511 ± 201
19	SMe	>C=CH_2	*N*MeIND	H	1.1	520 ± 141	717 ± 107	249 ± 103
20	Cl	>C=O	*N*MeIND	CHO	>5	≥10^3	≥10^3	≥10^3
21	SMe	>C=O	*N*MeIND	CHO	>5	≥10^3	≥10^3	≥10^3
22	Cl	>C=NOH	*N*MeIND	H	>5	365 ± 71	257 ± 39	≥10^3
23	SMe	>C=NOH	*N*MeIND	H	1.0	590 ± 235	240 ± 74	745 ± 102
24	Cl	>C=NOH	*N*MeIND	CN	0.2	57 ± 18	93 ± 9	195 ± 23
25	Cl	>C=CH_2	*N*MeIND	CHO	1.6	72 ± 15	38 ± 18	876 ± 45

26	SMe	>C=CH_2	*N*MeIND	CHO	1.2	64 ± 16	303 ± 60	573 ± 104
27	Cl	>C=CH_2	*N*MeIND	COOH	>5	≥10^3	≥10^3	≥10^3
28	SMe	>C=CH_2	*N*MeIND	COOH	4.7	≥10^3	≥10^3	≥10^3
29	Cl	>C=CH_2	*N*MeIND	CN	0.6	158 ± 58	74 ± 21	278 ± 106
30	SMe	>C=CH_2	*N*MeIND	CN	0.4	579 ± 96	604 ± 143	587 ± 203
31	Cl	>C=CH_2	*N*MeIND	$CONH_2$	2.3	82 ± 33	44 ± 15	38 ± 8
32	SMe	>C=CH_2	*N*MeIND	$CONH_2$	2.4	601 ± 210	223 ± 44	276 ± 68
33	SMe	>C=O	4-NMe_2Ph	H	>5	652 ± 24	435 ± 198	787 ± 38
33b	SMe	>C-OH	(4-NMe_2Ph)$_2$		>5	≥10^3	≥10^3	≥10^3
34	SMe	>C=CH_2	4-NMe_2Ph	H	3.8	328 ± 82	486 ± 215	928 ± 59
35	SMe	>C=NOH	4-NMe_2Ph	H	2.1	269 ± 36	213 ± 71	781 ± 112
36	SMe	>C=O	3-NMe_2Ph	H	>5	≥10^3	≥10^3	≥10^3
37	SMe	>C=CH_2	3-NMe_2Ph	H	>5	≥10^3	≥10^3	≥10^3
38	SMe	>C=NOH	3-NMe_2Ph	H	>5	≥10^3	≥10^3	≥10^3
39	SMe	>C=O	6-NMe_2-pyr-3-yl	H	>5	≥10^3	≥10^3	≥10^3
39a	SMe	>C-OH	2(6-NMe_2-pyr)	H	>5	≥10^3	≥10^3	≥10^3
40	SMe	>C=O	2-Naphth	H	>5	≥10^3	≥10^3	≥10^3
41	SMe	>C=CH_2	2-Naphth	H	>5	≥10^3	≥10^3	≥10^3
42	SMe	>C=NOH	2-Naphth	H	>5	≥10^3	≥10^3	≥10^3
43	SMe	-CH=CH-	4-MeO-Ph	H	3.8	≥10^3	≥10^3	≥10^3
44	SMe	-CH=CH-	*N*MeIND	H	>5	≥10^3	≥10^3	633 ± 211
CA-4	-	-	-	-	2.8	3	13	305
ABT-751	-	-	-	-	4000	388	-	514

[a] Concentration inhibiting 50% (IC_{50}) the polymerization of microtubular protein (TPI) *in vitro*. [b] IC_{50} values were calculated from concentration-response curves using the XTT assay as described in the Experimental Section. Data correspond to the mean values of three experiments performed in triplicate.

There is not a big difference in anti-proliferative potency when the pyridine A ring has two methylsulfanyl substituents or one chlorine and one methylsulfanyl (e.g. compare the pairs **9** *vs* **10**, **11** *vs* **12**, **13** *vs* **14**, **16** *vs* **17**, **18** *vs* **19**, and **22** *vs* **23**) except for the 3-substituted indoles, which experience a potency boost when combined with the 2-chloro-6-methylsulfanylpyridines but not with the 2,6-bis(methylsulfanyl)pyridines (e.g. compare the pairs **25** *vs* **26**, **29** *vs* **30**, and **31** *vs* **32**). Therefore, the combination of 3-substituted indoles with 2-chloro-6-methylsulfanylpyridines in the isocombretastatin (i.e. compounds **25**, **29**, and **31**) or ketoxime series (i.e. compound **24**) results in two of the most potent compounds. These results are in good agreement with previous studies showing that 3-substituted indoles make good B rings,[35] but that their effect is dependent on the structural context they are found in.[32, 34, 46] These favorable indole 3-substituents are aldehydes, amides, and nitrile groups, with similar

effects on the potency (e.g. compare **25**, **29**, and **31**), whereas carboxylic acids result in the loss of the potency, probably due to their ionized state in solution.

In summary, 2-chloro-6-methylsulfanylpyridine isocombretastatins or oximes with 3-formyl-, 3-carbamoyl- or 3-cyano- indoles are highly potent inhibitors of cell proliferation in the double-digit nanomolar range, comparable to reference compounds, even if devoid of the trimethoxyphenyl A ring.

2.2.2. Tubulin polymerization inhibition

To confirm the proposed effect on tubulin we have studied the *in vitro* inhibitory activity of the synthesized compounds on the polymerization of microtubular protein isolated from calf brain. The amounts of polymer mass formed in the presence and the absence (control) of the compounds were measured by turbidimetry, and the percentage of reduction was taken as the tubulin polymerization inhibitory activity. The compounds were initially tested at a concentration of 5 μM, and for those inhibiting more than 50%, we have determined the IC_{50} values (Table 2). Sixteen of the synthesized compounds have TPI IC_{50} values lower than 3 μM, comparable to reference compounds such as combretastatin A-4 or ABT-751, with TPI IC_{50} values of 2 μM and 4 μM respectively (Table 2). Remarkably, 4 compounds (**18**, **24**, **29**, and **30**) are highly potent sub-micromolar inhibitors and additionally, 6 more have TPI IC_{50} values lower than 2 μM (**11**, **17**, **19**, **23**, **25**, and **26**).

The TPI and the antiproliferative activity are strongly correlated, as almost all the compounds with TPI IC_{50} values lower than 5 μM show antiproliferative activity at sub-micromolar concentrations, thus indicating that interference with tubulin polymerization is their mechanism of action. However, there is not a strict correlation between the two values, with compounds with highly potent TPI in the sub-micromolar range (e.g. **18**, **29**, **30**, and **24**) showing significant differences in anti-proliferative potency, and compounds with not so high TPI potencies (i.e. **25** or **31**) amongst the more potent inhibitors of cell proliferation. This discrepancy has been

previously noted and justified by the fact that antiproliferative activity is dependent on the inhibition of polymerization dynamics at low (nanomolar) compound concentrations and not so much to polymer mass change at high protein and compound (micromolar) concentration. As a result of these differences, the observed SAR for TPI is slightly different from the anti-proliferative SAR previously discussed.

Concerning the bridge, more differences than in antiproliferative activity are found, with isocombretastatins (1,1-diarylethenes) being more potent than the ketone oximes that are in turn usually more potent than phenstatins (ketones) (e.g. compare **9** *vs* **11** *vs* **13**, **10** *vs* **12** *vs* **14**, **16** *vs* **18** *vs* **22**, **17** *vs* **19** *vs* **23**), with combretastatin **43** showing TPI activity. Similarly, more differences are observed for the B rings in TPI activity than in anti-proliferative activity, with the indolic analogs showing higher potencies than compounds with 4-methoxyphenyl or 4-dimethylaminophenyl moieties (e.g. compare **10** *vs* **17** *vs* **33**, **11** *vs* **18**, **12** *vs* **19** *vs* **34**, and **14** *vs* **23** *vs* **35**). On the other hand, less differences are observed between 2-chloro-6-methylsulfanylpyridines and bis(methylsulfanyl)pyridines (e.g. compare **9** *vs* **10**, **11** *vs* **12**, **13** *vs* **14**, , **16** *vs* **17**, and **18** *vs* **19**, but **22** *vs* **23**), especially in the case of compounds carrying 3-substituted indoles (e.g. compare **20** *vs* **21**, **25** *vs* **26**, **27** *vs* **28**, **29** *vs* **30**, and **31** *vs* **32**).

Replacement of the trimethoxyphenyl A ring with 2-chloro-6-methylsulfanylpyridines or 2,6-bis(methylsulfanyl)pyridines results in highly potent inhibitors of tubulin polymerization for isocombretastatins or ketone oximes with 3-formyl-, 3-carbamoyl- or 3-cyanoindoles as B rings, even more potent than combretastatin A-4.

2.2.3. Effects on cellular microtubules

To confirm that the actions of the compounds in cells are based on their effects on tubulin, we have studied the effect of representative compounds on the microtubule network in HeLa cells. To this end, we have selected compounds **24** and **25**, which showed the lowest anti-proliferative IC_{50} values and were highly potent inhibitors of tubulin polymerization *in vitro*.

Immunofluorescence confocal microscopy studies with the labeling of α-tubulin and nuclei showed that treatment with **24** and **25** promoted a drastic and severe disruption of the microtubule network (Figure 2) as assessed by immunofluorescence confocal microscopy (Figure 2), thus supporting that the above disrupting effects on microtube network were due to interaction of compounds **24** and **25** with tubulin.

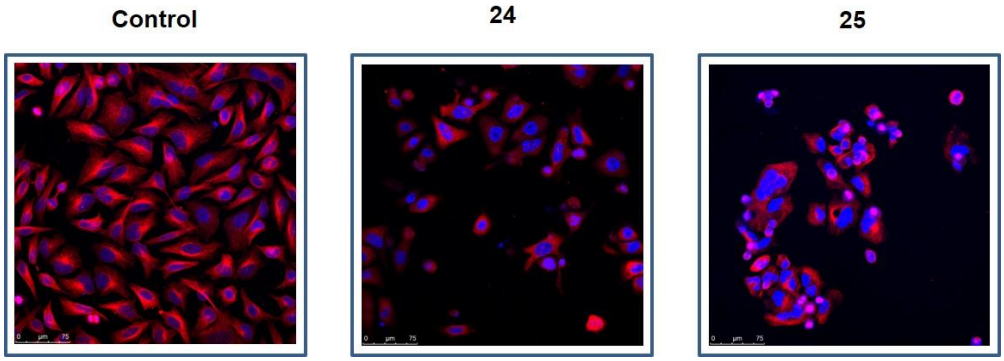

Figure 2. Effects of the treatment with compounds **24** and **25** on the microtubule network in HeLa cells. Cells were incubated in the absence (Control) or the presence of 1 µM of compounds **24** and **25** for 24 h, and then fixed and processed to analyze microtubules (red fluorescence) and nuclei (blue fluorescence) by confocal microscopy as described in the Experimental Section. Bar: 75 µm. The photomicrographs are representative of three independent experiments.

2.2.4 Effects on the cell cycle and induction of apoptosis

The effect of the most potent antiproliferative compounds (Table 2), **24** and **25**, on the cell cycle at different concentrations and times post-treatment was assessed by flow cytometry. Treatment of HeLa cells with **24** or **25** led to cell cycle arrest at G_2/M followed by the induction of apoptosis, as assessed by the appearance of cells with sub-G_0/G_1 DNA content (Figure 3). Treatment of HT-29 cells with **24** led also to a potent cell cycle arrest at G2/M, similar to the response observed in HeLa cells, albeit with a lower apoptotic response (Figure 3). However, compound **25** failed to promote a potent cell cycle arrest in HT-29 cells after 24 h treatment, and the overall response was lower than in HeLa cells (Figure 3). This is in agreement with our previous

observation that HL-60 and HeLa cells were more sensitive than HT-29 to compound **25** (Table 2).

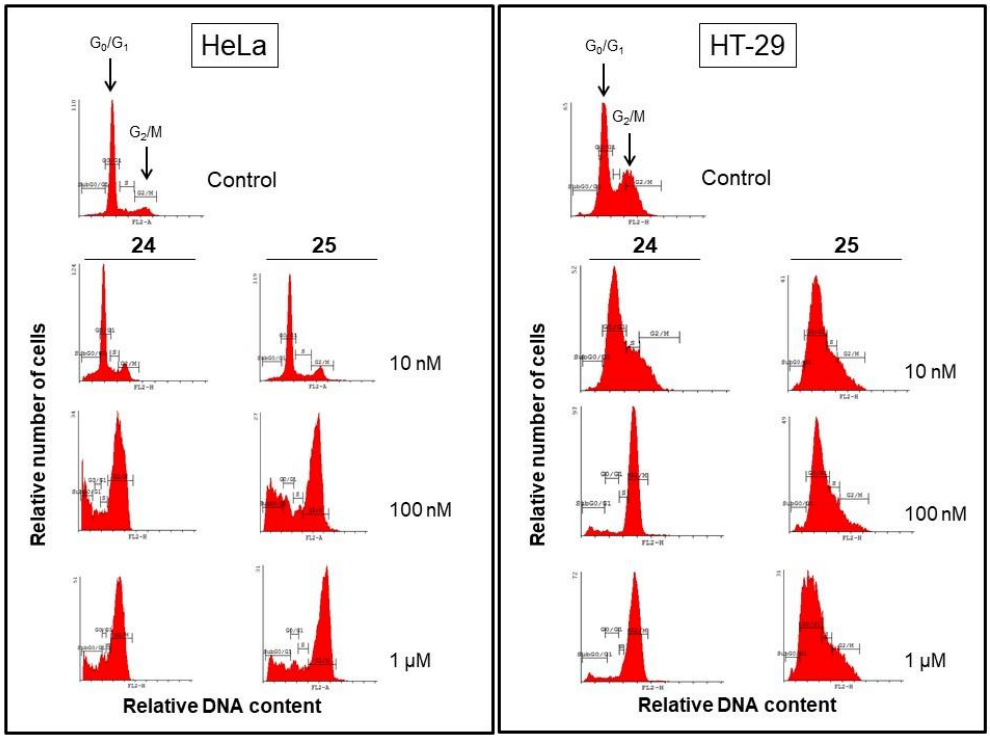

Figure 3. Dose-response of the effects of compounds **24** and **25** on cell cycle in HeLa and HT-29 cells. Cells were incubated with different concentrations of **24** and **25** for 24 h, and their DNA content was analyzed by fluorescence flow cytometry. The positions of the G_0/G_1 and G_2/M peaks are indicated by arrows, and the proportion of cells in each phase of the cell cycle was quantified by flow cytometry. The cell population in the sub-G_0/G_1 region represents cells with hypodiploid DNA content, an indicator of apoptosis. Untreated control cells were run in parallel. Data shown are representative of three independent experiments.

Next, we carried out a dose-response (at concentrations of 1 nM, 10 nM, 100 nM, 1 µM, and 10 µM) and time-course (at 24, 48, and 72 h post-treatment) analyses of the effects on the cell cycle of **24** and **25** in HL-60, HeLa and HT-29 cells (Figure 4).

At a concentration of 1 nM of **24** and **25**, the populations of cells at the different phases of the cell cycle (sub-G_0/G_1, G_0/G_1, S, and G_2/M) for the three cell lines at the three time points did not show differences with the untreated controls (data not shown) and can be used as references.

Incubation with compound **24** at only 100 nM (Figures 3 and 4) arrested most of the HL-60 and HT-29 cells at the G_2/M phase after 24 h (77.4% for HL-60 and 84.4% for HT-29). At the same time point and concentration, 73.2% of HeLa cells were arrested at the G_2/M phase and significant apoptosis induction was evidenced by a substantial number of cells at the sub-G_0/G_1 region (15.7%), with the sum of sub-G_0/G_1 and G_2/M accounting for a total of 88.9%. At later time points (48 h and 72 h), the percentage of cells at the sub-G_0/G_1 region progressively increased (22.7% at 48 h and 33.1% at 72 h for HL-60, 35.9% at 48 h and 83.3% at 72 h for HeLa, and 28.1% at 48h and 64.7% at 72 h for HT-29 cells) at the expense of the cells arrested at G_2/M phase (39.7% at 48 h and 23.3% at 72 h for HL-60, 46.9% at 48 h and 4.6% at 72 h for HeLa, and 54.9% at 48 h and 4.7% at 72 h for HT-29 cells), with the accumulated total of the two phases remaining roughly constant (62.4% at 48 h and 56.3% at 72 h for HL-60, 88.9% at 48 h and 82.8% at 72 h for HeLa, and 82.9% at 48h and 69.4% at 72 h for HT-29 cells). Interestingly, compound **24** at the low 10 nM concentration showed delayed apoptosis after 48h and 72 h in the more resistant HT-29 cell line. At micromolar concentrations (1 µM and 10 µM), the onset of apoptosis in HL-60 and HeLa cells occurs earlier, being already patent at 24 h, but the pattern of cell cycle phases distribution remains. For HT-29 the earlier apoptosis onset is not so apparent, and a significant reduction of the sum of the sub-G_0/G_1 and G_2/M populations is evident at 72 h (the sum equals 91.1% at 1 µM and 92.1% at 10 µM for the 48 h time point and 39.1 at 1 µM and 40.7% at 10 µM for the 72 h time point), as a result of a significative reduction in the G_2/M population.

Incubation with compound **25** at 100 nM (Figure 4) arrested most of the HL-60 cells at the G_2/M phase after 24 h (80.1%). At the same time point and concentration, 56.9% of HeLa cells were arrested at the G_2/M phase and significant apoptosis induction was evidenced by a substantial number of cells (25.2%) at the sub-G_0/G_1 region, with the sum of sub-G_0/G_1 and G_2/M accounting for a total of 82.0%. Under these conditions, HT-29 cells did not show effects on the distribution of the cell cycle phases. At later time points (48 h and 72 h), the percentage of HL-60 and HeLa cells at the sub-G_0/G_1 region progressively increased (20.9% at 48 h and 32.6% at 72 h for HL-60 and 47.6% at 48 h and 59.1% at 72 h for HeLa cells) at the expense of the cells arrested at G_2/M phase (40.5% at 48 h and 22.0% at 72 h for HL-60 and 30.4% at 48 h and 7.9% at 72 h for HeLa cells), with the accumulated total of the two phases remaining roughly constant (61.4% at 48 h and 54.6% at 72 h for HL-60 and 82.0% at 48 h and 78.0% at 72 h for HeLa cells). Under these experimental conditions (100 nM, 48 h, and 72 h incubation), HT-29 cells started to show increasing delayed apoptotic response (11.8% at 48 h and 15.1% at 72 h) in the absence of apparent G_2/M arrest. At higher drug concentrations (Figure 4), HL-60 and HeLa cells show cell cycle distribution patterns like those observed at 100 nM, and HT-29 cells showed augmented sub-G_0/G_1 regions.

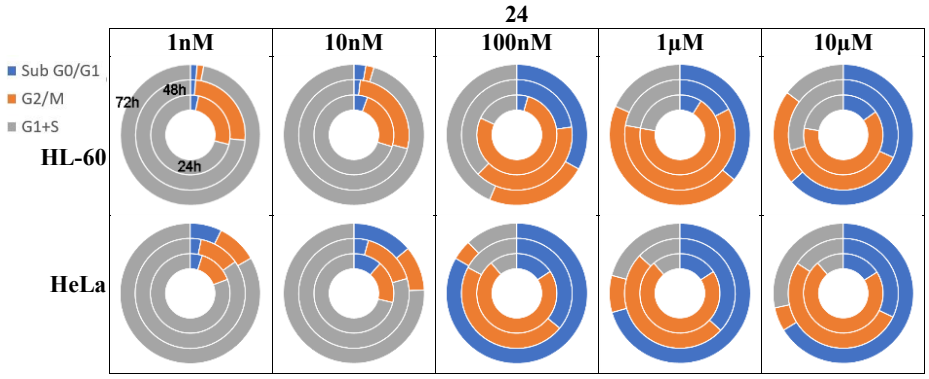

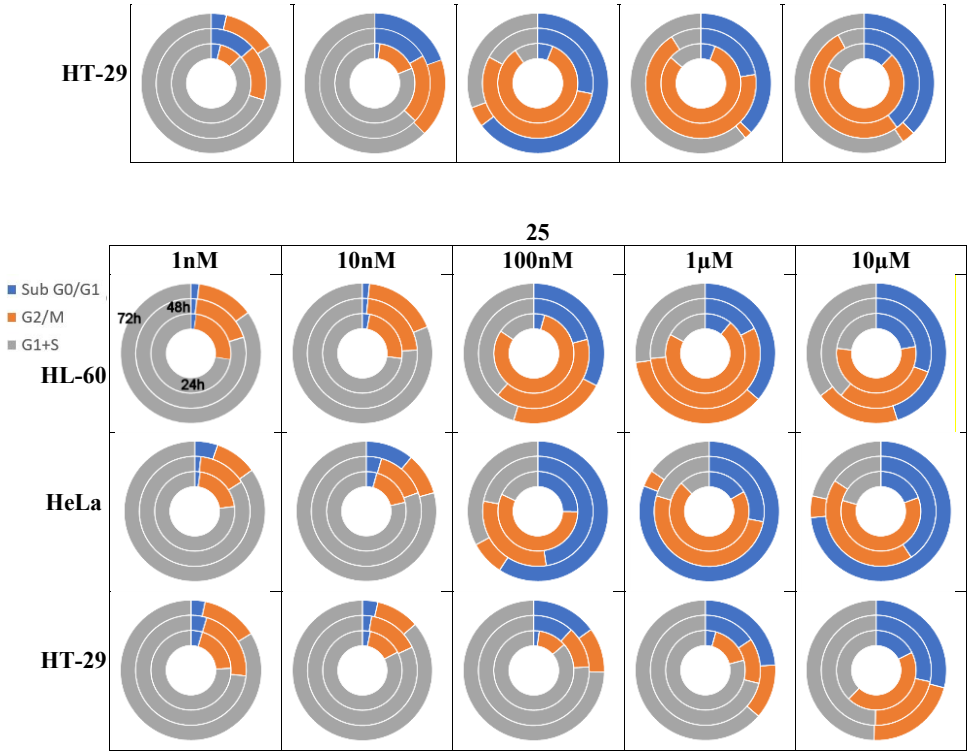

Figure 4. Time course of the effect of compounds **24** and **25** on the sub-G_0/G_1 and G_2/M cell cycle phases in HL-60, HeLa, and HT-29 cells. Compounds were incubated for 24, 48, and 72 h, and then their DNA content was analyzed by flow cytometry as described in the Experimental Section. The different cell cycle phases were quantified and represented in concentric hollow circles (24h inner, 48h center, and 72h outer) to easily visualize the evolution in time of the G_2/M arrest (■) and apoptotic responses (■ sub-G_0/G_1). Untreated control cells were run in parallel, and the percentage of untreated cells in the sub-G_0/G_1 region was less than 3% in all the cell lines assayed. Data shown are representative of at least three independent experiments.

The cell cycle distribution patterns for HL-60 and HeLa cells after treatment with **24** and **25** are very similar to each other, with mitotic arrest followed by an apoptotic response. These data suggest that the disruption of microtubule polymerization by **24** and **25** induce a potent mitotic arrest that eventually triggers an apoptotic response, thus rendering a substantial cell demise in the drug-treated population. On the other hand, HT-29 cells display quite a different cell cycle distribution profiles in response to the two compounds. With **24**, the observed pattern is like

those of HL-60 and HeLa cells, with arrest in the G_2/M arrest followed by the accumulation of apoptotic cells in the sub-G_0/G_1 region. However, after treatment with **25**, HT-29 cells undergo apoptotic response in the absence of patent G_2/M arrest. This different behavior is in accord with the observed difference in tubulin polymerization inhibitory potency of the two compounds (Table 2). Similar experiments on the non – tumorigenic embryonic kidney cell line HEK-293 show a similar mitotic arrest, but no apoptotic induction was observed after 24 h treatment (Supplementary Figure 2), thus suggesting a potential selectivity to induce apoptosis in human tumor cells.

In order to further support the above effects of compounds **24** and **25** on cell cycle arrest and apoptosis induction, we analyzed the expression of proteins related to these processes. Thus, we used the anti-mitotic proteins antibody MPM-2 that recognizes a phosphorylated epitope (S/T)P found in several phosphoproteins that result phosphorylated at the onset of mitosis. Our Western blot results shown in Figure 5 indicate a significant increase in the number of phosphoproteins recognized by MPM-2, simultaneously to the mitotic arrest observed at 24 h in the above cell cycle distribution studies. The lower intensity of the bands after 48 h treatment might likely be due to the onset of apoptosis. In this regard, we analyzed the cleavage of PARP (poly (ADP-ribose) polymerase), a typical caspase-3 substrate, as an early marker of apoptosis. The anti-PARP C2.10 monoclonal antibody detected the full length 116 kDa intact form as well as the 89 kDa cleaved form of PARP. Alongside with the observed sequential increase in the sub-G_0/G_1 population, we found an increase in the levels of cleaved PARP after treatment with 24 and 25, in good agreement with an apoptotic response induced by the sustained mitotic arrest.

Taken together, flow cytometry and biochemical evidences strongly indicate that compounds **24** and **25** behaved as anti-mitotic agents leading to M arrest and subsequent induction of apoptosis.

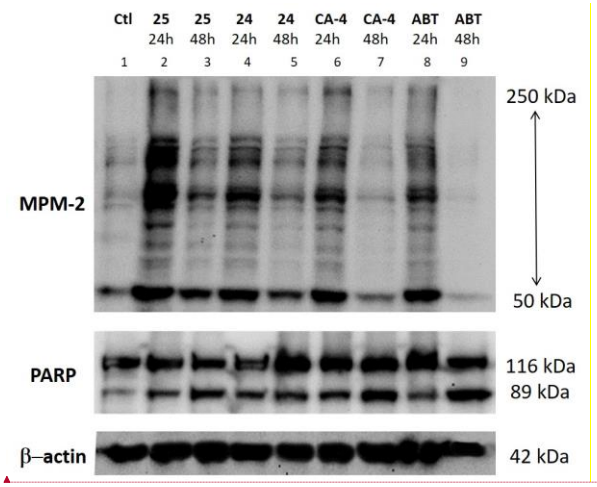

Figure 5. Effect of compounds **24** and **25**, and the reference compounds combretastatin A-4 (CA-4) and ABT-751 (ABT) on MPM-2 expression and PARP cleavage in HeLa cells after 24 and 48 h treatment. Lane 1: untreated HeLa (control Ctl). Lane 2: HeLa treated for 24h with 1 µM **25**. Lane 3: HeLa treated for 48h with 1 µM **25**. Lane 4: HeLa treated for 24 h with 1 µM **24**. Lane 5: HeLa treated for 48h with 1 µM **24**. Lane 6: HeLa treated for 24 h with 1 µM combretastatin A-4. Lane 7: HeLa treated for 48h with 1 µM combretastatin A-4. Lane 8: HeLa treated for 24 h with 1 µM ABT-751. Lane 9: HeLa treated for 48h with 1 µM ABT-751. β-Actin was used as a loading control. The migration positions of full-length PARP (p116) and its cleavage product p89 are indicated. Molecular weights areindicated in kDa. Western blot images are representative of three independent experiments.

Formatted: Highlight

Formatted: Highlight

2.3. Computational studies

Flexible docking studies of compounds **9** - **44** on the colchicine site of tubulin were carried out to establish the ligands' binding modes (Figure 7). The protein conformational space was sampled by using protein structures with 54 different pocket dispositions. 49 came from available X-ray crystal structures of complexes of tubulin with different colchicine site ligands.[46] 5 additional structures came from a molecular dynamics simulation of tubulin in complex with a 3-substituted indole containing ligand, as previously described.[35, 54] The docking poses were generated and scored by PLANTS[55] and AutoDock 4.2[56], two frequently used docking

programs with very different scoring functions. The docking scores of the two programs were combined to select the binding mode for each ligand (Table S1 of the supplementary material). The assignment of the occupancy of the ligands to zones of the colchicine domain (zones A, B, C, as previously described, and a deeper extension in β tubulin of zone C called zone D) of the binding site was performed in a fully automated way. The most favorable binding poses for all the compounds occupy zones A and B of the colchicine domain (corresponding to the pockets for the trimethoxyphenyl ring and the 3-hydroxy-4-methoxyphenyl ring of combretastatin A-4, respectively), probably reflecting a good steric fit of the bent diaryls to these pockets.[54, 57] In all instances, the substituted pyridines occupy the A zone and the other aromatic ring the zone B. This arrangement places the pyridine nitrogen in contact distance with the sulfur atom of Cys241β (Figure 7), a polar interaction deemed important for the binding of colchicine site ligands, while the rest of the moiety is contacting the hydrophobic sidechains of Leu239β, Leu245β, Ala247β, Leu252β, Ala315β, Lys352β, and Ala354β conforming the A site. The other aromatic ring stacks between the polar sidechain of Asn255β on helix H8 and those of Ala316β of sheet S8 and Lys352β of sheet S9 forming the floor of the site, and Met259β, Thr314β, and Val181α, also conforming zone B.

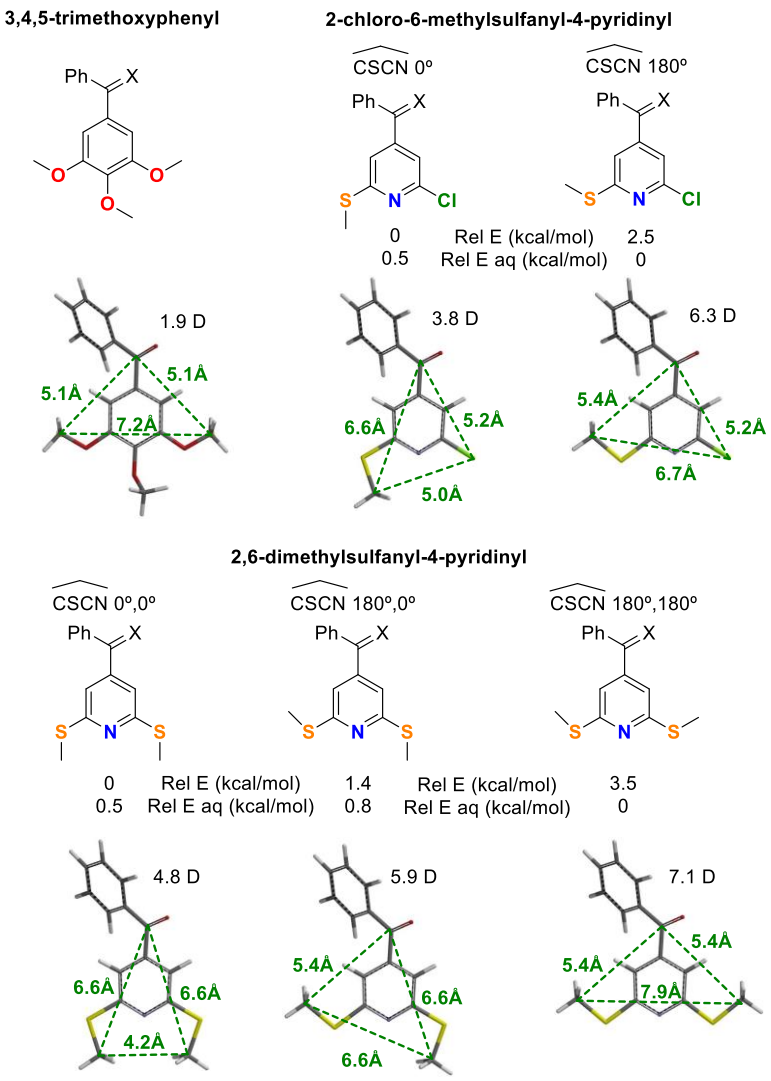

Figure 6. Comparison of the geometries of the trimethoxyphenyl ring taken as a reference A ring and the different conformers found for the 2-chloro-6-methylsulfanyl-4-pyridines and the 2,6-dimethylsulfanyl-4-pyridines. The results shown here are for the benzophenones, but similar results were obtained for oximes and isocombretastatins. The substituents on the pyridine are depicted in the 2D representation in the same dispositions as the 3D structures underneath. The green triangles indicate the dimensions of the A rings. The relative energies are in kcal/mol above the most stable, indicated as 0 kcal/mol. The calculated dipole moments for every conformer are also indicated.

Formatted: Highlight

The binding of the methylsulfanylpyridines to the A site always occurs with a rotation of the methylsulfanyl to place one of the sulfur lone pairs side by side to the pyridine nitrogen lone pair (CSCN dihedral angle of 180º, Figures 6 and 7). We have previously shown that this rotation is less unfavorable in methylsulfanyl than in methoxy groups.[46] We have performed DFT calculations to evaluate the energy penalty if any, of rotating the methylsulfanyl group to the observed rotamer in the docking studies (Figure 6) and the geometrical effects of such rotations. In water, the most favorable conformation places the pyridine and the sulfur lone pairs in the same direction (CSCN dihedral angle of 180º, Figure 6), thus increasing the molecule polarity and favoring interactions with water molecules. This should result in more favorable solvation, although solubility is not as high as expected (Table 1). In apolar media, represented by vacuum, the preferred rotamers place the methyl group of the methylsulfanyl close to the pyridine lone pair (CSCN dihedral angle of 0º, Figure 6). This would result in a larger size along the pyridine 1-4 axis and a masking of the nitrogen lone pair (Figure 6), but binding to the A zone as observed in the docking studies (Figure 7) requires a rotation to the polar conformer to reduce the steric demand along the pyridine long axis and to allow a polar interaction between the pyridine lone pair and the thiol group of Cys241β. Two identical methylsulfanyl groups provide an entropic advantage for the rotation, whereas the presence of one methylsulfanyl and one chlorine atom reduces the steric congestion in the long axis of the pyridine (Figure 6).

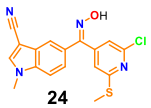

24

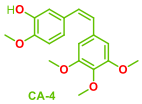

CA-4

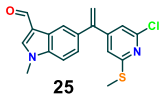

25

A

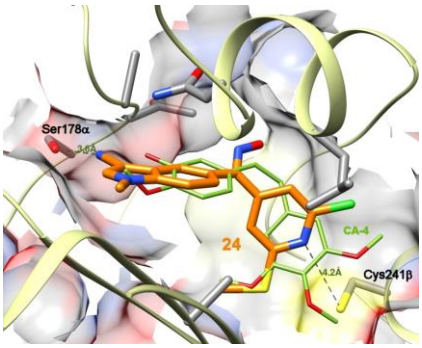

B

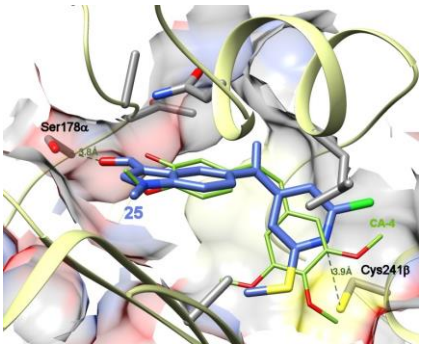

Figure 7. 2D structures of the compounds depicted in A and B. Proposed binding modes for compound **24** (carbons in orange) and **25** (carbons in aegean), superposed onto the X-ray structure of combretastatin A-4 (carbons in green) in their complexes with tubulin. The colchicine binding domain is depicted in lime (pdb ID 5LYJ), and the distances of the pyridine nitrogen to the sulfur atom of the sidechain of Cys241β and of the indole 3-substituent acceptor atom to the hydroxyl group of the sidechain of Ser178α is indicated in green.

Formatted: Highlight

The substituents at the 3 position of the indole ring enhance the antiproliferative potency of the 2-chloro-6-methylsulfanylpyridine derivatives. The docking models show that these polar groups hydrogen bond to the hydroxyl group of the sidechain of Ser178a (Figure 7), thus explaining the observed potency improvement. The preference of 2-chloro- versus 2-methylsulfanyl in the isocombretastatin and ketoxime series can be accounted for by the disposition of the methyl group towards the pyridine nitrogen (data not shown) due to conformational preferences and to a need of reducing the transversal size at the A zone (Figure 6) caused by steric hindrance of the site's walls, thus blocking the favorable polar interaction with the thiol group of Cys241β, which is maintained in the chloro derivatives. The unfavorable effect of the same substitution in the ketone (phenstatin) series is due to the higher conjugation of the bridge with the aromatic rings that results in flatter structures that collide with the site's walls when extended by substituents.[35] The combination of conformational and docking studies, therefore, provide a good rationale for the observed SAR of these new family of pyridine-based colchicine site ligands.

3. CONCLUSIONS

The successful replacement of the 3,4,5-trimethoxyphenyl ring by methylsulfanyl substituted pyridine rings in colchicine site ligands is reported. 2-Chloro-6-methylsulfanyl-4-pyridine and 2,6-dimethylsulfanyl-4-pyridines are polar entities that moderately improve the aqueous solubility to the compounds bearing them with respect to the trimethoxyphenyl analogues. The combination of methylsulfanyl substituted pyridine moieties with indole B rings gives diheteroaryl isocombretastatins, phenstatins, and ketone oximes which are potent inhibitors of tubulin polymerization and cytotoxic agents against several human cancer cell lines. The substitution of the indole at the 3 position with amides, nitriles, or formyl groups in the 2-chloro-6-methylsulfanyl-4-pyridine series further increases the polarity and provides optimal potency in the TPI and cytotoxicity assays. The most potent compound, the 3-cyanoindole 2-chloro-6-methylsulfanyl-4-pyridine oxime **24** disrupted the microtubule network of treated cells and arrested the cell cycle at the G_2/M phase after 24 h, followed by a high apoptosis-like cell response. The 3-formylindole 2-chloro-6-methylsulfanyl-4-pyridine isocombretastatin **25**, showed similar effects as **24** in the more sensitive HeLa and HL60 cells, wheres in the more resistant HT-29 cells a weak apoptotic response in the absence of G_2/M arrest is observed after 24 hours, which suggests that it might activate an additional cell death response to the microtubule effect by unknown mechanisms. Binding at the colchicine site is supported by docking studies that allocate the pyridine ring at the sub-pocket of the trimethoxyphenyl rings in the colchicine domain. Docking results combined with conformational studies suggest that binding to the thiol group of Cys241b is more favorable in 2-chloro-6-methylsulfanyl-4-pyridines than in 2,6-dimethylsulfanyl-4-pyridines, thus providing a rationale for their better activity profile. The synthesized compounds have improved aqueous solubility and good anti-mitotic potency and therefore the structural modifications here described could be applied in the design of new colchicine site ligands.

4. EXPERIMENTAL SECTION

4.1. Chemistry

4.1.1. General chemical techniques

Reagents were used as purchased without further purification. Solvents (THF, DMF, dichloromethane, and toluene) were dried and freshly distilled before use according to procedures described in the literature. TLC was performed on pre-coated silica gel polyester plates (0.25 mm thickness) with a UV fluorescence indicator 254 (Polychrome SI F254). Chromatographic separations were performed on silica gel columns by flash (Kieselgel 40, 0.040-0.063; Merck) or gravity (Kieselgel 60, 0.063-0.200 mm; Merck) chromatography. Melting points were determined on a Büchi 510 apparatus and are uncorrected. ^{1}H NMR and ^{13}C NMR spectra were recorded in $CDCl_3$ on a Bruker WP 200-SY spectrometer at 200/50 MHz or on a Bruker SY spectrometer at 400/100 MHz. Chemical shifts (δ) are given in ppm downfield from tetramethylsilane and coupling constants (*J* values) are in Hertz. IR spectra were run on a Nicolet Impact 410 Spectrophotometer. For FABHRMS analyses, a VG-TS250 apparatus (70 eV) was used. HPLCs were run on Waters X-Terra® MS C_{18} (5 mm, 4.6x150 mm) or C_8 (5 mm, 4.6x150 mm) with acetonitrile/water solvent gradients. All the compounds described here were obtained with at least 95% of purity by quantitative HPLC and/or elemental analysis, unless otherwise stated.

4.1.2. Chemical synthesis

General synthetic procedure for the preparation of diarylketones (Procedure 1)

1 equivalent of *n*BuLi (1.6 M in hexane) was added at -40 ºC onto a solution of the aromatic bromoderivative in dry THF. One hour later, 0.4 equivalents of the carboxylic acid in dry THF was added and the mixture was allowed to reach room temperature. After 24 h, the reaction was

poured onto ethyl formate, and then ethyl acetate and water were added. The mixture was partially evaporated, washed with brine, dried over anhydrous Na_2SO_4, filtered, and evaporated to dryness. The products obtained were purified by flash chromatography.

General synthetic procedure for the preparation of isocombretastatins (Procedure 2)

0.67 equivalents of *n*BuLi (1.6 M in hexane) were added to a slurry of the phosphonium salt in dry THF at -40 ºC and, after one-hour stirring, 0.33 equivalents of the diaryl ketone in dry THF was added and then the mixture was allowed to warm to room temperature and react for 24 hours. The mixture was poured onto a 5% solution of NH_4Cl at 0 ºC, ethyl acetate was added and the mixture was partially evaporated under vacuum. The organic layers were washed with brine, dried over anhydrous Na_2SO_4, filtered, and evaporated to dryness. The products were purified by flash chromatography.

General synthetic procedure for the preparation of oximes (Procedure 3)

A solution of the carbonyl compound in methanol, 10 equivalents of hydroxylamine hydrochloride, and 4 drops of pyridine were refluxed for 24 h. The crude was evaporated to dryness, dissolved in dichloromethane, and washed with brine. The organic phases were dried over anhydrous Na_2SO_4, filtered, and evaporated. The products were purified by flash chromatography giving a mixture of oximes (*E* and *Z*). Oximes were obtained as roughly 1:1 mixtures of the two isomers (proportions can significantly change depending on solvent composition), which readily interconvert in solution. Crystallization of one of the isomers is sometimes possible, but it readily regenerates the mixture in solution.

General indole formylation procedure (Procedure 4)

6 mmol of phosphorus oxychloride per mmol of indole derivative were added at 0 ºC onto dry DMF and stirred for 30 minutes. Then, the indole derivative was added and heated to 60 ºC for 2-24 h for benzophenones or kept 2 hours at room temperature for 1,1-diarylethenes. The solution was poured onto a large volume of ice water saturated with sodium acetate. After 24 h at 4 ºC, the precipitate was filtered, dissolved in dichloromethane, dried over anhydrous Na_2SO_4, filtered, and evaporated to dryness. The products were purified by flash chromatography

General synthetic procedure for the preparation of carbonitriles (Procedure 5)

A solution of the aldehyde in methanol and 4 drops of pyridine, and 10 equivalents of hydroxylamine hydrochloride was refluxed for 24 hours. The solvent was removed, and the product was dissolved in dichloromethane. The organic layer was washed with 2N HCl, brine until neutral pH, dried over anhydrous Na_2SO_4, filtered, and concentrated under vacuum. The crude was dissolved in pyridine and an excess of acetic anhydride and stirred for 24-48 hours at 130 ºC. The reaction was poured onto ice and extracted with dichloromethane, washed with 2N HCl, 5% $NaHCO_3$, brine until neutral pH, dried over anhydrous Na_2SO_4, filtered, and evaporated to dryness. The products were purified by flash chromatography.

2,6-Dichloropyridine-4-carboxylic acid (1)

45.1 g of citrazinic acid (291 mmol) and 31 g of tetramethylammonium chloride (282.8 mmol) in $POCl_3$ (80 mL) was heated to 90 °C until complete dissolution. Then, the temperature was gradually increased to 140 ºC. After 24 h, the mixture was cooled to room temperature and poured onto ice. The precipitate was filtered, washed with water and dried under vacuum. The solid was suspended in ethyl acetate, stirred for 15 min, and filtered to remove insoluble citrazinic acid. The filtrate was dried over anhydrous Na_2SO_4 and evaporated to obtain 42 g (218.8 mmol, 75.2%) of a brown solid corresponding to **1.** M.p. 203-204 ºC. IR (KBr): 2600-3300, 1724, 1596, 1547 cm^{-1}. ^1H NMR (200 MHz, DMSO-D_6): 7.83 (2H, s). ^{13}C NMR (50 MHz, CD_3OD): 124.0 (2) (CH), 145.4 (C), 152.2 (2) (C), 165.0 (C).

2-Chloro-6-methylsulfanylpyridine-4-carboxylic acid (2)

3.84 g (54.8 mmol) of sodium methanethiolate in 50 mL of dry DMF and 4 g of KOH were added onto a solution of 7 g (36.5 mmol) of 2,6-dichloropyridine-4-carboxylic acid (**1**) in 100 mL of dry DMF and the mixture was refluxed for 24 h. The reaction was cooled to room temperature, poured onto brine, and extracted with ethyl acetate. The organic phase was washed with 2N HCl and brine until neutral pH, dried over anhydrous Na_2SO_4, filtered and evaporated, obtaining 6.71 g (32.9 mmol, 90.1%) of 2-chloro-6-methylsulfanylpyridine-4-carboxylic acid (**2**). IR (film): 3100, 1706, 1588, 1545 cm^{-1}. ^1H NMR (200 MHz, CD_3OD): 2.46 (3H, s), 7.40 (1H, *d*, *J* = 1), 7.54 (1H, *d*, *J* = 1). ^{13}C NMR (50 MHz, CD_3OD): 13.7 (CH_3), 119.4 (CH), 120.3 (CH), 142.2 (C), 152.6 (C), 163.7 (C), 166.2 (C).

2,6-bis(methylsulfanyl)pyridine-4-carboxylic acid (3)

390 mg (1.92 mmol) of 2-chloro-6-methylsulfanylpyridine-4-carboxylic acid (**2**) and a 10 mol excess of sodium methanethiolate in 5 mL of dry DMF was refluxed for 72 h under N_2 atmosphere. The reaction was cooled down to room temperature, poured onto 2N HCl, and extracted with ethyl acetate. The organic phase was washed with brine until neutral pH, dried over anhydrous Na_2SO_4, filtered and evaporated, obtaining 216 mg (1.01 mmol, 53%) of 2,6-bis(methylsulfanyl)pyridine-4-carboxylic acid (**3**). ^{1}H NMR (200 MHz, CD_3OD): 2.48 (6H, *s*), 7.25 (2H, *s*). ^{13}C NMR (50 MHz, CD_3OD): 13.4 (2) (CH_3), 116.5 (2) (CH), 139.5 (C), 162.2 (2) (C), 167.5 (C).

(2,6-bis(methylsulfanyl)pyridin-4-yl)methanol (4)

290 mg (7.64 mmol) of LAH were slowly added to a cooled solution of 1.098 g (5.10 mmol) of 2,6-bis(methylsulfanyl)pyridine-4-carboxylic acid (**3**) in dry THF. After 1h, the mixture was poured onto cooled ethyl acetate. The organic phase was dried over anhydrous Na_2SO_4, filtered, and chromatographed using Hexane/Ethyl acetate 9/1 to yield 590 mg (2.9 mmol; 58%) of (2,6-bis(methylsulfanyl)pyridin-4-yl)methanol (**4**). ^{1}H NMR (200 MHz, $CDCl_3$): 2.57 (6H, *s*); 4.58 (2H, *s*); 6.84 (2H, *s*). ^{13}C NMR (50 MHz, $CDCl_3$): 13.4 (2) (CH_3), 63.0 (CH_2), 113.8 (2) (CH), 150.3 (C), 159.5 (2) (C). IR (film): 1539, 1581, 3351 cm^{-1}.

4-(bromomethyl)-2,6-bis(methylsulfanyl)pyridine (5)

361 mg (1.8 mmol) of (2,6-bis(methylsulfanyl)pyridin-4-yl)methanol (**4**) were dissolved in 5 mL of a 32% solution of HBr in acetic acid at 0 ºC and stirred for 6h. The reaction was poured onto ice and extracted with EtOAc. The organic layer was washed with 5% $NaHCO_3$ and brine, dried over anhydrous Na_2SO_4, filtered an evaporated to yield 405 mg (1.5 mmol; 86%) of 4-(bromomethyl)-2,6-bis(methylsulfanyl)pyridine (**5**). ^{1}H NMR (200 MHz, $CDCl_3$): 2.59 (6H, *s*), 4.24 (2H, *s*); 6.87 (2H, *s*). ^{13}C NMR (50 MHz, $CDCl_3$): 13.2 (2) (CH_3), 30.5 (CH_2), 116.4 (2) (CH), 146.0 (C), 156.0 (2) (C). IR (film): 1431, 1540, 1581, 1742 cm^{-1}.

((2,6-bis(methylsulfanyl)pyridin-4-yl)methyl)triphenylphosphonium bromide (6)

408 mg (1.6 mmol) of triphenylphosphine was added to a solution of 355 mg (1.34 mmol) of 4-(bromomethyl)-2,6-bis(methylsulfanyl)pyridine (**5**) in toluene. After 24 hours the White solid

formed was filtered to yield 323 mg (0.6 mmol; 46%) of ((2,6-bis(methylsulfanyl)pyridin-4-yl)methyl)triphenylphosphonium bromide (**6**). ^{1}H NMR (200 MHz, $CDCl_3$): 2.39 (6H, *s*), 5.65 (2H, *s*), 6.72 (2H, *s*), 7.80 (15H, *m*). IR (film): 1435, 1535, 1574 cm^{-1}.

1-Methyl-1*H*-indole-5-carbaldehyde (8)

1.04 g (26 mmol) of NaOH and 20 mg of *n*-Bu_4NHSO_4 were added to a stirred solution of 1*H*-indole-5-carbaldehyde (2.0 g, 13.8 mmol) in 40 mL of dry dichloromethane. After 1 h at room temperature 3 mL (40.2 mmol) of methyl iodide were added and the reaction was heated at 50 ºC. After 48 h, the reaction mixture was concentrated, re-dissolved in dichloromethane, washed with brine, dried over anhydrous Na_2SO_4, filtered and concentrated in vacuum to obtain 1.10 g (50.1%) of 1-methyl-1*H*-indole-5-carbaldehyde (**11**): M.p. 85-86 ºC (diethylether). ^{1}H NMR (200 MHz, $CDCl_3$): 3.76 (3H, *s*), 6.55 (1H, *d*, *J* = 3.3), 7.10 (1H, *d*, *J* = 3.3), 7.41(1H, *d*, *J* = 8.8), 7.80 (1H, *dd*, *J* = 8.8 and 1.9), 8.05 (1H, *d*, *J* = 1.9), 9.92 (1H, *s*). ^{13}C NMR (50 MHz, $CDCl_3$): 32.6 (CH_3), 103.1 (CH), 109.8 (CH), 121.4 (CH), 126.1 (CH), 128.2(C), 129.1 (C), 130.9 (CH), 139.8 (C), 192.3 (CH).

(2-chloro-6-(methylsulfanyl)pyridin-4-yl)(4-methoxyphenyl)methanone (**9**)

Following procedure 1, 11.5 ml (18.4 mmol) of *n*BuLi 1.6 M in hexanes were slowly added at -40 ºC to a solution of 2.33 ml (18.4 mmol) of 4-bromoanisole in 40 mL of dry THF. After 45 minutes, 1.5 g (7.37 mmol) of 2-chloro-6-methylsulfanylpyridine-4-carboxylic acid (**2**) dissolved in 15 mL of dry THF was added. Flash chromatography using Hexane/AcOEt (95/5) yielded 509 mg (1.73 mmol; 24%) of (2-chloro-6-(methylsulfanyl)pyridin-4-yl)(4-methoxyphenyl)methanone (**9**) and 864 mg (2.35 mmol; 32%) of ethyl 3-(2-chloro-6-(methylsulfanyl)pyridin-4-yl)-3-hydroxy-3-(4-methoxyphenyl)propanoate (**9a**).

(2-Chloro-6-(methylsulfanyl)pyridin-4-yl)(4-methoxyphenyl)methanone (**9**): ^{1}H NMR (200 MHz, $CDCl_3$): 2.55 (3H, *s*), 3.88 (3H, *s*), 6.95 (2H, *d*, *J* = 8.9), 7.16 (1H, *d*, *J* = 0.7), 7.26 (1H, *d*, *J* = 0.7), 7.77 (2H, *d*, *J* = 8.6). ^{13}C NMR (50 MHz, $CDCl_3$): 13.6 (CH_3), 55.7 (CH_3), 114.1 (2) (CH), 118.2 (CH), 119.0 (CH), 128.1 (C), 132.7 (2) (CH), 147.9 (C), 151.3 (C), 161.9 (C), 164.3 (C), 191.9 (C). IR (film): 1420, 1459, 1528, 1577, 1597, 1660 cm^{-1}. HRMS ($C_{14}H_{13}ClNO_2S$): calculated ($M+H^+$) 294.0350, found 294.0335.

Ethyl 3-(2-chloro-6-(methylsulfanyl)pyridin-4-yl)-3-hydroxy-3-(4-methoxyphenyl)propanoate (**9a**). ^{1}H NMR (200 MHz, $CDCl_3$): 1.20 (3H, *t*, *J* = 7.1), 2.54 (3H, *s*), 3.09 (1H, *d*, *J* = 16.5), 3.12 (1H, *dd*, *J* = 16.4), 3.77 (3H, s), 4.12 (2H, *c*, *J* = 7.1), 6.85 (2H, *d*, *J* = 8.9), 7.03 (1H, *d*, *J* = 1.4), 7.17 (1H, *d*, *J* = 1.4), 7.30 (2H, *d*, *J* = 8.9). ^{13}C NMR (50 MHz, $CDCl_3$): 13.5 (CH_3), 14.0 (CH_3), 44.6 (CH_2), 55.3 (CH_3), 61.4 (CH_2), 75.3 (C), 114.0 (2) (CH), 116.5 (CH), 116.7 (CH), 126.7 (2) (CH), 135.9 (C), 151.2 (C), 158.1 (C), 159.1 (C), 161.1 (C), 172.3 (C). IR (film): 1514, 1533, 1582, 1606, 1714, 3450 cm^{-1}. HRMS ($C_{18}H_{20}ClNO_4S$): calculated ($M+H^+$) 382.0874, found 382.0888.

(2,6-bis(methylsulfanyl)pyridin-4-yl)(4-methoxyphenyl)methanone (**10**)

Following procedure 1, 7.2 ml (11.6 mmol) of *n*BuLi 1.6 M in hexanes were slowly added at -40 ºC to a solution of 1.45 ml (11.6 mmol) of 4-bromoanisole in 40 mL of dry THF. After 45 minutes, 1g (4.6 mmol) of 2,6-bis(methylsulfanyl)pyridine-4-carboxylic acid (**3**) dissolved in 15 mL of dry THF was added. Flash chromatography using Hexane/AcOEt (95/5) yielded 626 mg (2.1 mmol; 45.7%) of (2,6-bis(methylsulfanyl)pyridin-4-yl)(4-methoxyphenyl)methanone (**10**). M.p. (Hex/CH_2Cl_2): 103 ºC. ^{1}H NMR (200 MHz, $CDCl_3$): 2.61 (6H, *s*), 3.89 (3H, *s*), 6.96 (2H, *d*, *J* = 8.8), 7.05 (2H, *s*), 7.80 (2H, *d*, *J* = 8.8). ^{13}C NMR (50 MHz, $CDCl_3$): 13.4 (2) (CH_3), 55.6 (CH_3), 113.9 (2) (CH), 115.6 (2) (CH), 128.6 (C), 132.6 (2) (CH), 145.3 (C), 160.2 (2) (C), 164.0 (C), 193,2 (C). IR (KBr): 1544, 1592, 1655 cm^{-1}. HRMS ($C_{15}H_{16}NO_2S_2$): calculated ($M+H^+$) 306.0617, found 306.0612.

2-chloro-4-(1-(4-methoxyphenyl)vinyl)-6-(methylsulfanyl)pyridine (11)

Following procedure 2, 0.8 ml (1.3 mmol) of *n*BuLi 1.6 M in hexanes were slowly added at -40 ºC to a solution of 790 mg (1.96 mmol) of methyltriphenylphosphonium iodide in 10 mL of dry THF. After 1 hour, 192 mg (0.65 mmol) of (2-chloro-6-(methylsulfanyl)pyridin-4-yl)(4-methoxyphenyl)methanone (**9**) dissolved in 10 mL of dry THF was added. Flash chromatography using Hexane/EtOAc (99/1) yielded 65 mg (0.22 mmol; 34%) of 2-chloro-4-(1-(4-methoxyphenyl)vinyl)-6-(methylsulfanyl)pyridine (**11**). ^{1}H NMR (200 MHz, $CDCl_3$): 2.56 (3H, *s*), 3.84 (3H, *s*), 5.47 (1H, *s*), 5.53 (1H, *s*), 6.88 (2H, *d*, *J* = 8.6), 6.95 (1H, *s*), 7.03 (1H, *s*), 7.20 (2H, *d*, *J* = 8.6). ^{13}C NMR (50 MHz, $CDCl_3$): 13.6 (CH_3), 55.4 (CH_3), 114.0 (2) (CH), 116.4 (CH_2), 118.6 (CH), 119.1 (CH), 129.3 (2) (CH), 113. 6 (C), 146.3 (C), 151.1 (C), 152.1 (C), 159.9 (C),

160.9 (C). IR (film): 1417, 1457, 1518, 1602 cm^{-1}. HRMS ($C_{15}H_{14}ClNOS$): Calculated ($M+H^+$) 292.0557 found 292.0572.

4-(1-(4-methoxyphenyl)vinyl)-2,6-bis(methylsulfanyl)pyridine (12)

Following procedure 2, 1.4 ml (2.2 mmol) of *n*BuLi 1.6 M in hexanes were slowly added at -40 ºC to a solution of 1.32 g (3.27 mmol) of methyltriphenylphosphonium iodide in 10 mL of dry THF. After 1 hour, 333 mg (1.09 mmol) of (2,6-bis(methylsulfanyl)pyridin-4-yl)(4-methoxyphenyl)methanone (**10**) dissolved in 10 mL of dry THF was added. Flash chromatography using Hexane/EtOAc (97/3) yielded 309 mg (1.02 mmol; 94 %) of 4-(1-(4-methoxyphenyl)vinyl)-2,6-bis(methylsulfanyl)pyridine (**12**). ^{1}H NMR (200 MHz, $CDCl_3$): 2.59 (6H, *s*), 3.83 (3H, *s*), 5.42 (1H, *d*, *J* = 1.1), 5.47 (1H, *d*, *J* = 1.1), 6.82 (2H, *s*), 6.86 (2H, *d*, *J* = 8.6), 7.21 (2H, *d*, *J* = 8.6). ^{13}C NMR (50 MHz, $CDCl_3$): 13.3 (2) (CH_3), 55.4 (CH_3), 113.8 (2) (CH), 115.4 (CH_2), 116.3 (2) (CH), 129.3 (2) (CH), 132.1 (C), 147.1 (C), 149.4 (C), 159.3 (2) (C), 159.7 (C). IR (película): 1523, 1593, 1654 cm^{-1}. HRMS ($C_{16}H_{17}NOS_2$): calculated ($M+H^+$) 304.0824, found 304.0835.

(*E*/*Z*)-(2-chloro-6-(methylsulfanyl)pyridin-4-yl)(4-methoxyphenyl)methanone oxime (13)

Following procedure 3, 229 mg (3.30 mmol) of hydroxylamine hydrochloride was added to a solution of 97 mg (0.33 mmol) of (2-chloro-6-(methylsulfanyl)pyridin-4-yl)(4-methoxyphenyl)methanone (**9**) in 15 mL of MeOH to yield 91 mg (0.29 mmol, 89%). The oximes crystalize in hexane/CH_2Cl_2 as a mixture of the oximes (E/Z)-(2-chloro-6-(methylsulfanyl)pyridin-4-yl)(4-methoxyphenyl)methanone oxime (**13**). M.p. (Hex/CH_2Cl_2): 100-105 ºC. ^{1}H NMR (200 MHz, $CDCl_3$): 2.55 (3H, *s*), 2.58 (3H, *s*), 3.83 (3H, *s*), 3.87 (3H, *s*), 6.87 (2H, *d*, *J* = 8.9), 6.98 (1H, *d*, *J* = 1.1), 6.99 (2H, *d*, *J* = 8.9), 7.05 (1H, *d*, *J* = 1.1), 7.09 (1H, *d*, *J* = 1.2), 7.14 (1H, *d*, *J* = 1.2), 7.33 (2H, *d*, *J* = 8.9), 7.37 (2H, *d*, *J* = 8.9). ^{13}C NMR (50 MHz, $CDCl_3$): 13.5 (CH_3), 55.3 (CH_3), 113.9 (CH), 114.0 (2) (CH), 118.9 (CH), 119.6 (CH), 126.5 (C), 128.8 (2) (CH), 130.8 (CH), 143.4 (C), 151.2 (C), 154.4 (C), 160.5 (C), 161.2 (C), 161.4 (C). IR (KBr): 1412, 1446, 1524, 1573, 1603, 3177 cm^{-1}. HRMS ($C_{14}H_{13}ClN_2O_2S$): Calculated ($M+H^+$) 309.0459, found 309.0438.

(*E*/*Z*)-(2,6-bis(methylthio)pyridin-4-yl)(4-methoxyphenyl)methanone oxime (14)

Following procedure 3, 403 mg (5.8 mmol) of hydroxylamine hydrochloride was added to a solution of 177 mg (0.58 mmol) of (2,6-bis(methylsulfanyl)pyridin-4-yl)(4-methoxyphenyl)methanone (**10**) in 15 mL of MeOH. The resulting product was chromatographed with hexane/EtOAc (9:1) to give 13 mg (0.04 mmol; 7%) of one oxime, and 141,2 mg (0,44 mmol; 76%) of the mixture of the two oximes (*E*/*Z*)-(2,6-bis(methylthio)pyridin-4-yl)(4-methoxyphenyl)methanone oxime (**14**), that crystalize in Hex/CH_2Cl_2. M.p. (Hex/CH_2Cl_2): 125 – 127 ºC. ^{1}H NMR (200 MHz, $CDCl_3$): 2.56 (6H, *s*), 3.86 (3H, *s*), 6.93 (2H, *s*), 6.98 (2H, *d*, *J* = 8.9), 7.36 (2H, *d*, *J* = 8.9). ^{1}H NMR (200 MHz, $CDCl_3$): 2.60 (6H, s), 3.81 (3H, s), 6.85 (2H, d, J = 8.9), 6.85 (2H, s), 7.36 (2H, d, J=8.9). ^{13}C NMR (50 MHz, $CDCl_3$): 13.4 (2) (CH_3), 55.4 (CH_3), 113.8 (2) (CH), 115.5 (2) (CH), 122.8 (C), 131.2 (2) (CH), 144.1 (C), 155.6 (C), 159.9 (2) (C), 160.6 (C). ^{13}C NMR (50 MHz, $CDCl_3$): 13.4 (2) (CH_3), 55.4 (CH_3), 114.1 (2) (CH), 116.3 (2) (CH), 126.7 (C), 129.0 (2) (CH), 140.9 (C), 155.3 (C), 159.9 (2) (C), 161.2 (C). IR (KBr): 1417, 1456, 1518, 1573, 1605, 3434 cm^{-1}. HRMS ($C_{15}H_{16}N_2O_2S_2$): calculated ($M+Na^+$) 343.0545, found 343.0562.

4-(1-(4-methoxyphenyl)ethyl)-2,6-bis(methylsulfanyl)pyridine (15)

16 mg (0.05 mmol) of 4-(1-(4-methoxyphenyl)vinyl)-2,6-bis(methylsulfanyl)pyridine **(12)** in 10 ml of AcOEt/EtOH (95/5) was vigorously stirred under H_2 atmosphere with Pd(C) catalysis for 24h. The reaction was filtered through celite©, evaporated and chromatographed by preparative thin layer chromatography with Hexane/EtOAc (98/2) to yield 7 mg (0.02 mmol; 45%) of 4-(1-(4-methoxyphenyl)ethyl)-2,6-bis(methylsulfanyl)pyridine **(15)**. ^{1}H NMR (200 MHz, $CDCl_3$): 1.55 (3H, *d*, *J* = 7.2), 2.56 (6H, *s*), 3.79 (3H, *s*), 3.90 (1H, *c*, *J* = 7.2), 6.71 (2H, *s*), 6,83 (2H, *d*, *J* = 8.8), 7,06 (2H, *d*, *J* = 8.8). ^{13}C NMR (50 MHz, $CDCl_3$): 13.3 (2) (CH_3), 21.2 (CH_3), 43.3 (CH), 55.4 (CH_3), 113.9 (2) (CH), 114.0 (C), 116.3 (2) (CH), 128.6 (2) (CH), 136.3 (2) (C), 155.5 (C), 159.0 (C). IR (film): 1456, 1513, 1533, 1575, 1610 cm^{-1}. HRMS ($C_{16}H_{19}NOS_2$): calculated ($M+H^+$) 306.0981, found 306.0987.

(2-Chloro-6-(methylsulfanyl)pyridin-4-yl)(1-methyl-1H-indol-5-yl)methanone (16)

Following procedure 1, 15.4 ml (24.6 mmol) of *n*BuLi 1.6 M in hexanes was slowly added to a solution of 5.16 g (24.6 mmol) of 5-bromo-*N*-methyl-1*H*-indol (**7**) in dry THF at -40 ºC. After 45 minutes, 2 g (9.8 mmol) of 2-chloro-6-methylsulfanylpyridine-4-carboxylic acid (**2**) in 10 mL of dry THF was added. The reaction product was flash chromatographed using Hexane/EtOAc (9/1) toyield 1.09 g (3.44 mmol, 35%) of (2-chloro-6-(methylsulfanyl)pyridin-4-yl)(1-methyl-1*H*-indol-5-yl)methanone (**16**) as white needles. M.p. (Hex/AcOEt): 116-123 ºC. ^{1}H NMR (200 MHz, $CDCl_3$): 2.60 (3H, *s*), 3.86 (3H, *s*), 6.63 (1H, *d*, *J* = 2.8), 7,16 (1H, *d*, *J* = 2.8), 7.25 (1H, *s*), 7.33 (1H, *s*), 7.40 (1H, *bd*, *J* = 8.9), 7.79 (1H, *bd*, *J* = 8,6), 8.06 (1H, *s*). ^{13}C NMR (50 MHz, $CDCl_3$): 13.7 (CH_3), 33.2 (CH_3), 103.5 (CH), 109.7 (CH), 118.5 (CH), 119.2 (CH), 123.4 (CH), 125.9 (CH), 127.3 (C), 127.9 (C), 131.0 (CH), 139.6 (C), 149.0 (C), 151.3 (C), 161.8 (C), 193.8 (C). IR (KBr): 1446, 1530, 1565, 1601, 1645 cm^{-1}. HRMS ($C_{16}H_{13}ClN_2OS$): calculated ($M+Na^+$) 339.0329, found 339.0316.

(2,6-Bis(methylsulfanyl)pyridin-4-yl)(1-methyl-1*H*-indol-5-yl)methanone (17)

Following procedure 1, 7.2 ml (11.5 mmol) of *n*BuLi 1.6 M in hexanes was slowly added to a solution of 2.44 g (11.5 mmol) of 5-bromo-*N*-methyl-1*H*-indol (**7**) in dry THF at -40 ºC. After 45 minutes, 1 g (4.6 mmol) of 2,6-bis(methylsulfanyl)pyridine-4-carboxylic acid (**3**) in 10 mL of dry THF was added. The reaction product was flash chromatographed using Hexane/EtOAc (9/1) to yield 412 mg (1.25 mmol; 27%) of (2,6-bis(methylsulfanyl)pyridin-4-yl)(1-methyl-1*H*-indol-5-yl)methanone (**17**). ^{1}H NMR (200 MHz, $CDCl_3$): 2.62 (6H, *s*), 3.85 (3H, *s*), 6.60 (1H, *d*, *J* = 3.2), 7.10 (2H, *s*), 7.15 (1H, *d*, *J* = 3.2), 7.38 (1H, *bd*, *J* = 8.8), 7.80 (1H, *dd*, *J* = 1.8, *J* = 8.8), 8.07 (1H, *d*, *J* = 1.8). ^{13}C NMR (50 MHz, $CDCl_3$): 13.5 (2) (CH_3), 33.2 (CH_3), 103.4 (CH), 109.6 (CH), 115.9 (2) (CH), 123.5 (CH), 125.8 (CH), 127.7 (C), 127.9 (C), 130.9 (CH), 139.5 (C), 146.4 (C), 160.1 (2) (C), 195.1 (C). IR (KBr): 1526, 1565, 1603, 1652 cm^{-1}. HRMS ($C_{17}H_{16}N_2OS_2$): calculated ($M+H^+$) 329.0777, found 329.0761.

5-(1-(2-Chloro-6-(methylsulfanyl)pyridin-4-yl)vinyl)-1-methyl-1*H*-indole (18)

Following procedure 2, 3.4 ml (5.4 mmol) of *n*BuLi 1.6 M in hexanes was slowly added to a stirred suspension of 3.251 g (8.07 mmol) of methyltriphenylphosphonium iodide in 50 mL of dry THF at -40 ºC. After 45 minutes, 852 mg (2.69 mmol) of (2-chloro-6-(methylsulfanyl)pyridin-4-yl)(1-methyl-1*H*-indol-5-yl)methanone (**16**) was added. Flash chromatography with

Hexane/EtOAc (98/2) yielded 194 mg (0.62 mmol; 23 %) of 5-(1-(2-chloro-6-(methylsulfanyl)pyridin-4-yl)vinyl)-1-methyl-1*H*-indole (**18**). ^{1}H NMR (200 MHz, $CDCl_3$): 2.60 (3H, *s*), 3.82 (3H, *s*), 5.53 (1H, *s*), 5.61 (1H, *s*), 6.50 (1H, *s*), 7.01 (1H, *s*), 7.10 (2H, *s*), 7.14 (1H, *bd*, *J* = 8,6), 7.33 (1H, *bd*, *J* = 8.6), 7.54 (1H, *s*). ^{13}C NMR (50 MHz, $CDCl_3$): 13.7 (CH_3), 33.0 (CH_3), 101.6 (CH), 109.4 (CH), 116.4 (CH_2), 118.9 (CH), 119.3 (CH), 120.9 (CH), 122.0 (CH), 128.5 (C), 129.9 (CH), 130.7 (C), 136.7 (C), 147.9 (C), 151.1 (C), 153.0 (C), 160.8 (C). IR (film): 1422, 1442, 1492, 1519, 1576 cm^{-1}. HRMS ($C_{17}H_{15}ClN_2S$): calculated ($M+H^+$) 315.0717, found 315.0723.

5-(1-(2,6-Bis(methylsulfanyl)pyridin-4-yl)vinyl)-1-methyl-1*H*-indole (19)

Following procedure 2, 1.1 ml (1.76 mmol) of *n*BuLi 1.6 M in hexanes was slowly added to a stirred suspension of 1.07 g (2.65 mmol) of methyltriphenylphosphonium iodide in 50 mL of dry THF at -40 ºC. After 45 minutes, 290 mg (0.88 mmol) of (2,6-bis(methylsulfanyl)pyridin-4-yl)(1-methyl-1*H*-indol-5-yl)methanone (**17**) was added. Flash chromatography with 95/5 Hexane/EtOAc yielded 134 mg (0.41 mmol; 47 %) of 5-(1-(2,6-bis(methylsulfanyl)pyridin-4-yl)vinyl)-1-methyl-1*H*-indole (**19**). ^{1}H NMR (200 MHz, $CDCl_3$): 2.63 (6H, *s*), 3.81 (3H, *s*), 5.51 (1H, *d*, *J* = 1.1), 5.59 (1H, *d*, *J* = 1.1), 6.50 (1H, *d*, *J* = 3.2), 6.94 (2H, *s*), 7.09 (1H, *d*, *J* = 3.2), 7.20 (1H, *dd*, *J* = 1.8, *J* = 8.8), 7.31 (1H, *bd*, *J* = 8.8), 7.58 (1H, *d*, *J* = 1.8). ^{13}C NMR (50 MHz, $CDCl_3$): 13.4 (2) (CH_3), 33.0 (CH_3), 101.5 (CH), 109.2 (CH), 115.4 (CH_2), 116.5 (2) (CH), 120.9 (CH), 122.1 (CH), 128.4 (C), 129.7 (CH), 131.2 (C), 136.6 (C), 148.7 (C), 150.3 (C), 159.2 (2) (C). IR (film): 1517, 1571, 1607 cm^{-1}. HRMS ($C_{18}H_{18}N_2S_2$): Calculated ($M+H_+$) 327.0984, found 329.1031.

5-(2-Chloro-6-(methylsulfanyl)isonicotinoyl)-1-methyl-1*H*-indole-3-carbaldehyde (20)

Following procedure 4, 0.35 ml (3.7 mmol) of $POCl_3$ was added to 2 mL of dry DMF at 0 ºC. After 30 minutes, 200 mg (0.63 mmol) of (2-chloro-6-(methylsulfanyl)pyridin-4-yl)(1-methyl-1*H*-indol-5-yl)methanone (**16**) was added and the mixture heated to 60 ºC. After precipitation, the filtrate was flash chromatographed with Hexane/EtOAc (1/1) to yield 140 mg (0.41 mmol, 64%) of 5-(2-chloro-6-(methylsulfanyl)isonicotinoyl)-1-methyl-1*H*-indole-3-carbaldehyde (**20**). ^{1}H NMR (200 MHz, $CDCl_3$): 2.59 (3H, *s*), 3.95 (3H, *s*), 7.22 (1H, *s*), 7.31 (1H, *s*), 7.46 (1H, *d*, *J* = 8.6), 7.81 (1H, *s*), 7.85 (1H, *dd*, *J* = 8.6; *J* = 1.4), 8.66 (1H, *s*), 9.99 (1H, *s*). ^{13}C NMR (50 MHz,

$CDCl_3$): 13.7 (CH_3), 34.1 (CH_3), 110.5 (CH), 118.4 (CH), 119.1 (CH), 122.4 (C), 124.8 (C), 125.7 (CH), 125.9 (CH), 130.5 (C), 140.7 (CH), 148.0 (C), 151.4 (C), 162.1 (C), 184.2 (CH), 193.6 (C). IR (film): 1466, 1530, 1607, 1658 cm^{-1}. HRMS ($C_{17}H_{13}ClN_2O_2S$): calculated ($M+H^+$) 345.0459, found 345.0444.

5-(2,6-bis(methylsulfanyl)isonicotinoyl)-1-methyl-1*H*-indole-3-carbaldehyde (21)

Following procedure 4, 0.15 ml (1.6 mmol) of $POCl_3$ was added to 2 mL of dry DMF at 0 ºC. After 30 minutes, 96 mg (0.29 mmol) of (2,6-bis(methylsulfanyl)pyridin-4-yl)(1-methyl-1*H*-indol-5-yl)methanone (**17**) was added and the mixture heated to 60 ºC for 2 hours. After precipitation, the filtrate was flash chromatographed with 1/1 Hexane/EtOAc to yield 45 mg (0.13 mmol; 44%) of 5-(2,6-bis(methylsulfanyl)isonicotinoyl)-1-methyl-1*H*-indole-3-carbaldehyde (**21**). ^{1}H NMR (200 MHz, $CDCl_3$): 2.62 (6H, *s*), 3.94 (3H, *s*), 7.10 (2H, *s*), 7.44 (1H, *bd*, *J* = 8.4), 7.79 (1H, *s*), 7.88 (1H, *dd*, *J* = 1.8, *J* = 8.4), 8.69 (1H, *d*, *J* = 1.8), 10.02 (1H, *s*). ^{13}C NMR (50 MHz, $CDCl_3$): 13.4 (2) (CH_3), 33.9 (CH_3), 110.2 (CH), 115.8 (2) (CH), 119.1 (C), 124.7 (C), 125.6 (CH), 125.7 (CH), 130.9 (C), 140.2 (CH), 145.3 (C), 160.3 (2) (C), 184.1 (CH), 194.9 (C). IR: (film): 1457, 1529, 1568, 1610, 1658 cm^{-1}. HRMS ($C_{18}H_{15}N_2NaO_2S_2$): calculated ($M+H^+$) 357.0731, found 357.0742.

(2-Chloro-6-(methylsulfanyl)pyridin-4-yl)(1-methyl-1*H*-indol-5-yl)methanone oxime (22)

Following procedure 3, 305 mg (4.39 mmol) of hydroxylamine hydrochloride was added onto a solution of 139 mg (0.43 mmol) of (2-chloro-6-(methylsulfanyl)pyridin-4-yl)(1-methyl-1*H*-indol-5-yl)methanone (**16**) in 20 mL of MeOH. 105 mg (0.32 mmol, 74%) of the mixture of oximes was crystalized in Hexane/CH_2Cl_2 from the reaction. (*E*/*Z*)-(2-chloro-6-(methylsulfanyl)pyridin-4-yl)(1-methyl-1*H*-indol-5-yl)methanone oxime (**22**). ^{1}H NMR (200 MHz, $CDCl_3$): 2.55 (3H, *s*), 2.60 (3H, *s*), 3.79 (3H, *s*), 3.83 (3H, *s*), 6.48 (1H, *d*, *J* = 3.0), 6.56 (1H, *d*, *J* = 3.0), 7.00 – 7.59 (2H, *m*), 7.71 (1H, *s*). ^{13}C NMR (50 MHz, $CDCl_3$): 13.7 (CH_3), 33.1 (CH3), 102.0 (CH), 102.1 (CH), 109.4 (CH), 109.8 (CH), 118.1 (CH), 118.7 (CH), 119.4 (CH), 119.9 (CH), 120.6 (CH), 121.5 (CH), 122.6 (CH), 124.3 (C), 125.5 (C), 128.2 (CH), 130.1 (CH), 137.1 (C), 137.6 (C), 144.5 (C), 147.7 (C), 151.2 (C), 155.8 (C), 156.2 (C), 161.3 (C), 161.5 (C). IR (film): 1441, 1524, 1577 cm^{-1}. HRMS ($C_{16}H_{14}N_3OSCl$): calculated ($M+H^+$) 332.0619, found 332.0610.

(E/Z)-(2,6-bis(methylsulfanyl)pyridin-4-yl)(1-methyl-1*H*-indol-5-yl)methanone oxime (23)

Following procedure 3, 284 mg (4.08 mmol) of hydroxylamine hydrochloride was added onto a solution of 134 mg (0.41 mmol) of (2,6-bis(methylsulfanyl)pyridin-4-yl)(1-methyl-1*H*-indol-5-yl)methanone (**17**) in 20 mL of MeOH. The mixture of oximes was chromatographed with 9/1 Hexane/EtOAc to yield 48 mg (0.14 mmol; 34%) of one isomer, 21 mg (0.06 mmol; 15%) of the other, and 52 mg (0.15 mmol; 37%) of the mixture of (*E*/*Z*)-(2,6-bis(methylsulfanyl)pyridin-4-yl)(1-methyl-1*H*-indol-5-yl)methanone oximes (**23**). ^{1}H NMR (200 MHz, $CDCl_3$), major isomer: 2.56 (6H, s), 3.84 (3H, *s*), 6.54 (1H, *d*, *J* = 3.2), 6.98 (2H, *s*), 7.12 (1H, *d*, *J* = 3.2), 7.24 (1H, *dd*, *J* = 1.8, *J* = 8.6), 7.40 (1H, *bd*, *J* = 8.6), 7.68 (1H, *d*, *J* = 1.8). ^{1}H NMR (200 MHz, $CDCl_3$), minor isomer: 2.61 (6H, *s*), 3.80 (3H, *s*), 6.46 (1H, *d*, *J* = 3.2), 6.90 (2H, *s*), 7.06 (1H, *d*, *J* = 3.2), 7.29 (1H, *bd*, *J* = 8.6), 7.47 (1H, *d*, *J* = 1.8), 7.51 (1H, *dd*, *J* = 1.8, *J* = 8.6). ^{13}C NMR (50 MHz, $CDCl_3$): 13.3 (2) (CH_3), 32.9 (CH_3), 102.0 (CH), 109.4 (CH), 116.5 (2) (CH), 120.6 (CH), 121.6 (CH), 125.5 (C), 128.1 (C), 129.8 (CH), 137.5 (C), 141.5 (C), 156.9 (C), 159.7 (2) (C). IR: (film): 1435, 1517, 1571, 3214 cm^{-1}. HRMS ($C_{17}H_{17}N_3OS_2$): calculated ($M+H^+$) 344.0886, found 344.0870.

(*E/Z*)-5-((2-chloro-6-(methylsulfanyl)pyridin-4-yl)(hydroxyimino)methyl)-1-methyl-1*H*-indole-3-carbonitrile (24)

Following procedure 3, 282 mg (4.06 mmol) of hydroxylamine hydrochloride was added onto a solution of 140 mg (0.41 mmol) of 5-(2-chloro-6-(methylsulfanyl)isonicotinoyl)-1-methyl-1*H*-indole-3-carbaldehyde (**20**) in 20 mL of MeOH, yielding 129 mg (0.34 mmol; 84%) of a mixture of oximes. The oximes were dissolved in 1 mL of pyridine and 0.5 mL of acetic anhydride, following procedure 5 to yield 103 mg (0.26 mmol; 76%) of (*E/Z*)-5-((2-chloro-6-(methylsulfanyl)pyridin-4-yl)(acetoxyimino)methyl)-1-methyl-1*H*-indole-3-carbonitrile, that was dissolved in 3 mL of MeOH and 1 mL of 10% NaOH and stirred for 72 hours at room temperature. The mixture was poured onto CH_2Cl_2 and the organic layer was washed with brine until neutral pH, dried over anhydrous Na_2SO_4, filtered and evaporated to dryness, yielding 89 mg. Column chromatography using 95/5 CH_2Cl_2/EtOAc gave 45 mg (0.13 mmol; 50%) of (*E/Z*)-5-((2-chloro-6-(methylsulfanyl)pyridin-4-yl)(hydroxyimino)methyl)-1-methyl-1*H*-indole-3-carbonitrile (**24**) as light yellow needles (CH_2Cl_2/Hexane). ^{1}H NMR (200 MHz, $CDCl_3$): 2.46 (3H, *s*), 2.52 (3H, *s*), 3.80 (3H, *s*), 3.84 (3H, *s*), 6.93 (1H, *s*), 6.99 (1H, *s*), 7.01 (1H, *s*), 7.04 (1H, *s*), 7.18 (1H, *d*, *J* = 1,6), 7.22 (1H, *d*, *J* = 8.6), 7.30 (1H, *d*, *J* = 8.6), 7.43 (1H, *d*, *J* = 8.6), 7.53 (1H, *s*), 7.58 (1H, *s*), 7.63 (1H, *s*), 7.71 (1H, *s*). ^{13}C NMR (50 MHz, $CDCl_3$): 13.5 (CH_3), 33.8 (CH_3),

110.7 (CH), 115.3 (C), 117.4 (CH), 118.3 (CH), 119.0 (C), 119.7 (CH), 121.0 (CH), 123.1 (C), 124.5 (CH), 127.6 (C), 136.2 (C), 136.7 (CH), 146.6 (C), 151.2 (C), 155.1 (C), 161.6 (C), 175.8 (C). IR (film): 1428, 1448, 1527, 1574, 2219, 3316, 3338 cm^{-1}. HRMS ($C_{17}H_{13}ClN_4OS$): calculated ($M+Na^+$) 379.0391, found 379.0389.

5-(1-(2-chloro-6-(methylsulfanyl)pyridin-4-yl)vinyl)-1-methyl-1*H*-indole-3-carbaldehyde (25)

Following procedure 4, 0.16 ml (1.7 mmol) of $POCl_3$ was added to 2 mL of dry DMF at 0 ºC. After 30 minutes, 89 mg (0.28 mmol) of 5-(1-(2-chloro-6-(methylsulfanyl)pyridin-4-yl)vinyl)-1-methyl-1*H*-indole (**18**) was added stirred for 2 hours at room temperature. After precipitation, the filtrate was flash chromatographed with Hexane/EtOAc (4/6) to yield 67 mg (0.20 mmol; 70%) of 5-(1-(2-chloro-6-(methylsulfanyl)pyridin-4-yl)vinyl)-1-methyl-1*H*-indole-3-carbaldehyde (**25**). ^{1}H NMR (200 MHz, $CDCl_3$): 2.56 (3H, *s*), 3.92 (3H, *s*), 5.62 (1H, *s*), 5.65 (1H, *s*), 6.94 (1H, *d*, *J* = 1.4), 7.03 (1H, *d*, *J* = 1.4), 7.17 (1H, *dd*, *J* = 1.8; *J* = 8.2), 7.34 (1H, *bd*, *J* = 8.2), 7.73 (1H, *s*), 8.29 (1H, *d*, *J* = 1.8), 10.0 (1H, *s*). ^{13}C NMR (50 MHz, $CDCl_3$): 13.6 (CH_3), 33.9 (CH_3), 110.0 (CH), 118.0 (CH_2), 118.3 (C), 118.5 (CH), 119.0 (CH), 121.8 (CH), 124.5 (CH), 125.4 (C), 134.5 (C), 137.8 (C), 140.2 (CH), 147.2 (C), 151.1 (C), 152.3 (C), 160.9 (C), 184.4 (CHO). IR (film): 1528, 1577, 1657 cm^{-1}. HRMS ($C_{18}H_{15}ClN_2OS$): calculated ($M+H^+$) 343.0666, found 343.0666.

5-(1-(2,6-bis(methylsulfanyl)pyridin-4-yl)vinyl)-1-methyl-1*H*-indole-3-carbaldehyde (26)

Following procedure 4, 309 µl (3.38 mmol) of $POCl_3$ was added to 2 mL of dry DMF at 0 ºC. After 30 minutes, 184 mg (0.56 mmol) of 5-(1-(2,6-bis(methylsulfanyl)pyridin-4-yl)vinyl)-1-methyl-1*H*-indole (**19**) was added and the mixture stirred for 2 hours at room temperature. After precipitation, the filtrate was flash chromatographed with 6/4 Hexane/EtOAc to yield 183 mg (0.51 mmol; 92%) of 5-(1-(2,6-bis(methylsulfanyl)pyridin-4-yl)vinyl)-1-methyl-1*H*-indole-3-carbaldehyde (**26**) ^{1}H NMR (200 MHz, $CDCl_3$): 2.57 (6H, *s*), 3.88 (3H, *s*), 5.56 (1H, *s*), 5.60 (1H, *s*), 6.82 (2H, *s*), 7.17 (1H, *bd*, *J* = 8.6), 7.32 (1H, *bd*, *J* = 8.6), 7.70 (1H, *s*), 8.29 (1H, *s*), 9.98 (1H, *s*). ^{13}C NMR (50 MHz, $CDCl_3$): 13.3 (2) (CH_3), 33.8 (CH_3), 109.9 (CH), 116.1 (2) (CH), 116.9 (CH_2), 118.2 (C), 121.6 (CH), 124.5 (CH), 125.3 (C), 134.9 (C), 137.7 (C), 140.2 (CH), 148.0 (C), 149.5 (C), 159.3 (2) (C), 184.3 (CH). IR (film): 1456, 1481, 1524, 1572, 1652, 2918 cm^{-1}. HRMS ($C_{19}H_{18}N_2OS_2$): calculated ($M+H^+$) 355.0933, found 355.0939.

5-(1-(2-Chloro-6-(methylsulfanyl)pyridin-4-yl)vinyl)-1-methyl-1*H*-indole-3-carboxylic acid (27)

393 µl (0.74 mmol) of phosgene was added to a solution of 85 mg (0.27 mmol) of 5-(1-(2-chloro-6-(methylsulfanyl)pyridin-4-yl)vinyl)-1-methyl-1*H*-indole-3-carbaldehyde (**25**) in 20 mL of dry CH_2Cl_2 at 0 ºC. After stirring 72 hours at room temperature the reaction is poured onto iced water and extracted with EtOAc. The organic layer were washed with 4% NaOH and brine until neutral pH, dried over anhydrous Na_2SO_4, filtered and evaporated to dryness, yielding 66 mg (0.19 mmol; 71%) of 5-(2-chloro-6-(methylsulfanyl)isonicotinoyl)-1-methyl-1*H*-indole-3-carbaldehyde (**20**). The basic waters were acidified with 2N HCl and extracted with EtOAc. The organic layer was washed with brine until neutral pH, dried over anhydrous Na_2SO_4, filtered and evaporated to dryness, yielding 13 mg (0.04 mmol; 13%) of 5-(1-(2-chloro-6-(methylsulfanyl)pyridin-4-yl)vinyl)-1-methyl-1*H*-indole-3-carboxylic acid (**27**). ^{1}H NMR (200 MHz, $CDCl_3$): 2.48 (3H, *s*), 3.81 (3H, *s*), 5.55 (1H, *s*), 5.58 (1H, *s*), 6.89 (1H, *d*, *J* = 1.1), 6.97 (1H, *d*, *J* = 1.1), 7.05 (1H, *bd*, *J* = 8.5), 7.26 (1H, *bd*, *J* = 8.5), 7.83 (1H, *s*), 8.12 (1H, *s*). IR (film): 1465, 1532, 1577, 1610, 1662 cm^{-1}. HRMS ($C_{18}H_{15}ClN_2O_2S$): calculated (M+Na$^+$) 381.0435, found 381.0453.

5-(1-(2,6-Bis(methylsulfanyl)pyridin-4-yl)vinyl)-1-methyl-1*H*-indole-3-carboxylic acid (28)

125 µl (0.24 mol) of phosgene was added to a solution of 79 mg (0.24 mmol) of 5-(1-(2,6-bis(methylsulfanyl)pyridin-4-yl)vinyl)-1-methyl-1*H*-indole (**19**) in 20 mL of dry CH_2Cl_2 at 0 ºC. After stirring 72 hours at room temperature the reaction is poured onto iced water, basified with 4% NaOH and extracted with CH_2Cl_2. The basic aqueous layer was acidified with HCl 2N and extracted with CH_2Cl_2. The organic layer was washed with and brine until neutral pH, dried over anhydrous Na_2SO_4, filtered and evaporated to dryness, yielding 22 mg (0.06 mmol; 25%) of 5-(1-(2,6-bis(methylsulfanyl)pyridin-4-yl)vinyl)-1-methyl-1*H*-indole-3-carboxylic acid (**28**). ^{1}H NMR (200 MHz, $CDCl_3$): 2.58 (6H, *s*), 3.88 (3H, *s*), 5.58 (1H, *s*), 5.61 (1H, *s*), 6.84 (2H, *s*), 7.12 (1H, *bd*, *J* = 8.9), 7.31 (1H, *bd*, *J* = 8.9), 7.90 (1H, *s*), 8.22 (1H, *s*). ^{13}C NMR (50 MHz, DMSO-D_6): 12.7 (2) (CH_3), 33.1 (CH_3), 106.5 (C), 110.9 (CH), 115.3 (2) (CH), 117.1 (CH_2), 120.2 (CH), 122.4 (CH), 126.4 (C), 132.7 (C), 136.9 (CH), 147.4 (C), 149.6 (C), 159.2 (2) (C), 165.5 (C). IR (KBr): 1422, 1482, 1523, 1573, 1615, 1656 cm^{-1}. HRMS ($C_{19}H_{18}N_2O_2S_2$): calculated (M+H$^+$) 371.0882, found 371.0886.

5-(1-(2-Chloro-6-(methylsulfanyl)pyridin-4-yl)vinyl)-1-methyl-1*H*-indole-3-carbonitrile (29)

Following procedure 3, 324 mg (4.67 mmol) of hydroxylamine hydrochloride was added onto a solution of 160 mg (0.46 mmol) of 5-(1-(2-chloro-6-(methylsulfanyl)pyridin-4-yl)vinyl)-1-methyl-1*H*-indole-3-carbaldehyde (**25**) in 20 mL of MeOH, yielding 149 mg (0.42 mmol; 90%) of a mixture of oximes. The oximes were dissolved in 1 mL of pyridine and 0.5 mL of acetic anhydride, following procedure 5. Column chromatography using 7/3 Hexane/EtOAc gave 106 mg (0.31 mmol; 74%) of 5-(1-(2-chloro-6-(methylsulfanyl)pyridin-4-yl)vinyl)-1-methyl-1*H*-indole-3-carbonitrile (**29**). ^{1}H NMR (200 MHz, $CDCl_3$): 2.56 (3H, *s*), 3.88 (3H, *s*), 5.62 (1H, *s*), 5.63 (1H, *s*), 6.93 (1H, *s*, *J* = 1.2), 7.02 (1H, *s*, *J* = 1.2), 7.20 (1H, *dd*, *J* = 1.6, *J* = 8.6), 7.37 (1H, *bd*, *J* = 8.6), 7.61 (1H, *s*), 7.70 (1H, *s*). ^{13}C NMR (50 MHz, $CDCl_3$) 13.5 (CH_3), 33.8 (CH_3), 110.4 (CH), 115.6 (C), 117.9 (CH_2), 118.4 (CH), 119.0 (CH), 119.5 (CH), 124.3 (CH), 127.9 (C), 133.8 (C), 135.9 (C), 136.3 (CH), 146.8 (C), 151.1 (C), 151.9 (C), 161.0 (C). IR (film): 1526, 1576, 2218 cm^{-1}. HRMS (C18H14ClN3S): calculated (M+H+) 340.0670, found 340.0673.

5-(1-(2,6-bis(methylsulfanyl)pyridin-4-yl)vinyl)-1-methyl-1*H*-indole-3-carbonitrile (30)

Following procedure 3, 271 mg (3.89 mmol) of hydroxylamine hydrochloride was added onto a solution of 138 mg (0.39 mmol) of 5-(1-(2,6-bis(methylsulfanyl)pyridin-4-yl)vinyl)-1-methyl-1*H*-indole-3-carbaldehyde (**26**) in 20 mL of MeOH, yielding 138 mg (0.37 mmol; 95%) of 5-(1-(2,6-bis(methylthio)pyridin-4-yl)vinyl)-1-methyl-1*H*-indole-3-carbaldehyde oxime. The oximes were dissolved in 1 mL of pyridine and 0.5 mL of acetic anhydride, following procedure 5. Column chromatography using 3/1 Hexane/EtOAc gave 51 mg (0.15 mmol; 39%) of 5-(1-(2,6-bis(methylsulfanyl)pyridin-4-yl)vinyl)-1-methyl-1*H*-indole-3-carbonitrile (**30**). ^{1}H NMR (200 MHz, $CDCl_3$): 2.55 (6H, *s*), 3.77 (3H, *s*), 5.48 (1H, *s*), 5.49 (1H, *s*), 6.72 (2H, *s*), 7.13 (1H, *bd*, *J* = 8.8), 7.26 (1H, *bd*, *J* = 8.8), 7.50 (1H, *s*), 7.60 (1H, *s*). ^{13}C NMR (50 MHz, $CDCl_3$): 13.6 (2) (CH_3), 34.2 (CH_3), 110.7 (CH), 116.1 (C), 116.5 (2) (CH), 117.3 (CH_2), 119.8 (CH), 124.8 (CH), 128.2 (C), 134.7 (C), 136.2 (C), 136.6 (CH), 148.0 (C), 159.6 (C), 159.7 (2) (C). IR (film): 1484, 1527, 1573, 1714, 2218 cm^{-1}. HRMS ($C_{19}H_{17}N_3S_2$): calculated ($M+H^+$) 352.0937, found 352.0939.

5-(1-(2-chloro-6-(methylsulfanyl)pyridin-4-yl)vinyl)-1-methyl-1*H*-indole-3-carboxamide (31)

12 ul (0.14 mmol) of chlorosulfonylisocyanide was added to a solution of 29 mg (0.09 mmol) of 5-(1-(2-chloro-6-(methylsulfanyl)pyridin-4-yl)vinyl)-1-methyl-1*H*-indole (**18**) in 2 mL of 1,2-dichloroethane and the mixture stirred 24 hours at room temperature under N_2. The mixture was poured onto ice and extracted with CH_2Cl_2. The organic layer was washed with brine until neutral pH, dried over anhydrous Na_2SO_4, filtered, evaporated to dryness, and subjected to preparative thin layer chromatography, yielding 12 mg (0.03 mmol; 31%) of 5-(1-(2-chloro-6-(methylsulfanyl)pyridin-4-yl)vinyl)-1-methyl-1*H*-indole-3-carboxylic acid (**27**) and 10 mg (0.03 mmol; 31%) of 5-(1-(2-chloro-6-(methylsulfanyl)pyridin-4-yl)vinyl)-1-methyl-1*H*-indole-3-carboxamide (**31**). ^{1}H NMR (200 MHz, $CDCl_3$): 2.55 (3H, *s*); 3.86 (3H, *s*); 5.56 (2H, *s*); 5.60 (1H, *s*); 5.62 (1H, *s*); 6.95 (1H, *d*, *J* = 1.2); 7.03 (1H, *d*, *J* = 1.2); 7.13 (1H, *dd*, *J* = 1.7; *J* = 8.6); 7.33 (1H, *bd*, *J* = 8.6); 7.68 (1H, *s*); 7.95 (1H, *d*, *J* = 1.7). ^{13}C NMR (50 MHz, $CDCl_3$): 13.5 (CH_3), 33.5 (CH_3), 110.0 (CH), 110.2 (C), 117.6 (CH), 118.5 (CH), 119.0 (CH), 120.4 (CH_2), 123.3 (CH), 125.9 (C), 133.3 (CH), 137.1 (C), 147.4 (C), 151.1 (C), 152.3 (C), 159.5 (C), 166.6 (C). IR: (film): 1519, 1574, 1651, 2925, 3342 cm^{-1}. HRMS ($C_{18}H_{16}ClN_3OS$): calculated (M+H$^+$) 358.0775, found 358.0780.

5-(1-(2,6-bis(methylsulfanyl)pyridin-4-yl)vinyl)-1-methyl-1*H*-indole-3-carboxamide (32)

29 ul (0.32 mmol) of chlorosulfonylisocyanide was added to a solution of 70 mg (0.21 mmol) of 5-(1-(2,6-bis(methylsulfanyl)pyridin-4-yl)vinyl)-1-methyl-1*H*-indole (**19**) in 2 mL of 1,2-dichloroethane and the mixture stirred 24 hours at room temperature under N_2. The mixture was poured onto ice and extracted with CH_2Cl_2. The organic layer was washed with brine until neutral pH, dried over anhydrous Na_2SO_4, filtered, evaporated to dryness, and chromatographed with 99:1 CH_2Cl_2/MeOH to yield 24 mg (0.06 mmol; 31%) of 5-(1-(2,6-bis(methylsulfanyl)pyridin-4-yl)vinyl)-1-methyl-1*H*-indole-3-carboxamide (**32**). ^{1}H NMR (200 MHz, $CDCl_3$): 2.51 (6H, *s*), 3.78 (3H, *s*), 5.50 (1H, *s*), 5.51 (1H, *s*), 5.66 (2H, *s*), 6.76 (2H, *s*), 7.08 (1H, *dd*, *J* = 1.6, *J* = 8.6), 7.24 (1H, *bd*, *J* = 8.6), 7.63 (1H, *s*), 7.86 (1H, *d*, *J* = 1.6). ^{13}C NMR (50 MHz, $CDCl_3$): 13.3 (2) (CH_3), 33.5 (CH_3), 110.0 (CH), 110.1 (C), 116.2 (2) (CH), 120.1 (CH_2), 123.4 (CH), 125.6 (CH), 133.6 (C), 133.8 (CH), 137.1 (C), 148.1 (C), 149.5 (C), 159.2 (2) (C), 166.7 (C). IR (film): 1462, 1519, 1573, 1651, 2924, 3341cm^{-1}. HRMS ($C_{19}H_{19}N_3OS_2$): calculated (M+H$^+$) 370.1042, found 370.1051.

(2,6-bis(methylsulfanyl)pyridin-4-yl)(4-(dimethylamino)phenyl)methanone (33)

Following procedure 1, 7.3 ml (11.6 mmol) of *n*BuLi 1.6 M in hexanes was slowly added to a solution of 2.32 g (11.6 mmol) of 4-bromo-*N,N*-dimethylaniline in dry THF at -40 ºC. After 45 minutes, 1 g (4.6 mmol) of 2,6-bis(methylsulfanyl)pyridine-4-carboxylic acid (**3**) in 10 mL of dry THF was added. The reaction product was flash chromatographed using 98/2 Hexane/EtOAc to yield 81 mg (0.18 mmol; 4%) of (2,6-bis(methylsulfanyl)pyridin-4-yl)bis(4-(dimethylamino)phenyl)methanol and 669 mg (2.1 mmol; 46%) of (2,6-bis(methylsulfanyl)pyridin-4-yl)(4-(dimethylamino)phenyl)methanone (**33**). M.p. (Hex/EtOAc): 103 - 105 ºC. ^{1}H NMR (200 MHz, $CDCl_3$): 2.61 (6H, *s*), 3.09 (6H, *s*), 6.67 (2H, *d*, *J* = 9.2), 7.04 (2H, *s*), 7.75 (2H, *d*, *J* = 9.2). ^{13}C NMR (50 MHz, $CDCl_3$): 13.3 (2) (CH_3), 40.1 (2) (CH_3), 110.7 (2) (CH), 115.6 (2) (CH), 123.4 (C), 132.6 (2) (CH), 146.5 (C), 153.7 (C), 159.8 (2) (C), 192.6 (C). IR (KBr): 1435, 1523, 1591, 1639 cm^{-1}. HRMS ($C_{16}H_{18}N_2OS_2$): calculated ($M+H^+$) 319.0933, found 319.1221. (2,6-bis(methylsulfanyl)pyridin-4-yl)bis(4-(dimethylamino)phenyl)methanol: ^{1}H NMR (200 MHz, $CDCl_3$): 2.55 (6H, *s*), 2.94 (12H, *s*), 6.66 (4H, *d*, *J* = 8.8), 6.91 (2H, *s*), 7.09 (4H, *d*, *J* = 8.8). ^{13}C NMR (50 MHz, $CDCl_3$): 13.2 (2) (CH_3), 40.4 (4) (CH_3), 80.7 (C), 111.7 (4) (CH), 115.9 (2) (CH), 128.6 (4) (CH), 133.6 (2) (C), 149.7 (2) (C), 156.5 (C), 158.6 (2) (C). IR (KBr): 1522, 1576, 1608, 2921, 3432 cm^{-1}. HRMS ($C_{24}H_{29}N_3OS_2$): calculated ($M+H^+$) 440.1825, found 440.1838.

4-(1-(2,6-bis(methylsulfanyl)pyridin-4-yl)vinyl)-*N*,*N*-dimethylaniline (34)

Following procedure 2, 1.5 ml (2.4 mmol) of *n*BuLi 1.6 M in hexanes was slowly added to a stirred suspension of 1.33 g (3.3 mmol) of methyltriphenylphosphonium iodide in 50 mL of dry THF at -40 ºC. After 45 minutes, 302 mg (0.95 mmol) of (2,6-bis(methylsulfanyl)pyridin-4-yl)(4-(dimethylamino)phenyl)methanone (**33**) was added. Flash chromatography with 97/3 Hexane/EtOAc yielded 118 mg (0.37 mmol; 39 %) of 4-(1-(2,6-bis(methylsulfanyl)pyridin-4-yl)vinyl)-*N*,*N*-dimethylaniline (**34**). ^{1}H NMR (200 MHz, $CDCl_3$): 2.59 (6H, *s*); 2.99 (6H, *s*); 5.31 (1H, *d*, *J* = 1.0); 5.45 (1H, *d*, *J* = 1.0); 6.69 (2H, *d*, *J* = 9.2); 6.86 (2H, *s*); 7.18 (2H, *d*, *J* = 9.2). ^{13}C NMR (50 MHz, $CDCl_3$): 13.2 (2) (CH_3), 40.4 (2) (CH_3), 111.7 (2) (CH), 113.5 (CH_2), 116.4 (2) (CH), 127.5 (C), 128.8 (2) (CH), 147.3 (C), 149.9 (C), 150.3 (C), 159.0 (2) (C). IR (film): 1519, 1572, 1606 cm^{-1}. HRMS ($C_{17}H_{20}N_2S_2$): calculated ($M+H^+$) 317.1141, found 317.1142.

(E/Z)-(2,6-bis(methylthio)pyridin-4-yl)(4-(dimethylamino)phenyl)methanone oximes (35).

Following procedure 3, 432 mg (6.22 mmol) of hydroxylamine hydrochloride was added onto a solution of 198 mg (0.62 mmol) of (2,6-bis(methylsulfanyl)pyridin-4-yl)(4-(dimethylamino)phenyl)methanone (**33**) in 20 mL of MeOH. The mixture of oximes was chromatographed with 9/1 Hexane/EtOAc to yield 141 mg (0.42 mmol; 69%) of the mixture of (E/Z)-(2,6-bis(methylthio)pyridin-4-yl)(4-(dimethylamino)phenyl)methanone oximes (**35**). Major isomer: ^{1}H NMR (200 MHz, $CDCl_3$): 2.59 (6H, *s*), 2.99 (6H, *s*), 6.62 (2H, *d*, *J* = 9.0), 6.83 (2H, *s*), 7.30 (2H, *d*, *J* = 9.0). ^{13}C NMR (50 MHz, $CDCl_3$): 13.2 (2) (CH_3), 40.2 (2) (CH_3), 111.7 (2) (CH), 116.4 (2) (CH), 128.4 (C), 128.4 (2) (CH), 137.8 (C), 151.3 (C), 155.7 (C), 159.6 (2) (C). IR (KBr): 1524, 1574, 1605, 3246, 3273 cm^{-1}. HRMS ($C_{16}H_{20}N_3OS_2$): calculated ($M+Na^+$) 356.0867, found 356.1157. Minor isomer: ^{1}H NMR (200 MHz, $CDCl_3$): 2.57 (6H, *s*), 3.02 (6H, *s*), 6.72 (2H, *d*, *J* = 8.9), 6.96 (2H, *s*), 7.36 (2H, *d*, *J* = 8.9). ^{13}C NMR (50 MHz, $CDCl_3$): 13.3 (2) (CH_3), 40.1 (2) (CH_3), 111.2 (2) (CH), 115.9 (2) (CH), 118.0 (C), 121.7 (C), 131.1 (2) (CH), 150.9 (C), 155.6 (C), 159.5 (2) (C).

(2,6-bis(methylsulfanyl)pyridin-4-yl)(3-(dimethylamino)phenyl)methanone (36)

Following procedure 1, 7.3 ml (11.6 mmol) of *n*BuLi 1.6 M in hexanes was slowly added to a solution of 1.29 ml (8.75 mmol) of 3-bromo-*N,N*-dimethylaniline in dry THF at -40 ºC. After 45 minutes, 754 mg (3.5 mmol) of 2,6-bis(methylsulfanyl)pyridine-4-carboxylic acid (**3**) in 10 mL of dry THF was added. The reaction product was flash chromatographed using 95/5 Hexane/EtOAc to yield 590 mg (1.85 mmol; 53%) of (2,6-bis(methylsulfanyl)pyridin-4-yl)(3-(dimethylamino)phenyl)methanone (**36**). M.p. (Hex/CH_2Cl_2): 114 – 116 ºC. ^{1}H NMR (200 MHz, $CDCl_3$): 2.61 (6H, *s*), 3.00 (6H, *s*), 6.96 (1H, *dd*, *J* = 1.7, *J* = 8.6), 7.02 (1H, *dd*, *J* = 7.6), 7.15 (2H, *s*), 7.16 (1H, *d*, *J* = 1.7), 7.31(1H, *t*, *J* = 7.9). ^{13}C NMR (50 MHz, $CDCl_3$): 13.3 (2) (CH_3), 40.5 (2) (CH_3), 112.6 (CH), 115.4 (2) (CH), 117.3 (CH), 118.7 (CH), 129.0 (CH), 136.6 (C), 144.9 (C), 150.4 (C), 160.1 (2) (C), 195.5 (C). IR (KBr): 1525, 1568, 1596, 1656 cm^{-1}. HRMS ($C_{16}H_{18}N_2OS_2$): calculated (M+H) 319.0939, found 319.0938.

3-(1-(2,6-bis(methylsulfanyl)pyridin-4-yl)vinyl)-*N*,*N*-dimethylaniline (37)

Following procedure 2, 1.22 ml (1.95 mmol) of *n*BuLi 1.6 M in hexanes was slowly added to a stirred suspension of 1.18 g (2.93 mmol) of methyltriphenylphosphonium iodide in 50 mL of dry THF at -40 ºC. After 45 minutes, 312 mg (0.98 mmol) of (2,6-bis(methylsulfanyl)pyridin-4-yl)(3-

(dimethylamino)phenyl)methanone (**36**) was added. Flash chromatography with 97/3 Hexane/EtOAc yielded 118 mg (0.37 mmol; 39 %) of 112 mg (0.35 mmol; 36 %) of 3-(1-(2,6-bis(methylsulfanyl)pyridin-4-yl)vinyl)-*N*,*N*-dimethylaniline (**37**). ^{1}H NMR (200 MHz, $CDCl_3$): 2.59 (6H, *s*), 2.94 (6H, *s*), 5.52 (1H, *d*, *J* = 1.2), 5.54 (1H, *d*, *J* = 1.2), 6.62 (1H, *dd*, *J* = 6.7), 6.64 (1H, *s*), 6.73 (1H, *dd*, *J* = 6.7), 6.85 (2H, *s*), 7.21 (1H, *t*, *J* = 8.1). ^{13}C NMR (50 MHz, $CDCl_3$): 13.4 (2) (CH_3), 40.7 (2) (CH_3), 112.4 (CH), 112.5 (CH), 116.3 (2) (CH), 116.5 (CH_2), 116.8 (CH), 129.1 (CH), 140.6 (C), 148.4 (C), 149.2 (C), 150.5 (C), 159.2 (2) (C). IR (film): 1517, 1571, 1596 cm^{-1}. HRMS ($C_{17}H_{20}N_2S_2$): calculated ($M+Na^+$) 339.0960, found 339.0959.

(*E/Z*)-(2,6-bis(methylsulfanyl)pyridin-4-yl)(3-(dimethylamino)phenyl)methanone oxime (38)

Following procedure 3, 465 mg (6.69 mmol) of hydroxylamine hydrochloride was added onto a solution of 213 mg (0.67 mmol) of (2,6-bis(methylsulfanyl)pyridin-4-yl)(3-(dimethylamino)phenyl)methanone (**36**) in 20 mL of MeOH. The mixture of oximes was chromatographed with 9/1 Hexane/EtOAc to yield 182 mg (0.55 mmol; 82%) of the mixture of (*E/Z*)-(2,6-bis(methylsulfanyl)pyridin-4-yl)(3-(dimethylamino)phenyl)methanone oximes (**38**). Major isomer: ^{1}H NMR (200 MHz, $CDCl_3$): 2.57 (6H, *s*), 2.96 (6H, *s*), 6.59 (1H, *m*), 6.61 (1H, *bd*, *J* = 8.2), 6.80 (1H, *bd*, *J* = 8.2), 6.98 (2H, *s*), 7.33 (1H, *t*, *J* = 8.2). ^{13}C NMR (50 MHz, $CDCl_3$): 13.4 (2) (CH_3), 40.5 (2) (CH_3), 112.3 (CH), 113.5 (CH), 115.1 (2) (CH), 116.6 (CH), 129.3 (CH), 131.7 (C), 143.7 (C), 150.4 (C), 156.9 (C), 159.6 (2) (C). IR (film): 1521, 1572, 1597, 2921, 3265 cm^{-1}. HRMS ($C_{16}H_{19}N_3OS_2$): calculated ($M+H^+$) 334.1042, found 334.1042. Minor isomer: ^{1}H NMR (200 MHz, $CDCl_3$): 2.59 (6H, *s*), 2.92 (6H, *s*), 6.61 (1H, *d*, *J* = 7.9), 6.63 (1H, *m*), 6.78 (1H, *bd*, *J* = 7.9), 6.87 (2H, *s*), 7.18 (1H, *t*, *J* = 7.9). ^{13}C NMR (50 MHz, $CDCl_3$): 13.4 (2) (CH_3), 40.7 (2) (CH_3), 111.2 (CH), 112.6 (CH), 114.5 (CH), 116.5 (2) (CH), 129.3 (CH), 135.2 (C), 141.0 (C), 150.5 (C), 156.2 (C), 159.7 (2) (C).

(2,6-bis(methylsulfanyl)pyridin-4-yl)(6-(dimethylamino)pyridin-3-yl)methanone (39)

7.3 ml (11.6 mmol) of *n*BuLi 1.6 M in hexanes was slowly added to a solution of 1.167 g (5.80 mmol) of 5-bromo-*N*,*N*-dimethylpyridin-2-amine in dry THF at -40 ºC and stirred for 1 hour. 215 mg (8,96 mmol) of NaH was added to a solution of 1 g (4.6 mmol) of 2,6-bis(methylsulfanyl)pyridine-4-carboxylic acid (**3**) in 10 mL of dry THF and stirred for 1 hour at 0

ºC. The first solution was slowly added onto the second and stirred for 24 hours. 2 mL of ethyl formate was added and the miture was poured onto 5% NH_4Cl and EtOAc. The mixture was partially evaporated and the organic layer was washed with 2N HCl, 5% $NaHCO_3$, and brine, dried over anhydrous Na_2SO_4, filtered and evaporated. The reaction product was flash chromatographed using 8/2 Hexane/EtOAc to yield 71 mg (0.16 mmol; 3%) of (2,6-bis(methylsulfanyl)pyridin-4-yl)bis(6-(dimethylamino)pyridin-3-yl)methanol and 97 mg (0.30 mmol; 5%) of (2,6-bis(methylsulfanyl)pyridin-4-yl)(6-(dimethylamino)pyridin-3-yl)methanone (**39**). ^{1}H NMR (200 MHz, $CDCl_3$): 2.61 (6H, *s*), 3.21 (6H, *s*), 6.55 (1H, *bd*, *J* = 9.2), 7.04 (2H, *s*), 7.98 (1H, *dd*, *J* = 2.2, *J* = 9.2), 8.57 (1H, *d*, *J* = 2.2). ^{13}C NMR (50 MHz, $CDCl_3$): 13.4 (2) (CH_3), 38.1 (2) (CH_3), 105.3 (CH), 115.5 (2) (CH), 119.9 (C), 138.3 (CH), 145.5 (C), 153.1 (CH), 160.2 (2) (C), 160.7 (C), 191.8 (C). IR (KBr): 1524, 1593, 1645 cm^{-1}. HRMS ($C_{15}H_{17}N_3OS_2$): calculated ($M+H^+$) 320.0886, found 320.0901. (2,6-bis(methylsulfanyl)pyridin-4-yl)bis(6-(dimethylamino)pyridin-3-yl)methanol: M.p. (Hex/CH_2Cl_2): 175 – 177 ºC. ^{1}H NMR (200 MHz, $CDCl_3$): 2.55 (6H, *s*), 3.09 (12H, *s*), 6.45 (2H, *bd*, *J* = 8.8), 6.86 (2H, *s*), 7.36 (2H, *dd*, *J* = 2.4, *J* = 8.8), 7,95 (2H, *d*, *J* = 2.4). ^{13}C NMR (50 MHz, $CDCl_3$): 13.3 (2) (CH_3), 38.2 (4) (CH_3), 78.2 (C), 105.5 (2) (CH), 115.6 (2) (CH), 128.1 (2) (C), 137.2 (2) (CH), 146.9 (2) (CH), 155.3 (C), 158.4 (2) (C), 159.2 (2) (C). IR (KBr): 1515, 1568, 1605, 2924 cm^{-1}. HRMS ($C_{22}H_{27}N_5OS_2$): calculated ($M+H^+$) 442.1730, found 442.1722.

(2,6-bis(methylsulfanyl)pyridin-4-yl)(naphthalen-2-yl)methanone (40)

Following procedure 1, 7.2 ml (11.5 mmol) of *n*BuLi 1.6 M in hexanes was slowly added to a solution of 2.41 g (11.5 mmol) of 2-bromonaphthalene in dry THF at -40 ºC. After 45 minutes, 1 g (4.6 mmol) of 2,6-bis(methylsulfanyl)pyridine-4-carboxylic acid (**3**) in 10 mL of dry THF was added. The reaction product was flash chromatographed using 95/5 Hexane/EtOAc to yield 709 mg (2.18 mmol; 47%) of (2,6-bis(methylsulfanyl)pyridin-4-yl)(naphthalen-2-yl)methanone (**40**). ^{1}H NMR (200 MHz, $CDCl_3$): 2.61 (6H, *s*), 7.17 (2H, *s*), 7.4 - 8.3 (7H, *m*). ^{13}C NMR (50 MHz, $CDCl_3$): 13.5 (2) (CH_3), 116.2 (2) (CH), 124.3 (CH), 125.5 (CH), 126.8 (CH), 128.0 (CH), 128.6 (CH), 129.5 (CH), 132.9 (CH), 130.8 (C), 133.8 (C), 134.1 (C), 145.1 (C), 160.8 (2) (C), 196.4 (C). IR (film): 1529, 1570, 1665 cm^{-1}.

2,6-bis(methylsulfanyl)-4-(1-(naphthalen-2-yl)vinyl)pyridine (41)

Following procedure 2, 1.91 ml (3.06 mmol) of *n*BuLi 1.6 M in hexanes was slowly added to a stirred suspension of 1.85 g (5.49 mmol) of methyltriphenylphosphonium iodide in 50 mL of dry THF at -40 ºC. After 45 minutes, 497 mg (1.53 mmol) of (2,6-bis(methylsulfanyl)pyridin-4-yl)(naphthalen-2-yl)methanone (**40**) was added. Flash chromatography with 97/3 Hexane/EtOAc yielded 118 mg (0.37 mmol; 39 %) of 293 mg (0.91 mmol; 59 %) of 2,6-bis(methylsulfanyl)-4-(1-(naphthalen-2-yl)vinyl)pyridine (**41**). ^{1}H NMR (200 MHz, $CDCl_3$): 2.56 (6H, s), 5.53 (1H, d, J = 1.1), 6.08 (1H, d, J = 1.1), 6.81 (2H, s), 7.2 – 7.7 (7H, *m*). ^{13}C NMR (50 MHz, $CDCl_3$): 13.4 (2) (CH_3), 114.7 (2) (CH), 120.0 (CH_2), 125.5 (CH), 126.1 (2) (CH), 126.4 (CH), 127.6 (CH), 128.5 (CH), 128.7 (CH), 131.6 (C), 133.8 (C), 138.0 (C), 146.2 (C), 148.5 (C), 159.6 (2) (C). IR (film): 1519, 1570 cm^{-1}. HRMS ($C_{19}H_{17}NS_2$): calculated ($M+H^+$) 324.0875, found 324.0893.

(*E/Z*)-(2,6-bis(methylsulfanyl)pyridin-4-yl)(naphthalen-2-yl)methanone oxime (42)

Following procedure 3, 199 mg (0.29 mmol) of hydroxylamine hydrochloride was added onto a solution of 93 mg (0.29 mmol) of (2,6-bis(methylsulfanyl)pyridin-4-yl)(naphthalen-2-yl)methanone (**40**) in 20 mL of MeOH. The mixture of oximes was chromatographed with 9/1 Hexane/EtOAc to yield 188 mg (0.26 mmol; 89%) of the mixture of (*E/Z*)-(2,6-bis(methylsulfanyl)pyridin-4-yl)(naphthalen-2-yl)methanone oxime (**43**). Major isomer: ^{1}H NMR (200 MHz, $CDCl_3$): 2.53 (6H, *s*), 6.95 (2H, *s*), 7.2 - 8.0 (7H, *m*). ^{13}C NMR (50 MHz, $CDCl_3$): 13.4 (2) (CH_3), 114.4 (2) (CH), 125.4 (2) (CH), 126.3 (CH), 126.5 (CH), 127.0 (CH), 127.3 (C),128.7 (CH), 129.8 (CH), 130.2 (C), 133.6 (C), 143.3 (C), 155.6 (C), 159.9 (2) (C). IR: (película): 1435, 1522, 1571, 3271, 3295 cm^{-1}. HRMS ($C_{18}H_{16}N_2OS_2$): calculated ($M+H^+$) 341.0777, found 341.0792. Minor isomer: ^{1}H NMR (200 MHz, $CDCl_3$): 2.55 (6H, *s*), 7.01 (2H, *s*), 7.4 – 8.0 (7H, *m*). ^{13}C NMR (50 MHz, $CDCl_3$): 13.4 (2) (CH_3), 114.4 (CH), 116.8 (CH), 125.4 (2) (CH), 126.5 (CH), 127.0 (CH), 128.5 (CH), 129.7 (CH), 130.2 (CH), 131.5 (C), 133.9 (C), 140.6 (C), 143.4 (C), 154.8 (C), 155.5 (C), 159.8 (2) (C).

(*Z*)-4-(4-methoxystyryl)-2,6-bis(methylsulfanyl)pyridine (43)

Following procedure 2, 0.25 ml (0.40 mmol) of *n*BuLi 1.6 M in hexanes was slowly added to a stirred suspension of 189 mg (0.36 mmol) of ((2,6-bis(methylthio)pyridin-4-yl)methyl)triphenylphosphonium bromide (**6**) in 50 mL of dry THF at -40 ºC. After 45 minutes, a

solution of 0.13 ml (1.10 mmol) of 4-methoxybenzaldehyde in 5 mL of dry THF was added over 30 minutes. Flash chromatography with 97/3 Hexane/EtOAc yielded 118 mg (0.37 mmol; 39 %) of 59 mg (0.19 mmol; 54%) of (*E*)-4-(4-methoxystyryl)-2,6-bis(methylsulfanyl)pyridine (**43*E***) and 19 mg (0.06 mmol; 17%) of (*Z*)-4-(4-methoxystyryl)-2,6-bis(methylsulfanyl)pyridine (**43**). ^{1}H NMR (200 MHz, $CDCl_3$): 2.49 (6H, *s*), 3.79 (3H, *s*), 6.25 (1H, *d*, *J* = 12), 6.65 (1H, *d*, *J* = 12), 6.73 (2H, *s*), 6.78 (2H, *d*, *J* = 8.2), 7.16 (2H, *d*, *J* = 8.2). ^{13}C NMR (50 MHz, $CDCl_3$): 13.3 (2) (CH_3), 55.3 (CH_3), 113.8 (2) (CH), 116.3 (2) (CH), 125.5 (CH), 128.4 (C), 130.3 (2) (CH), 132.8 (C), 133.6 (CH), 145.5 (C), 159.4 (2) (C). IR (KBr): 1512, 1566, 1604 cm^{-1}. HRMS ($C_{16}H_{17}NOS_2$): calculated ($M+H^+$) 304.0824, found 304.0823. (*E*)-4-(4-methoxystyryl)-2,6-bis(methylsulfanyl)pyridine (**43*E***): ^{1}H NMR (200 MHz, $CDCl_3$): 2.61 (6H, *s*), 3.84 (3H, *s*), 6.73 (1H, *d*, *J* = 16), 6.91 (2H, *d*, *J* = 8.6), 6.94 (2H, *s*), 7.18 (1H, *d*, *J* = 16), 7.45 (2H, *d*, *J* = 8.6). ^{13}C NMR (50 MHz, $CDCl_3$): 13.4 (2) (CH_3), 55.4 (CH_3), 114.0 (2) (CH), 114.3 (2) (CH), 123.3 (CH), 128.4 (2) (CH), 128.9 (C), 132.8 (C), 132.9 (CH), 159.4 (2) (C). Falta un C. IR (KBr): 1517, 1571, 1604, 1635 cm^{-1}. HRMS ($C_{16}H_{18}NOS_2$): calculated ($M+H^+$) 304.0830, found 304.0823.

(*Z*)-5-(2-(2,6-bis(methylsulfanyl)pyridin-4-yl)vinyl)-1-methyl-1*H*-indole (44)

Following procedure 2, 0.4 ml (0.64 mmol) of *n*BuLi 1.6 M in hexanes was slowly added to a stirred suspension of 139 mg (0.26 mmol) of ((2,6-bis(methylthio)pyridin-4-yl)methyl)triphenylphosphonium bromide (**6**) in 50 mL of dry THF at -40 ºC. After 45 minutes, a solution of 252 mg (1.58 mmol) of *N*-methyl-1*H*-indole-5-carbaldehyde in 5 mL of dry THF was added over 30 minutes. Flash chromatography with 98/2 Hexane/EtOAc yielded 22 mg (0.07 mmol; 26%) of (*E*)-5-(2-(2,6-bis(methylsulfanyl)pyridin-4-yl)vinyl)-1-methyl-1*H*-indole (**44*E***) and 12 mg (0.04 mmol; 14%) of (*Z*)-5-(2-(2,6-bis(methylsulfanyl)pyridin-4-yl)vinyl)-1-methyl-1*H*-indole (**44**). ^{1}H NMR (200 MHz, $CDCl_3$): 2.45 (6H, *s*), 3.77 (3H, *s*), 6.26 (1H, *d*, *J* = 12), 6.43 (1H, *d*, *J* = 3.2), 6.78 (2H, *s*), 6.86 (1H, *d*, *J* = 12), 7.03 (1H, *d*, *J* = 3.2), 7.12 (1H, *bd*, *J* = 8.6), 7.12 (1H, *bd*, *J* = 8.6), 7.52 (1H, *s*). ^{13}C NMR (50 MHz, $CDCl_3$): 13.4 (2) (CH_3),33.1 (CH_3), 101.7 (CH), 109.7 (CH), 114.0 (2) (CH), 120.5 (CH), 120.8 (CH), 122.5 (CH), 124.7 (C), 127.8 (C), 128.8 (C), 129.8 (CH), 134.9 (CH), 145.5 (C), 159.3 (2) (C). IR (film): 1521, 1571, 1608, 1626 cm^{-1}. HRMS ($C_{18}H_{18}N_2S_2$): calculated ($M+H^+$) 327.0984, found 327.1001.

4.1.3. Determination of Aqueous Solubility.

The aqueous solubility was determined by the shaking-flask method. Roughly 2 mg of the compound was shaken in 0.3 mL of pH 7.0 phosphate buffer for 72 h at room temperature. The saturated supernatant was passed through a 45 µm filter and the absorbance of the filtrate measured at the maximum UV absorbance wavelength for every compound in a Helios Alfa Spectrophotometer. The aqueous solubility was calculated by comparison with a calibration curve.

4.2. Biology

4.2.1. Inhibition of tubulin polymerization.

Bovine brain tubulin was isolated as previously described.[35] Tubulin polymerization assays were carried out with 1.5 mg/mL protein at pH 6.7 in assay buffer containing 0.1 M MES buffer, 1.5 mM GTP, 1 mM EGTA, 1 mM β-ME, 1 mM $MgCl_2$, and the required ligand concentration. Samples were incubated 30 min at 20 °C, followed by cooling on ice for 10 min. Tubulin polymerization was assessed by the UV absorbance increase at 450 nm due to the turbidity caused by a temperature shift from 4 ºC to 37 ºC. When a stable plateau was reached and maintained for at least 20 minutes, the temperature was switched back to 4 ºC to ascertain the return to the initial absorption values, to confirm the reversibility of the process. The degree of tubulin assembly for each experiment was calculated as the difference in amplitude between the stable plateau and the initial baseline of the curves. Control experiments in identical conditions but the absence of ligand were taken as 100% tubulin polymerization. In a first screening, all the compounds were assayed at 5 µM in at least two independent measurements. For those compounds with TPI values higher than 40% on average, the IC_{50} values of tubulin polymerization were determined by measuring the tubulin polymerization inhibitory activity at different ligand concentrations. The obtained values of the mole ratio of total ligand to total tubulin in solution were fitted to mono-exponential curves and the IC_{50} values of tubulin polymerization inhibition calculated from the best-fitting curves.

4.2.2. Cell culture.

HL-60 (human acute myeloid leukemia) and HT-29 (human colon carcinoma) cell lines were grown at 37 °C in humidified 95% air and 5% CO_2 in RPMI-1640 culture medium containing 10% (v/v) heat-inactivated fetal bovine serum (FBS), 100 U/mL penicillin, 100 µg/mL streptomycin, and 2 mM L-glutamine. HeLa (human cervical carcinoma) cell line was grown at 37 °C in humidified 95% air and 5% CO_2 in DMEM culture medium containing 10% (v/v) heat-inactivated fetal bovine serum (FBS), 2 mM L-glutamine, 100 U/mL penicillin, and 100 µg/mL streptomycin. Cells were periodically tested for *Mycoplasma* infection and found to be negative.

4.2.3. Cell Growth Inhibition Assay.

The effect of the compounds on the proliferation of human tumor cell lines (cytostatic activity) was determined using the XTT (sodium 3′-[1-(phenylaminocarbonyl)-3,4-tetrazolium]-bis(4-methoxy-6-nitro)-benzenesulfonic acid hydrate) cell proliferation kit (Roche Molecular Biochemicals, Mannheim, Germany) according to the manufacturer's instructions as previously described.[51] Cells (5×10^3 HL-60, 1.5×10^3 HeLa, or 3×10^3 HT-29 in 100 µL) were incubated for 72 h in 96-well flat-bottomed microtiter plates at 37 °C in a humidified atmosphere of air/CO_2 (19/1) in culture medium containing 10% heat-inactivated FBS in the absence (control) and the presence of the indicated compounds at concentrations ranging from 10^{-5} to 10^{-13} M. After incubation, the XTT assay was performed. Each experiment was repeated three times and measurements were performed in triplicate. The IC_{50} (50% inhibitory concentration) value, defined as the drug concentration required to cause 50% inhibition in cellular proliferation with respect to the untreated controls, was determined for each compound by nonlinear curve fitting of the experimental data.

4.2.4. Cell Cycle Analysis.

For cell cycle analyses, untreated and drug-treated cells ($2-4 \times 10^5$) were centrifuged and fixed overnight in 70% ethanol at 4 °C. Then cells were washed three times with PBS, incubated for 1 h with 1 mg/mL RNase A and 20 µg/mL propidium iodide at room temperature, and analyzed with a Becton Dickinson fluorescence-activated cell sorter (FACSCalibur) flow cytometer (San Jose, CA) as previously described.[58, 59] Quantification of apoptotic cells was calculated as the percentage of cells in the sub-G_0/G_1 region in cell cycle analysis.[58, 59]

4.2.5. Confocal Microscopy.

HeLa cells were grown on 0.01% poly-L-lysine coated coverslips, and after drug treatment, the coverslips were washed three times with HPEM buffer (25 mM HEPES, 60 mM PIPES, 10 mM EGTA, 3 mM $MgCl_2$, pH 6.6), fixed with 4% formaldehyde in HPEM buffer for 20 min, and permeabilized with 0.5% Triton X-100 as previously described.[53] Coverslips were incubated with a specific Ab-1 anti-α-tubulin mouse monoclonal antibody (diluted 1:150 in PBS) (Calbiochem, San Diego, CA) for 1 h, washed four times with PBS, and then incubated with CY3-conjugated sheep anti-mouse IgG (diluted 1:100 in PBS) (Jackson ImmunoResearch, West Grove, PA) for 1 h at 4 °C. After four washes with PBS, a drop of SlowFade light antifading reagent (Molecular Probes, Eugene, OR), with DAPI (Sigma, St. Louis, MO) to stain cell nuclei, was added to preserve fluorescence. The samples were analyzed by confocal microscopy using a ZeissLSM 310 laser scan confocal microscope. Negative controls, lacking the primary antibody or using an irrelevant antibody, showed no staining.

4.2.6.Western Blot Analysis.

About 5×10^6 cells were pelleted by centrifugation, washed with PBS, lysed, and subjected to Western blot analysis as described previously.[58] Proteins (15 µg) were separated through 8% sodium dodecyl sulfate-polyacrylamide gels under reducing conditions, transferred to nitrocellulose filters, blocked with 5% nonfat dry milk, and incubated overnight with the

corresponding antibodies (anti-mitotic proteins mouse monoclonal antibody MPM-2, Abcam; C2.10 anti-PARP mouse monoclonal antibody, Cell Signaling). Signals were developed using an enhanced chemiluminescence (ECL) detection kit (Amersham). Immunoblotting with the mouse monoclonal anti-β-actin antibody AC15 (Sigma) was used as an internal loading control, revealing equivalent amounts of protein in each lane of the gel.

4.3. Computational studies

4.3.1. Chemical Structure.

Calculations were performed consecutively using the Spartan 08 software package at the molecular mechanics (MMFF94s), semiempirical (AM1), and B3LYP 6-31+G* DFT levels. Conformational analyses were performed by systematically rotating the bonds between the rings in 18° steps with AM1 and the substituents on the pyridine ring were subjected to final unrestrained energy minimization until convergence at the B3LYP/6-31+G* DFT level of theory.

4.3.2. Docking Experiments.

The coordinates of the tubulin – colchicine site ligands complexes available were retrieved from the pdb [60] and chains C−E were removed. Five representative structures selected from previous studies of energy minimization and molecular dynamics simulations at 300 K on 1SA1.pdb using AMBER14[61], initially with a restrained backbone and later 200 ns unrestrained were also used.[54] The ligands were built with Spartan 08[62] and prepared with AutodockTools. Docking experiments were run with PLANTS[55] using default settings and 10 runs per ligand and AutoDock 4.2 [56, 63], by running the Lamarckian genetic algorithm (LGA) 100−300 times with a maximum of 2.5×10^6 energy evaluations, 150 individuals in the population, and a maximum of 27000 generations. The occupancy of the colchicine site sub-pockets by the obtained binding poses was automatically determined, and the results tabulated using in-house KNIME pipelines. The binding energies were converted to *z*-scores and used for

comparison across programs. The results were analyzed with Chimera,[64] AutoDockTools,[56, 63] Marvin,[65] OpenEye[66] and with JADOPPT.[67] The selection of the docking poses was done by searching for automatically determined similar docking poses coming from the two docking programs and scored in the two first quartiles and by comparing them to the alternative binding modes based on the combined *z* scoring.

ACKNOWLEDGMENTS

We thank the people at Frigoríficos Salamanca S.A. slaughterhouse for providing us with the calf brains and “Servicio General de NMR” and “Servicio General de Espectrometría de Masas” of the Universidad de Salamanca for equipment. L.A. acknowledges a predoctoral fellowship from the Junta de Castilla y León. A.V.B acknowledges a predoctoral fellowship from the Spanish Ministerio de Educación, Cultura y Deporte (FPU15/02457).

FUNDING SOURCES

This work was supported by the Consejería de Educación de la Junta de Castilla y León (SA030U16 and SA262P18), co-funded by the EU's European Regional Development Fund-FEDER, and the Spanish Ministry of Science, Innovation, and Universities (RTI2018-099474-B-I00 and SAF2017-89672-R).

REFERENCES

[1] C. Dumontet, M.A. Jordan, Microtubule-binding agents: a dynamic field of cancer therapeutics, Nature reviews. Drug discovery, 9 (2010) 790-803. D.O.I.:10.1038/nrd3253

[2] A. Vicente-Blazquez, M. Gonzalez, R. Alvarez, S. Del Mazo, M. Medarde, R. Pelaez, Antitubulin sulfonamides: The successful combination of an established drug class and a multifaceted target, Medicinal research reviews, (2018). D.O.I.:10.1002/med.21541

[3] R. Gaspari, A.E. Prota, K. Bargsten, A. Cavalli, M.O. Steinmetz, Structural Basis of cis- and trans-Combretastatin Binding to Tubulin, Chem, 2 (2017) 102-113. D.O.I.:https://doi.org/10.1016/j.chempr.2016.12.005

[4] F. Mollinedo, C. Gajate, Microtubules, microtubule-interfering agents and apoptosis, Apoptosis : an international journal on programmed cell death, 8 (2003) 413-450.

[5] M.J. Perez-Perez, E.M. Priego, O. Bueno, M.S. Martins, M.D. Canela, S. Liekens, Blocking Blood Flow to Solid Tumors by Destabilizing Tubulin: An Approach to Targeting Tumor Growth, Journal of medicinal chemistry, 59 (2016) 8685-8711. D.O.I.:10.1021/acs.jmedchem.6b00463
[6] E.M. Agency, European Medicines Agency, in, 2020.
[7] W. Liang, Y. Ni, F. Chen, Tumor resistance to vascular disrupting agents: mechanisms, imaging, and solutions, Oncotarget, 7 (2016) 15444-15459. D.O.I.:10.18632/oncotarget.6999
[8] G.M. Tozer, C. Kanthou, G. Lewis, V.E. Prise, B. Vojnovic, S.A. Hill, Tumour vascular disrupting agents: combating treatment resistance, The British journal of radiology, 81 Spec No 1 (2008) S12-20. D.O.I.:10.1259/bjr/36205483
[9] L.M. Greene, M.J. Meegan, D.M. Zisterer, Combretastatins: more than just vascular targeting agents?, The Journal of pharmacology and experimental therapeutics, 355 (2015) 212-227. D.O.I.:10.1124/jpet.115.226225
[10] R. Kaur, G. Kaur, R.K. Gill, R. Soni, J. Bariwal, Recent developments in tubulin polymerization inhibitors: An overview, European journal of medicinal chemistry, 87 (2014) 89-124. D.O.I.:10.1016/j.ejmech.2014.09.051
[11] Y. Lu, J. Chen, M. Xiao, W. Li, D.D. Miller, An overview of tubulin inhibitors that interact with the colchicine binding site, Pharmaceutical research, 29 (2012) 2943-2971. D.O.I.:10.1007/s11095-012-0828-z
[12] L.M. Greene, N.M. O'Boyle, D.P. Nolan, M.J. Meegan, D.M. Zisterer, The vascular targeting agent Combretastatin-A4 directly induces autophagy in adenocarcinoma-derived colon cancer cells, Biochemical pharmacology, 84 (2012) 612-624. D.O.I.:10.1016/j.bcp.2012.06.005
[13] M.A. Soussi, S. Aprile, S. Messaoudi, O. Provot, E. Del Grosso, J. Bignon, J. Dubois, J.D. Brion, G. Grosa, M. Alami, The metabolic fate of isocombretastatin A-4 in human liver microsomes: identification, synthesis and biological evaluation of metabolites, ChemMedChem, 6 (2011) 1781-1788. D.O.I.:10.1002/cmdc.201100193
[14] S. Aprile, E. Del Grosso, G.C. Tron, G. Grosa, In vitro metabolism study of combretastatin A-4 in rat and human liver microsomes, Drug metabolism and disposition: the biological fate of chemicals, 35 (2007) 2252-2261. D.O.I.:10.1124/dmd.107.016998
[15] G.C. Tron, T. Pirali, G. Sorba, F. Pagliai, S. Busacca, A.A. Genazzani, Medicinal chemistry of combretastatin A4: present and future directions, Journal of medicinal chemistry, 49 (2006) 3033-3044. D.O.I.:10.1021/jm0512903
[16] Z.S. Seddigi, M.S. Malik, A.P. Saraswati, S.A. Ahmed, A.O. Babalghith, H.A. Lamfon, A. Kamal, Recent advances in combretastatin based derivatives and prodrugs as antimitotic agents, MedChemComm, 8 (2017) 1592-1603. D.O.I.:10.1039/c7md00227k
[17] A.M. Malebari, L.M. Greene, S.M. Nathwani, D. Fayne, N.M. O'Boyle, S. Wang, B. Twamley, D.M. Zisterer, M.J. Meegan, beta-Lactam analogues of combretastatin A-4 prevent metabolic inactivation by glucuronidation in chemoresistant HT-29 colon cancer cells, European journal of medicinal chemistry, 130 (2017) 261-285. D.O.I.:10.1016/j.ejmech.2017.02.049
[18] D. Simoni, G. Grisolia, G. Giannini, M. Roberti, R. Rondanin, L. Piccagli, R. Baruchello, M. Rossi, R. Romagnoli, F.P. Invidiata, S. Grimaudo, M.K. Jung, E. Hamel, N. Gebbia, L. Crosta, V. Abbadessa, A. Di Cristina, L. Dusonchet, M. Meli, M. Tolomeo, Heterocyclic and phenyl double-bond-locked combretastatin analogues possessing potent apoptosis-inducing activity in HL60 and in MDR cell lines, Journal of medicinal chemistry, 48 (2005) 723-736. D.O.I.:10.1021/jm049622b
[19] W. Li, H. Sun, S. Xu, Z. Zhu, J. Xu, Tubulin inhibitors targeting the colchicine binding site: a perspective of privileged structures, Future medicinal chemistry, 9 (2017) 1765-1794. D.O.I.:10.4155/fmc-2017-0100
[20] A. Vicente-Blazquez, M. Gonzalez, R. Alvarez, S. Del Mazo, M. Medarde, R. Pelaez, Antitubulin sulfonamides: The successful combination of an established drug class and a multifaceted target, Medicinal research reviews, 39 (2019) 775-830. D.O.I.:10.1002/med.21541
[21] M. Borowiak, W. Nahaboo, M. Reynders, K. Nekolla, P. Jalinot, J. Hasserodt, M. Rehberg, M. Delattre, S. Zahler, A. Vollmar, D. Trauner, O. Thorn-Seshold, Photoswitchable Inhibitors of Microtubule

Dynamics Optically Control Mitosis and Cell Death, Cell, 162 (2015) 403-411. D.O.I.:10.1016/j.cell.2015.06.049
[22] G.R. Pettit, B. Toki, D.L. Herald, P. Verdier-Pinard, M.R. Boyd, E. Hamel, R.K. Pettit, Antineoplastic agents. 379. Synthesis of phenstatin phosphate, Journal of medicinal chemistry, 41 (1998) 1688-1695. D.O.I.:10.1021/jm970644q
[23] C. Alvarez, R. Alvarez, P. Corchete, C. Perez-Melero, R. Pelaez, M. Medarde, Exploring the effect of 2,3,4-trimethoxy-phenyl moiety as a component of indolephenstatins, European journal of medicinal chemistry, 45 (2010) 588-597. D.O.I.:10.1016/j.ejmech.2009.10.047
[24] N. Sirisoma, A. Pervin, H. Zhang, S. Jiang, J.A. Willardsen, M.B. Anderson, G. Mather, C.M. Pleiman, S. Kasibhatla, B. Tseng, J. Drewe, S.X. Cai, Discovery of N-(4-methoxyphenyl)-N,2-dimethylquinazolin-4-amine, a potent apoptosis inducer and efficacious anticancer agent with high blood brain barrier penetration, Journal of medicinal chemistry, 52 (2009) 2341-2351. D.O.I.:10.1021/jm801315b
[25] I. Khelifi, T. Naret, A. Hamze, J. Bignon, H. Levaique, M.C. Garcia Alvarez, J. Dubois, O. Provot, M. Alami, N,N-bis-heteroaryl methylamines: Potent anti-mitotic and highly cytotoxic agents, European journal of medicinal chemistry, 168 (2019) 176-188. D.O.I.:10.1016/j.ejmech.2019.02.038
[26] S. Messaoudi, A. Hamze, O. Provot, B. Treguier, J. Rodrigo De Losada, J. Bignon, J.M. Liu, J. Wdzieczak-Bakala, S. Thoret, J. Dubois, J.D. Brion, M. Alami, Discovery of isoerianin analogues as promising anticancer agents, ChemMedChem, 6 (2011) 488-497. D.O.I.:10.1002/cmdc.201000456
[27] R. Alvarez, C. Alvarez, F. Mollinedo, B.G. Sierra, M. Medarde, R. Pelaez, Isocombretastatins A: 1,1-diarylethenes as potent inhibitors of tubulin polymerization and cytotoxic compounds, Bioorganic & medicinal chemistry, 17 (2009) 6422-6431. D.O.I.:10.1016/j.bmc.2009.07.012
[28] S. Messaoudi, B. Treguier, A. Hamze, O. Provot, J.F. Peyrat, J.R. De Losada, J.M. Liu, J. Bignon, J. Wdzieczak-Bakala, S. Thoret, J. Dubois, J.D. Brion, M. Alami, Isocombretastatins a versus combretastatins a: the forgotten isoCA-4 isomer as a highly promising cytotoxic and antitubulin agent, Journal of medicinal chemistry, 52 (2009) 4538-4542. D.O.I.:10.1021/jm900321u
[29] A. Hamze, M. Alami, O. Provot, Developments of isoCombretastatin A-4 derivatives as highly cytotoxic agents, European journal of medicinal chemistry, 190 (2020) 112110. D.O.I.:10.1016/j.ejmech.2020.112110
[30] L.M. Greene, S. Wang, N.M. O'Boyle, S.A. Bright, J.E. Reid, P. Kelly, M.J. Meegan, D.M. Zisterer, Combretazet-3 a novel synthetic cis-stable combretastatin A-4-azetidinone hybrid with enhanced stability and therapeutic efficacy in colon cancer, Oncology reports, 29 (2013) 2451-2458. D.O.I.:10.3892/or.2013.2379
[31] K. Ohsumi, R. Nakagawa, Y. Fukuda, T. Hatanaka, Y. Morinaga, Y. Nihei, K. Ohishi, Y. Suga, Y. Akiyama, T. Tsuji, Novel combretastatin analogues effective against murine solid tumors: design and structure-activity relationships, Journal of medicinal chemistry, 41 (1998) 3022-3032. D.O.I.:10.1021/jm980101w
[32] M. Gonzalez, Y. Ellahioui, R. Alvarez, L. Gallego-Yerga, E. Caballero, A. Vicente-Blazquez, L. Ramudo, M. Marin, C. Sanz, M. Medarde, R. Pelaez, The Masked Polar Group Incorporation (MPGI) Strategy in Drug Design: Effects of Nitrogen Substitutions on Combretastatin and Isocombretastatin Tubulin Inhibitors, Molecules, 24 (2019). D.O.I.:10.3390/molecules24234319
[33] M. Lawson, A. Hamze, J.F. Peyrat, J. Bignon, J. Dubois, J.D. Brion, M. Alami, An efficient coupling of N-tosylhydrazones with 2-halopyridines: synthesis of 2-alpha-styrylpyridines endowed with antitumor activity, Organic & biomolecular chemistry, 11 (2013) 3664-3673. D.O.I.:10.1039/c3ob40263k
[34] R. Alvarez, C. Gajate, P. Puebla, F. Mollinedo, M. Medarde, R. Pelaez, Substitution at the indole 3 position yields highly potent indolecombretastatins against human tumor cells, European journal of medicinal chemistry, 158 (2018) 167-183. D.O.I.:10.1016/j.ejmech.2018.08.078
[35] R. Alvarez, P. Puebla, J.F. Diaz, A.C. Bento, R. Garcia-Navas, J. de la Iglesia-Vicente, F. Mollinedo, J.M. Andreu, M. Medarde, R. Pelaez, Endowing indole-based tubulin inhibitors with an anchor for derivatization: highly potent 3-substituted indolephenstatins and indoleisocombretastatins, Journal of medicinal chemistry, 56 (2013) 2813-2827. D.O.I.:10.1021/jm3015603

Formatted: Highlight

[36] C. Jimenez, Y. Ellahioui, R. Alvarez, L. Aramburu, A. Riesco, M. Gonzalez, A. Vicente, A. Dahdouh, A. Ibn Mansour, C. Jimenez, D. Martin, R.G. Sarmiento, M. Medarde, E. Caballero, R. Pelaez, Exploring the size adaptability of the B ring binding zone of the colchicine site of tubulin with para-nitrogen substituted isocombretastatins, European journal of medicinal chemistry, 100 (2015) 210-222. D.O.I.:10.1016/j.ejmech.2015.05.047
[37] I. Khelifi, T. Naret, D. Renko, A. Hamze, G. Bernadat, J. Bignon, C. Lenoir, J. Dubois, J.D. Brion, O. Provot, M. Alami, Design, synthesis and anticancer properties of IsoCombretaQuinolines as potent tubulin assembly inhibitors, European journal of medicinal chemistry, 127 (2017) 1025-1034. D.O.I.:10.1016/j.ejmech.2016.11.012
[38] W. Li, F. Xu, W. Shuai, H. Sun, H. Yao, C. Ma, S. Xu, H. Yao, Z. Zhu, D.H. Yang, Z.S. Chen, J. Xu, Discovery of Novel Quinoline-Chalcone Derivatives as Potent Antitumor Agents with Microtubule Polymerization Inhibitory Activity, Journal of medicinal chemistry, 62 (2019) 993-1013. D.O.I.:10.1021/acs.jmedchem.8b01755
[39] M.A. Soussi, O. Provot, G. Bernadat, J. Bignon, D. Desravines, J. Dubois, J.D. Brion, S. Messaoudi, M. Alami, IsoCombretaQuinazolines: Potent Cytotoxic Agents with Antitubulin Activity, ChemMedChem, 10 (2015) 1392-1402. D.O.I.:10.1002/cmdc.201500069
[40] T. Naret, I. Khelifi, O. Provot, J. Bignon, H. Levaique, J. Dubois, M. Souce, A. Kasselouri, A. Deroussent, A. Paci, P.F. Varela, B. Gigant, M. Alami, A. Hamze, 1,1-Diheterocyclic Ethylenes Derived from Quinaldine and Carbazole as New Tubulin-Polymerization Inhibitors: Synthesis, Metabolism, and Biological Evaluation, Journal of medicinal chemistry, 62 (2019) 1902-1916. D.O.I.:10.1021/acs.jmedchem.8b01386
[41] S. Banerjee, K.E. Arnst, Y. Wang, G. Kumar, S. Deng, L. Yang, G.B. Li, J. Yang, S.W. White, W. Li, D.D. Miller, Heterocyclic-Fused Pyrimidines as Novel Tubulin Polymerization Inhibitors Targeting the Colchicine Binding Site: Structural Basis and Antitumor Efficacy, Journal of medicinal chemistry, 61 (2018) 1704-1718. D.O.I.:10.1021/acs.jmedchem.7b01858
[42] T.J. Ritchie, S.J. Macdonald, R.J. Young, S.D. Pickett, The impact of aromatic ring count on compound developability: further insights by examining carbo- and hetero-aromatic and -aliphatic ring types, Drug discovery today, 16 (2011) 164-171. D.O.I.:10.1016/j.drudis.2010.11.014
[43] T.J. Ritchie, S.J. Macdonald, The impact of aromatic ring count on compound developability--are too many aromatic rings a liability in drug design?, Drug discovery today, 14 (2009) 1011-1020. D.O.I.:10.1016/j.drudis.2009.07.014
[44] F. Xu, W. Li, W. Shuai, L. Yang, Y. Bi, C. Ma, H. Yao, S. Xu, Z. Zhu, J. Xu, Design, synthesis and biological evaluation of pyridine-chalcone derivatives as novel microtubule-destabilizing agents, European journal of medicinal chemistry, 173 (2019) 1-14. D.O.I.:10.1016/j.ejmech.2019.04.008
[45] W. Shuai, X. Li, W. Li, F. Xu, L. Lu, H. Yao, L. Yang, H. Zhu, S. Xu, Z. Zhu, J. Xu, Design, synthesis and anticancer properties of isocombretapyridines as potent colchicine binding site inhibitors, European journal of medicinal chemistry, 197 (2020) 112308. D.O.I.:10.1016/j.ejmech.2020.112308
[46] R. Alvarez, L. Aramburu, C. Gajate, A. Vicente-Blazquez, F. Mollinedo, M. Medarde, R. Pelaez, Potent colchicine-site ligands with improved intrinsic solubility by replacement of the 3,4,5-trimethoxyphenyl ring with a 2-methylsulfanyl-6-methoxypyridine ring, Bioorganic chemistry, 98 (2020) 103755. D.O.I.:10.1016/j.bioorg.2020.103755
[47] R. Schobert, K. Effenberger-Neidnicht, B. Biersack, Stable combretastatin A-4 analogues with sub-nanomolar efficacy against chemoresistant HT-29 cells, International journal of clinical pharmacology and therapeutics, 49 (2011) 71-72.
[48] K.E. Henegar, S.W. Ashford, T.A. Baughman, J.C. Sih, R.-L. Gu, Practical Asymmetric Synthesis of (S)-4-Ethyl-7,8-dihydro-4-hydroxy-1H-pyrano[3,4-f]indolizine- 3,6,10(4H)-trione, a Key Intermediate for the Synthesis of Irinotecan and Other Camptothecin Analogs, The Journal of organic chemistry, 62 (1997) 6588-6597. D.O.I.:10.1021/jo970173f
[49] J. Fernandes, C.R. Gattass, Topological polar surface area defines substrate transport by multidrug resistance associated protein 1 (MRP1/ABCC1), Journal of medicinal chemistry, 52 (2009) 1214-1218. D.O.I.:10.1021/jm801389m

[50] J. Chen, Z. Wang, C.M. Li, Y. Lu, P.K. Vaddady, B. Meibohm, J.T. Dalton, D.D. Miller, W. Li, Discovery of novel 2-aryl-4-benzoyl-imidazoles targeting the colchicines binding site in tubulin as potential anticancer agents, Journal of medicinal chemistry, 53 (2010) 7414-7427. D.O.I.:10.1021/jm100884b
[51] M.H. David-Cordonnier, C. Gajate, O. Olmea, W. Laine, J. de la Iglesia-Vicente, C. Perez, C. Cuevas, G. Otero, I. Manzanares, C. Bailly, F. Mollinedo, DNA and non-DNA targets in the mechanism of action of the antitumor drug trabectedin, Chemistry & biology, 12 (2005) 1201-1210. D.O.I.:10.1016/j.chembiol.2005.08.009
[52] C. Alvarez, R. Alvarez, P. Corchete, J.L. Lopez, C. Perez-Melero, R. Pelaez, M. Medarde, Diarylmethyloxime and hydrazone derivatives with 5-indolyl moieties as potent inhibitors of tubulin polymerization, Bioorganic & medicinal chemistry, 16 (2008) 5952-5961. D.O.I.:10.1016/j.bmc.2008.04.054
[53] A.B. Maya, C. Perez-Melero, C. Mateo, D. Alonso, J.L. Fernandez, C. Gajate, F. Mollinedo, R. Pelaez, E. Caballero, M. Medarde, Further naphthylcombretastatins. An investigation on the role of the naphthalene moiety, Journal of medicinal chemistry, 48 (2005) 556-568. D.O.I.:10.1021/jm0310737
[54] R. Alvarez, M. Medarde, R. Pelaez, New ligands of the tubulin colchicine site based on X-ray structures, Current topics in medicinal chemistry, 14 (2014) 2231-2252.
[55] O. Korb, T. Stutzle, T.E. Exner, Empirical scoring functions for advanced protein-ligand docking with PLANTS, Journal of chemical information and modeling, 49 (2009) 84-96. D.O.I.:10.1021/ci800298z
[56] S. Forli, R. Huey, M.E. Pique, M.F. Sanner, D.S. Goodsell, A.J. Olson, Computational protein-ligand docking and virtual drug screening with the AutoDock suite, Nature protocols, 11 (2016) 905-919. D.O.I.:10.1038/nprot.2016.051
[57] A. Massarotti, A. Coluccia, R. Silvestri, G. Sorba, A. Brancale, The tubulin colchicine domain: a molecular modeling perspective, ChemMedChem, 7 (2012) 33-42. D.O.I.:10.1002/cmdc.201100361
[58] C. Gajate, A.M. Santos-Beneit, A. Macho, M. Lazaro, A. Hernandez-De Rojas, M. Modolell, E. Munoz, F. Mollinedo, Involvement of mitochondria and caspase-3 in ET-18-OCH(3)-induced apoptosis of human leukemic cells, International journal of cancer, 86 (2000) 208-218.
[59] C. Gajate, I. Barasoain, J.M. Andreu, F. Mollinedo, Induction of apoptosis in leukemic cells by the reversible microtubule-disrupting agent 2-methoxy-5-(2',3',4'-trimethoxyphenyl)-2,4,6-cycloheptatrien-1-one: protection by Bcl-2 and Bcl-X(L) and cell cycle arrest, Cancer research, 60 (2000) 2651-2659.
[60] S. Aprile, E. Del Grosso, G. Grosa, Identification of the human UDP-glucuronosyltransferases involved in the glucuronidation of combretastatin A-4, Drug metabolism and disposition: the biological fate of chemicals, 38 (2010) 1141-1146. D.O.I.:10.1124/dmd.109.031435
[61] D.A. Case, T.E. Cheatham, 3rd, T. Darden, H. Gohlke, R. Luo, K.M. Merz, Jr., A. Onufriev, C. Simmerling, B. Wang, R.J. Woods, The Amber biomolecular simulation programs, Journal of computational chemistry, 26 (2005) 1668-1688. D.O.I.:10.1002/jcc.20290
[62] I. WAVEFUNCTION, Spartan08, in, 2008.
[63] G.M. Morris, R. Huey, W. Lindstrom, M.F. Sanner, R.K. Belew, D.S. Goodsell, A.J. Olson, AutoDock4 and AutoDockTools4: Automated docking with selective receptor flexibility, Journal of computational chemistry, 30 (2009) 2785-2791. D.O.I.:10.1002/jcc.21256
[64] E.F. Pettersen, T.D. Goddard, C.C. Huang, G.S. Couch, D.M. Greenblatt, E.C. Meng, T.E. Ferrin, UCSF Chimera--a visualization system for exploratory research and analysis, Journal of computational chemistry, 25 (2004) 1605-1612. D.O.I.:10.1002/jcc.20084
[65] Marvin 17.8 in, ChemAxon (http://www.chemaxon.com), 2017.
[66] W. Li, Y. Yin, W. Shuai, F. Xu, H. Yao, J. Liu, K. Cheng, J. Xu, Z. Zhu, S. Xu, Discovery of novel quinazolines as potential anti-tubulin agents occupying three zones of colchicine domain, Bioorganic chemistry, 83 (2019) 380-390. D.O.I.:10.1016/j.bioorg.2018.10.027
[67] C. Garcia-Perez, R. Pelaez, R. Theron, J. Luis Lopez-Perez, JADOPPT: java based AutoDock preparing and processing tool, Bioinformatics, 33 (2017) 583-585. D.O.I.:10.1093/bioinformatics/btw677

Declaration of interests

☒ The authors declare that they have no known competing financial interests or personal relationships that could have appeared to influence the work reported in this paper.

☐The authors declare the following financial interests/personal relationships which may be considered as potential competing interests:

Methylsulfanylpyridine based diheteroaryl isocombretastatin analogs as potent anti-proliferative agents.

Raquel Álvarez,[a,c,d] Laura Aramburu,[a,c,d] Consuelo Gajate,[b] Alba Vicente-Blázquez,[a,b,c,d] Faustino Mollinedo,[b] Manuel Medarde[a,c,d] and Rafael Peláez*[,a,c,d]

[a] Laboratorio de Química Orgánica y Farmacéutica, Departamento de Ciencias Farmacéuticas, Universidad de Salamanca, Campus Miguel de Unamuno, E-37007 Salamanca, Spain.
[b] Laboratory of Cell Death and Cancer Therapy, Department of Molecular Biomedicine, Centro de Investigaciones Biológicas Margarita Salas, Consejo Superior de Investigaciones Científicas (CSIC), E-28040 Madrid, Spain.
[c] Instituto de Investigación Biomédica de Salamanca (IBSAL), Facultad de Farmacia, Universidad de Salamanca, Campus Miguel de Unamuno, E-37007 Salamanca, Spain.
[d] Centro de Investigación de Enfermedades Tropicales de la Universidad de Salamanca (CIETUS). Facultad de Farmacia, Universidad de Salamanca, Campus Miguel de Unamuno, E-37007 Salamanca, Spain.

e-mail addresses:

Laura Aramburu	lauramvil@usal.es
Raquel Álvarez	raquelalvarez@usal.es
Consuelo Gajate	cgajate@cib.csic.es
Alba Vicente Blázquez	avicenteblazquez@usal.es
Faustino Mollinedo	fmollin@cib.csic.es
Manuel Medarde	medarde@usal.es
Rafael Peláez	pelaez@usal.es

* Corresponding author:
Phone: 00 34 923294528; 00 34 677554890. FAX: 00 34 923294515.
e-mail: pelaez@usal.es.
Address: Laboratorio de Química Orgánica y Farmacéutica, Departamento de Ciencias Farmacéuticas, Facultad de Farmacia, Campus Miguel de Unamuno, E-37007 Salamanca, Spain.

Graphical abstract

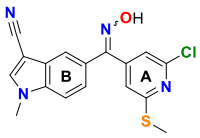

Tubulin inhibition

G_2/M arrest

Apoptosis

Binding to colchicine site

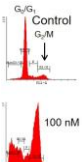

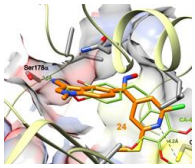

Highlights

- 2-Chloro-6-methylsulfanyl-4-pyridyl isocombretastatins are potent antimitotics
- Indole substitution increases potency
- Solubility improvements
- Disruption of microtubules in cells, G_2/M cell cycle arrest, and induction of apoptosis.
- Binding at the colchicine site of tubulin

Abstract

Isocombretastatins are the not isomerizable 1,1-diarylethene isomers of combretastatins. Both families of antimitotics are poorly soluble and new analogs with improved water solubility are needed. The ubiquitous 3,4,5-trimethoxyphenyl ring and most of its replacements contribute to the solubility problem. 39 new compounds belonging to two series of isocombretastatin analogs with 2-chloro-6-methylsulfanyl-4-pyridinyl or 2,6-bis(methylsulfanyl)-4-pyridinyl moieties replacing the 3,4,5-trimethoxyphenyl have been synthesized and their antimitotic activity and aqueous solubility have been studied. We show here that 2-chloro-6-methylsulfanylpyridines are more successful replacements than 2,6-bis(methylsulfanyl)pyridines, giving highly potent tubulin inhibitors and cytotoxic compounds with improved water solubilities. The optimal combination is with indole rings carrying polar substitutions at the three position. The resulting diheteroaryl isocombretastatin analogs showed potent cytotoxic activity against human cancer cell lines caused by tubulin inhibition, as shown by *in vitro* tubulin polymerization inhibitory assays, cell cycle analysis, and confocal microscopy studies. Cell cycle analysis also showed apoptotic responses following G_2/M arrest after treatment. Conformational analysis and docking studies were applied to propose binding modes of the compounds at the colchicine site of tubulin and were in good agreement with the observed SAR. 2-Chloro-6-methylsulfanylpyridines represent a new and successful trimethoxyphenyl ring substitution for the development of improved colchicine site ligands.

Keywords

Isocombretastatins and phenstatin oximes

Pyridine analogues

Solubility improvement

Tubulin polymerization inhibition

G_2/M arrest and apoptosis

Docking

1. INTRODUCTION

The microtubules of the eukaryotic cells are hollow dynamic tubes formed by polymerization and depolymerization of αβ-tubulin heterodimers, referred to as tubulin. This dynamic equilibrium is essential for their functioning and the aim of microtubule-targeting agents or MTAs, acting as anti-tumor and anti-parasitic drugs.[1] MTAs bind to tubulin in at least seven structurally characterized binding sites, some of them favoring (microtubule-stabilizing agents or MSAs) and some of them opposing polymerization (microtubule destabilizing agents or MDAs).[2] The combretastatins are a family of natural products that bind to the colchicine domain of tubulin, located at the interface between the αβ-tubulin heterodimers. Binding of combretastatins to the colchicine site hampers the curved to straight transition of tubulin dimers necessary for polymerization, and therefore they behave as MDAs.[3] MDAs inhibition of tubulin polymerization is especially patent in the highly dynamic mitotic microtubules and, therefore, they arrest cells at the metaphase to anaphase transition, which results in an enhanced population of cells in the G_2/M phases of the cell cycle, and a late apoptosis onset of cancer cells.[4] Furthermore, combretastatins act as vascular disrupting agents or VDAs, causing a rapid collapse of the tumor neo-vasculature *in vivo* and tumor death.[5] The phosphate prodrug of combretastatin A-4 (CA4P, fosbretabulin) as fosbretabulin tromethamine (Fig. 1) has been granted the orphan drug designation for the treatment of ovarian adenocarcinoma, gastroenteropancreatic and neuroendocrine cancers, and anaplastic thyroid cancer, and the combretastatin A-1 diphosphate prodrug Oxi4503 (Fig. 1) for the treatment of relapsed/refractory Acute Myeloid Leukemia (AML) in combination with cytarabine.[6]

Despite their clinical success, the combretastatins present several properties that limit their therapeutic potential and have therefore been the aim of many medicinal chemistry programs: they are highly hydrophobic compounds with low aqueous solubility, the double bond linking the two aromatic rings is configurationally unstable, they are inactivated *in vivo* by phase I and II

metabolic transformations, and their vascular disrupting activity which causes tumor necrosis leaves a peripheral rim of undamaged cancer cells that rapidly regenerates the tumor mass.[7-15] The solubility problem has been tackled by the formation of highly soluble prodrugs such as phosphates on the hydroxyl groups.[16] However, the hydroxyl group is also involved in phase II metabolic transformations leading to resistance.[17] The double bond isomerization problem has been solved by the inclusion of the bridge in different cycles,[10, 11, 18] by the replacement of the double bond by configurationally stable bridges of different lengths[19] or by bridges preferentially adopting *cisoid* conformations, such as the sulfonamides,[20] and has even been turned into an advantageous feature for photodynamic therapy.[21] A very successful strategy has been the reduction of the two - atom bridge of combretastatins to one - atom bridges as in benzophenones (phenstatins),[22] oximes,[23] diarylamines,[24, 25] 1,1-diarylethanes,[26] and 1,1-diarylethenes (isocombretastatins, the regioisomers of combretastatins).[27-29] Avoidance of the metabolic transformations has been pursued by modifications on the bridge[17] and the aromatic rings,[30] and combination therapy and increased cytotoxic potency have been proposed to escape the resistance to VDAs.[8] However, many of these improvements are often achieved at the expense of others (e.g. replacement of the guaiacol ring to avoid metabolic transformation reduces the solubility).

The B ring of combretastatins and isocombretastatins has been the subject of multiple replacements showing a permissive SAR requirement in this region.[15] However, few of them have addressed the increase in hydrophobicity associated with its replacement by naphthalene, indole, or differently substituted phenyl rings. The substitution of the hydroxyl group by amino substituents,[31] the replacement of the phenyl by pyridine rings,[25, 32, 33] and the introduction of polar groups on otherwise lipophilic moieties such as the indole rings [34, 35] are representative examples of such attempts. We have shown that the efficiency of these promising modifications is highly dependent on the structural context in which they are introduced,[34-36], and therefore needs to be ascertained in every structural context.

The 3,4,5-trimethoxyphenyl ring of combretastatin A-4 (A ring) due to its large size and hydrophobic nature is the target of metabolic transformations of combretastatins[14] and isocombretastatins,[13] and also represents a highly desirable target for solubility improvements. However, SAR studies have firmly established its importance for high cytotoxic potency.[15] Recently, successful replacements of the trimethoxyphenyl ring by quinolines[37, 38] and quinazolines[39] and related heterocycles have been described.[25, 40, 41] These potent benzo-fused heterocyclic compounds however unwillingly increase the hydrophobic area and the ring count.[42, 43] Successful replacements with smaller pyridine or related heterocycles have been less frequent and require hydrophobic substituents to compensate for the size reduction.[38, 44, 45] We have recently shown that replacement of the trimethoxyphenyl ring by pyridines can be favorably achieved with methylsulfanyl and methoxy substituents and that the encountered difficulties in the direct replacement of the phenyl ring of the trimetoxyphenyl ring by similarly substituted pyridines are due to unfavorable conformational preferences.[46] Furthermore, docking experiments showed optimal adjustment to complexes of tubulin with a chloro-furopyrimidine,[41] thus suggesting a region for further improvement devoid of the mentioned conformational issues. In all these instances, the polar interaction with the sidechain of Cys241of β-tubulin is preserved through the pyridine nitrogen.

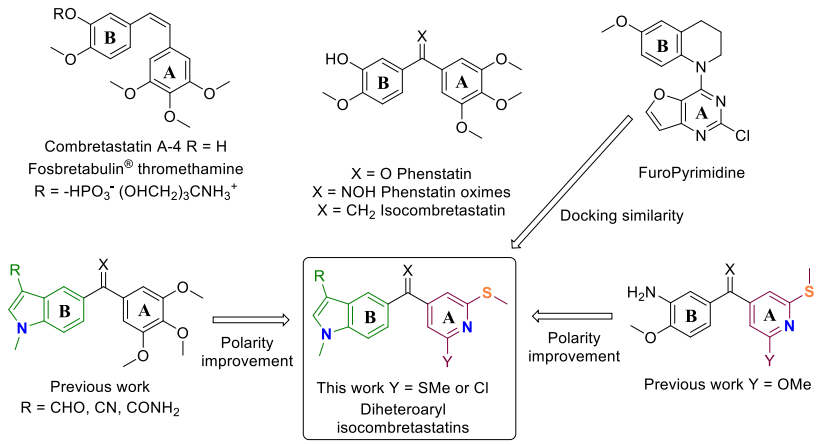

Figure 1. Chemical structure of combretastatins and one-atom bridged analogs, and design rationale for the compounds described in this work.

A long-term goal of the design of new combretastatin and related analogs involves the replacement of the 3,4,5-trimethoxyphenyl ring (A ring) with polar moieties with higher intrinsic water solubility, thus allowing the removal of the troublesome solubilizing hydroxyl substituent of the B ring. The aim is to piece a piece enhance the overall polarity of the compounds in a way tolerated by the highly hydrophobic colchicine domain such that a solubility increase is accompanied by potent tubulin inhibition. We have combined two previous successful strategies of structural modification, the first one affecting and consisting in the replacement of ring A with substituted pyridines and the second involving modifications of ring B that remove the troublesome groups while allowing additional polarity enhancements. On the pyridine A ring we have further explored the methylsulfanyl groups that have less conformational penalties than the methoxy groups to partially compensate for the size reduction associated with the removal of the central methoxy group, and based on previous docking results we have also combined them with chlorine substituents. We have done so in the context of 1,2-ethenylene (combretastatin) and 1,1-ethenylidene (isocombretastatin), carbonyl (phenstatin), and ketoxime bridges that avoid the undesired isomerization of the bridge. Substantial solubility improvements

were accomplished, and highly potent tubulin inhibitors were found. Potencies higher than the reference combretastatin A-4 in tubulin inhibition were attained, along with cytotoxic potencies in the mid nanomolar range in a more consistent way than with previous pyridine-based series against sensitive HeLa human cervix epithelioid carcinoma and HL-60 human acute myeloid leukemia cell lines. Submicromolar antiproliferative activity against the combretastatin A-4-resistant colon adenocarcinoma (HT-29) cell line was also achieved.[12, 17, 30, 47] Treatment with the most potent compounds at concentrations of 100 nM resulted after 24 hours in the accumulation of cells in the G_2/M phases of the cell cycle, followed by significant increases of the sub-G_0/G_1 cell populations 48 hours post-treatment. The effects of the compounds on the cytoskeleton were confirmed by immunofluorescence studies. Conformational analysis combined with docking studies suggest binding at the colchicine site with association energies dependent on the conformational preferences of the pyridine substituents. These results show that pyridine A rings can be a favorable modification in colchicine site ligands with improved water solubility and potent cytotoxic activity through tubulin polymerization inhibition for the development of new antimitotic drugs.

2. RESULTS AND DISCUSSION

2.1. Chemistry

2.1.1. Chemical synthesis

Nucleophilic additions of aryl-lithium derivatives to disubstituted pyridinecarboxylic acids prepared from citrazinic acid (scheme 1) were applied for the synthesis of the key intermediate diarylketones (schemes 2 and 3). Diarylketones were, in turn, converted into the 1,1-diarylethenes by Wittig reactions and into the oximes by treatment with hydroxylamine hydrochloride. The combretastatin analogs were synthesized using Wittig reactions with pyridinemethylphosponium salts.

Citrazinic acid was converted in neat phosphorous oxychloride to 2,6-dichloroisonicotinic acid (**1**),[48] which was the key intermediate for aromatic nucleophilic substitutions with sodium methanethiolate to give the mono- and disubstituted acids **2** and **3** (Scheme 1). Reduction of **3** with LAH to the benzylic alcohol **4**, nucleophilic substitution with HBr to benzylic bromide **5**, and then with triphenylphosphine gave triphenylphosphonium salt **6**, used for the Wittig reactions in the synthesis of the combretastatins (scheme 3).

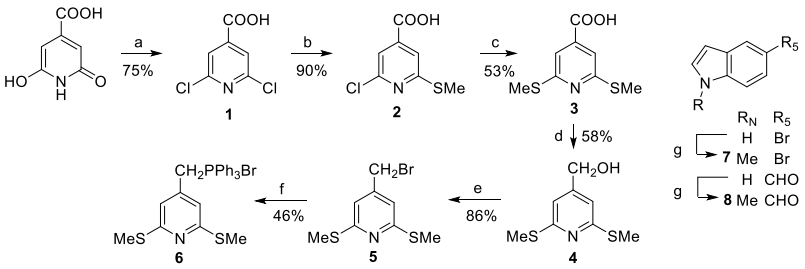

Scheme 1. Reagents and conditions: a) Me_4NBr, $POCl_3$, 90 - 140 ºC, 24 h; b) 1.5 eq NaSMe, DMF, reflux, 24-48 h; c) excess NaSMe, DMF, reflux, 24-48 h; d) LAH, THF, 0 ºC - r.t., 24 h; e) HBr, AcOH, 0 ºC - r.t., 24 h; f) PPh_3, Toluene, 24h, r.t.; g) MeI, NaOH, Bu_4NHSO_4, CH_2Cl_2, r.t., 24 h.

Diarylketones (phenstatins) **9**, **10**, **16**, **17**, **33**, **36**, **39**, and **40** were synthesized (schemes 2 and 3) by nucleophilic additions of aryl-lithium reagents, prepared by treatment of the corresponding aryl bromides with *n*BuLi, to isonicotinic acids **2** and **3**. 1,1-Diarylethenes (isocombretastatins) **11**, **12**, **18**, **19**, **34**, **37**, and **41** were prepared by Wittig reaction of the diarylketones with methyltriphenylphosphonium iodide, while treatment with hydroxylamine rendered the mixtures of *E* and *Z* oximes **13**, **14**, **22**, **23**, **24**, **35**, **38**, and ***42***. Hydrogenation of **12** yielded diarylethane **15**. The introduction of substituents at position 3 of the indole rings to obtain more polar analogs is shown in scheme 2. 3-Formylindoles **20**, **21**, **25**, and **26** were prepared under Vilsmeier – Haack conditions. Formyl indoles were converted into the oximes by treatment with hydroxylamine and then to the 3-cyanoindoles **24**, **29**, and **30** by acetylation followed by thermal elimination. Indoleamides **31** and **32** were prepared from the unsubstituted indoles by reaction

with CSI and indole carboxylic acids **27** and **28** by aromatic electrophilic substitution with phosgene followed by hydrolysis.

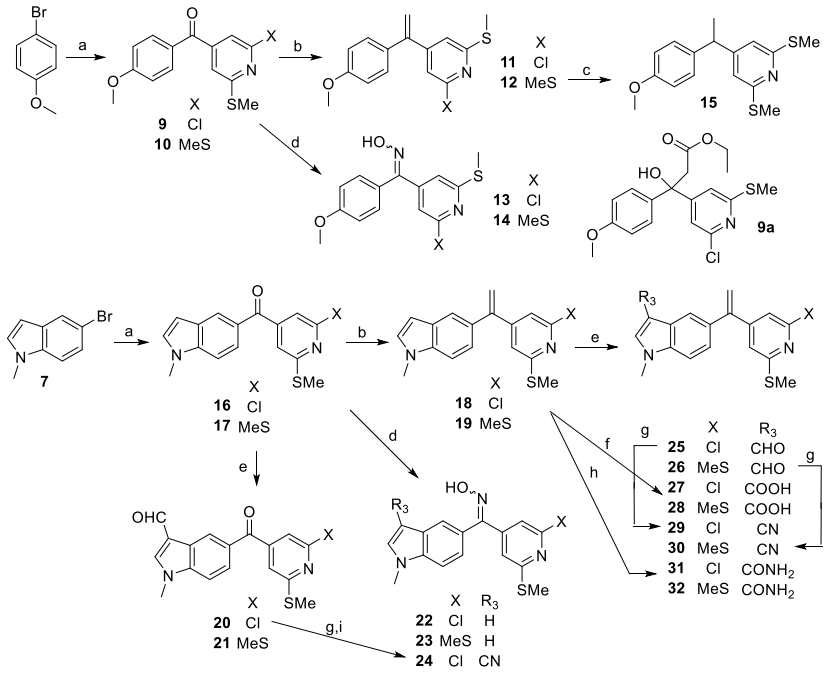

Scheme 2. Synthesis of *p*-methoxyphenyl and *N*-methyl-1*H*-indolyl analogs. Reagents and conditions: (a) i) *n*BuLi, dry THF, -40 ºC, 1 h; ii) **2** or **3**, dry THF, -40 ºC - r.t., 24 h; (b) i) CH_3PPh_3Br, *n*BuLi, dry THF, -40 ºC, 1 h; ii) **9, 10**, **16** or **17**, dry THF, -40 ºC - r.t., 24 h; (c) H_2, Pd(C), r.t., 24-48 h; (d) $NH_2OH{\cdot}HCl$, MeOH, pyridine, reflux, 24 h; (e) i) $POCl_3$, dry DMF, 0 ºC, 30 min; ii) **16** or **17** and heat to 60 ºC 2 h, or **18** or **19** and heat to room temperature 2 h; (f) Phosgene, CH_2Cl_2, room temperature, 24-48 h; (g) i) $NH_2OH{\cdot}HCl$, MeOH, pyridine, reflux, 24 h; ii) Ac_2O, pyridine, 130 ºC, 24-48 h; (h) CSI, 1,2-dichloroethane, r.t., 24 h; (i) 10% NaOH, MeOH, r.t., 72 h.

Wittig reactions between the phosphonium ylide formed by treatment of **6** with *n*BuLi and *N*-methylindole-5-carbaldehyde **11** (scheme 1) or *p*-anisaldehyde gave the combretastatins A (1,2-diarylethenes) **43** and **44** (scheme 3), whose *E* and *Z* isomers were chromatographically separated.

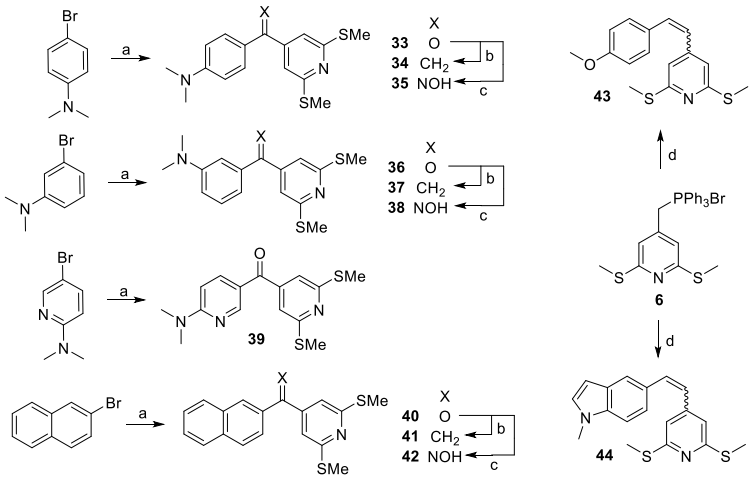

Scheme 3. Synthesis of analogs **33** - **44**. Reagents and conditions: (a) i) ArBr, *n*BuLi, dry THF, -40 ºC, 1 h, then **3**; ii) room temperature, 24 h; (b) i) CH_3-PPh_3I, *n*BuLi, dry THF, -40 ºC, 1 h; ii) **33**, **36** or **40**, r.t., 24 h; (c) NH_2OH·HCl, MeOH, pyridine, reflux, 24 h; (d) i) **6**, dry THF, *n*BuLi, -40 ºC, 1 h; ii) *p*-methoxybenzaldehyde or **8**, dry THF, -40 ºC - r.t., 24 h.

Different B ring modifications and bridges have been combined with methylsulfanylpyridine rings and thus provide a significative sample of the potential of the new pyridine analogs as cytotoxic and tubulin polymerization inhibitory agents, which were subsequently used in the biological assays.

2.1.2. Aqueous solubility

Colchicine site ligands are highly lipophilic due to the mainly hydrophobic nature of the colchicine domain, which results in low water solubilities. The established solution has been the formation of prodrugs that increase the aqueous solubility, but the anchor points are the substrate for metabolism and loss of activity, and alternative strategies are needed. Replacing highly hydrophobic phenyl rings by heterocycles of higher polarity, such as the pyridines here described, should improve water solubility. The solubility of representative compounds (Table 1) was determined by shaking the compounds in phosphate buffer at pH 7.0 until equilibration,

microfiltration, and quantification of the dissolved compound by UV absorbance. Most of the compounds show solubilities higher than the 1 µg/mL of combretastatin A-4, but the increase is in many cases modest although improvements of more than ten-fold are also observed. There is no clear SAR in the solubility values, as evidenced by a comparison of matched pairs. There is not a great difference in solubility between methylsulfanyl groups and chlorine atoms as pyridine substituents (e.g. compare the pairs **11** *vs* **12**, **25** *vs* **26**, but **29** *vs* **30**), or between the bridges, despite their different polarity and hydrogen bonding capabilities (e.g. compare **33**-**35**, **36**-**38**, **11** *vs* **13**, **18** *vs* **22** or **24** *vs* **29**). For the B rings, the *p*-methoxyphenyl seems somewhat more favorable, and in some instances, substitutions at the indole 3 position result in good solubilities (e.g. **21**, **28**, **30**), but unpredictably, possibly due to complex solvation interactions.

Table 1. Solubility of representative compounds in phosphate buffer at pH 7.0

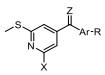

Comp	X	Z	Ar	R	Solubility (µg/mL)	TPSA (Å²)[49]
CA-4	-	-	-	-	1.04[50]	57
10	SMe	O	4-MeO-Ph	H	1.5	90
11	Cl	CH_2	4-MeO-Ph	H	48.9	47
12	SMe	CH_2	4-MeO-Ph	H	35.7	73
13	Cl	NOH	4-MeO-Ph	H	41.7	80
18	Cl	CH_2	*N*MeIND	H	12.3	43
21	SMe	O	*N*MeIND	CHO	230.2	103
22	Cl	NOH	*N*MeIND	H	14.8	76
24	Cl	NOH	*N*MeIND	CN	5.1	125
25	Cl	CH_2	*N*MeIND	CHO	6.3	60
26	SMe	CH_2	*N*MeIND	CHO	7.6	85
28	SMe	CH_2	*N*MeIND	COOH	102.7	106
29	Cl	CH_2	*N*MeIND	CN	3.2	67
30	SMe	CH_2	*N*MeIND	CN	46.3	92
33	SMe	O	4-NMe_2Ph	H	1.0	84
34	SMe	CH_2	4-NMe_2Ph	H	6.9	67
35	SMe	NOH	4-NMe_2Ph	H	1.1	99
36	SMe	O	3-NMe_2Ph	H	1.3	84
37	SMe	CH_2	3-NMe_2Ph	H	2,4	67
38	SMe	NOH	3-NMe_2Ph	H	14.7	99
39	SMe	O	6-NMe_2-pyr-3-yl	H	47.1	103
41	SMe	CH_2	2-Naphthyl	H	1.9	63

2.2. Biology.

2.2.1. Cell proliferation inhibitory activity

The cell proliferation inhibitory activity of the synthesized compounds against three human cancer cell lines has been assayed by measuring cell viability with the XTT method (Table 2).[51] The three selected cell lines show different sensitivities to treatment with combretastatin A-4:[52] HeLa (human cervix epithelioid carcinoma) and HL-60 (human acute myeloid leukemia) are sensitive, whereas HT-29 (human colon adenocarcinoma) are resistant.[12, 17, 30, 47] Most of the synthesized diarylmethane derivatives show anti-proliferative activity against the sensitive cell lines with sub-micromolar potencies, and many also against HT-29, although with reduced potencies. A handful of the compounds inhibit proliferation with IC_{50} values in the double-digit nanomolar range, with values 3−20 times higher than those of combretastatin A-4, but lower than ABT-751 (Table 2), an oral antimitotic drug that binds to the colchicine site and has reached clinical trials. These results confirm that the selected diarylmethane skeleton is a good scaffold for anti-proliferative activity and that the trimethoxyphenyl ring can be successfully substituted by the pyridine moieties here considered. Computational prediction of the sites of metabolism for the most potent compounds suggest that oxidation of the methylsulfanyl is the most likely point of metabolic transformation in this series (Supple~~m~~mentary figure 1).

Formatted: Not Highlight

Concerning the bridges between the two aryl groups, there is no big difference in anti-proliferative activity for ethenes (isocombretastatins) or ketone oximes, with the ketones (phenstatins) showing lower potencies for the methoxyphenyl ring B series (e.g. compare the triplets **9** *vs* **11** *vs* **13**, **10** *vs* **12** *vs* **14**, or **33** *vs* **34** *vs* **35**) and more similar in the indoles (e.g. compare the triplets **16** *vs* **18** *vs* **22**, or **17** *vs* **19** *vs* **23**). The oximes are stable in aqueous solution for more than 72 hours (data not shown) and computational prediction of the sites of metabolism do not point at them as significant transformation points (Supplementary figure 1)

Formatted: Not Highlight

and therefore their potency is not apparently due to hydrolysis to the ketones, which are in fact less potent. The combretastatins **43** and **44** did not consistently reach sub-micromolar potencies.

Among the B rings, which were selected because they had been previously shown to give active analogs, 4-methoxyphenyl,[27, 28] 3-substituted and unsubstituted *N*-methyl-5-indolyl,[34, 35] and 4-dimethylaminophenyl[36] containing analogs led to sub-micromolar inhibitors, whereas 3-dimethylaminophenyl[32] and 2-naphthyl[27, 53] rings were inactive. Similar potencies are observed for the 4-methoxyphenyl, 4-dimethylaminophenyl and the unsubstituted *N*-methylindole series (e.g. compare **12** *vs* **34** *vs* **19** or **14** *vs* **35** *vs* **23** respectively), while the substituted indoles showed slightly improved potencies only when combined with 2-chloro-6-methylsulfanylpyridines as A ring (e.g. compare **18** *vs* **25**, **29**, and **31** for 2-chloro-6-methylsulfanylpyridines and **19** *vs* **26**, **30**, and **32** for 2,6-bis(methylsulfanyl)pyridines).

Table 2. Tubulin Polymerization Inhibitory Activity and Cytotoxic Activity against Human Cancer Cell Lines.

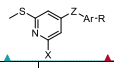

N	X	Z	Ar	R	IC_{50} TPI (μM)[a]	IC_{50} Hela (nM)[b]	IC_{50} HL-60 (nM)[b]	IC_{50} HT-29 (nM)[b]
9	Cl	>C=O	4-MeO-Ph	H	>5	≥10^3	≥10^3	≥10^3
9a	Cl	>C(OH)AcOH	4-MeO-Ph	H	>5	≥10^3	≥10^3	≥10^3
10	SMe	>C=O	4-MeO-Ph	H	>5	≥10^3	≥10^3	≥10^3
11	Cl	>C=CH_2	4-MeO-Ph	H	1.5	628 ± 256	464 ± 142	485 ± 103
12	SMe	>C=CH_2	4-MeO-Ph	H	2.0	399 ± 122	306 ± 114	550 ± 261
13	Cl	>C=NOH	4-MeO-Ph	H	4.6	518 ± 49	613 ± 207	≥10^3
14	SMe	>C=NOH	4-MeO-Ph	H	3.0	457 ± 94	299 ± 106	292 ± 54
15	SMe	>C(H)CH_3	4-MeO-Ph	H	>5	≥10^3	≥10^3	≥10^3
16	Cl	>C=O	*N*MeIND	H	2.4	388 ± 168	490 ± 106	≥10^3
17	SMe	>C=O	*N*MeIND	H	1.7	233 ± 81	222 ± 64	549 ± 79
17b	SMe	>C-OH	(*N*MeIND)$_2$	H	>5	≥10^3	≥10^3	≥10^3
18	Cl	>C=CH_2	*N*MeIND	H	0.3	176 ± 28	416 ±159	511 ± 201
19	SMe	>C=CH_2	*N*MeIND	H	1.1	520 ± 141	717 ± 107	249 ± 103
20	Cl	>C=O	*N*MeIND	CHO	>5	≥10^3	≥10^3	≥10^3
21	SMe	>C=O	*N*MeIND	CHO	>5	≥10^3	≥10^3	≥10^3
22	Cl	>C=NOH	*N*MeIND	H	>5	365 ± 71	257 ± 39	≥10^3
23	SMe	>C=NOH	*N*MeIND	H	1.0	590 ± 235	240 ± 74	745 ± 102
24	Cl	>C=NOH	*N*MeIND	CN	0.2	57 ± 18	93 ± 9	195 ± 23
25	Cl	>C=CH_2	*N*MeIND	CHO	1.6	72 ± 15	38 ± 18	876 ± 45

Formatted: Not Highlight
Field Code Changed
Formatted: Not Highlight
Formatted: Not Highlight
Formatted: Not Highlight
Formatted: Not Highlight
Formatted: Not Highlight
Formatted: Not Highlight
Formatted: Not Highlight
Formatted: Not Highlight
Formatted: Not Highlight
Formatted: Not Highlight
Formatted: Not Highlight
Formatted: Not Highlight
Formatted: Not Highlight
Formatted: Not Highlight
Formatted: Not Highlight
Formatted: Not Highlight
Formatted: Not Highlight
Formatted: Not Highlight

26	SMe	>C=CH_2	*N*MeIND	CHO	1.2	64 ± 16	303 ± 60	573 ± 104
27	Cl	>C=CH_2	*N*MeIND	COOH	>5	≥10^3	≥10^3	≥10^3
28	SMe	>C=CH_2	*N*MeIND	COOH	4.7	≥10^3	≥10^3	≥10^3
29	Cl	>C=CH_2	*N*MeIND	CN	0.6	158 ± 58	74 ± 21	278 ± 106
30	SMe	>C=CH_2	*N*MeIND	CN	0.4	579 ± 96	604 ± 143	587 ± 203
31	Cl	>C=CH_2	*N*MeIND	$CONH_2$	2.3	82 ± 33	44 ± 15	38 ± 8
32	SMe	>C=CH_2	*N*MeIND	$CONH_2$	2.4	601 ± 210	223 ± 44	276 ± 68
33	SMe	>C=O	4-NMe_2Ph	H	>5	652 ± 24	435 ± 198	787 ± 38
33b	SMe	>C-OH	(4-NMe_2Ph)$_2$		>5	≥10^3	≥10^3	≥10^3
34	SMe	>C=CH_2	4-NMe_2Ph	H	3.8	328 ± 82	486 ± 215	928 ± 59
35	SMe	>C=NOH	4-NMe_2Ph	H	2.1	269 ± 36	213 ± 71	781 ± 112
36	SMe	>C=O	3-NMe_2Ph	H	>5	≥10^3	≥10^3	≥10^3
37	SMe	>C=CH_2	3-NMe_2Ph	H	>5	≥10^3	≥10^3	≥10^3
38	SMe	>C=NOH	3-NMe_2Ph	H	>5	≥10^3	≥10^3	≥10^3
39	SMe	>C=O	6-NMe_2-pyr-3-yl	H	>5	≥10^3	≥10^3	≥10^3
39a	SMe	>C-OH	2(6-NMe_2-pyr)	H	>5	≥10^3	≥10^3	≥10^3
40	SMe	>C=O	2-Naphth	H	>5	≥10^3	≥10^3	≥10^3
41	SMe	>C=CH_2	2-Naphth	H	>5	≥10^3	≥10^3	≥10^3
42	SMe	>C=NOH	2-Naphth	H	>5	≥10^3	≥10^3	≥10^3
43	SMe	-CH=CH-	4-MeO-Ph	H	3.8	≥10^3	≥10^3	≥10^3
44	SMe	-CH=CH-	*N*MeIND	H	>5	≥10^3	≥10^3	633 ± 211
CA-4	-	-	-	-	2.8	3	13	305
ABT-751	-	-	-	-	4000	388	-	514

[a] Concentration inhibiting 50% (IC_{50}) the polymerization of microtubular protein (TPI) *in vitro*. [b] IC_{50} values were calculated from concentration-response curves using the XTT assay as described in the Experimental Section. Data correspond to the mean values of three experiments performed in triplicate.

There is not a big difference in anti-proliferative potency when the pyridine A ring has two methylsulfanyl substituents or one chlorine and one methylsulfanyl (e.g. compare the pairs **9** *vs* **10**, **11** *vs* **12**, **13** *vs* **14**, **16** *vs* **17**, **18** *vs* **19**, and **22** *vs* **23**) except for the 3-substituted indoles, which experience a potency boost when combined with the 2-chloro-6-methylsulfanylpyridines but not with the 2,6-bis(methylsulfanyl)pyridines (e.g. compare the pairs **25** *vs* **26**, **29** *vs* **30**, and **31** *vs* **32**). Therefore, the combination of 3-substituted indoles with 2-chloro-6-methylsulfanylpyridines in the isocombretastatin (i.e. compounds **25**, **29**, and **31**) or ketoxime series (i.e. compound **24**) results in two of the most potent compounds. These results are in good agreement with previous studies showing that 3-substituted indoles make good B rings,[35] but that their effect is dependent on the structural context they are found in.[32, 34, 46] These favorable indole 3-substituents are aldehydes, amides, and nitrile groups, with similar

effects on the potency (e.g. compare **25**, **29**, and **31**), whereas carboxylic acids result in the loss of the potency, probably due to their ionized state in solution.

In summary, 2-chloro-6-methylsulfanylpyridine isocombretastatins or oximes with 3-formyl-, 3-carbamoyl- or 3-cyano- indoles are highly potent inhibitors of cell proliferation in the double-digit nanomolar range, comparable to reference compounds, even if devoid of the trimethoxyphenyl A ring.

2.2.2. Tubulin polymerization inhibition

To confirm the proposed effect on tubulin we have studied the *in vitro* inhibitory activity of the synthesized compounds on the polymerization of microtubular protein isolated from calf brain. The amounts of polymer mass formed in the presence and the absence (control) of the compounds were measured by turbidimetry, and the percentage of reduction was taken as the tubulin polymerization inhibitory activity. The compounds were initially tested at a concentration of 5 μM, and for those inhibiting more than 50%, we have determined the IC_{50} values (Table 2). Sixteen of the synthesized compounds have TPI IC_{50} values lower than 3 μM, comparable to reference compounds such as combretastatin A-4 or ABT-751, with TPI IC_{50} values of 2 μM and 4 μM respectively (Table 2). Remarkably, 4 compounds (**18**, **24**, **29**, and **30**) are highly potent sub-micromolar inhibitors and additionally, 6 more have TPI IC_{50} values lower than 2 μM (**11**, **17**, **19**, **23**, **25**, and **26**).

The TPI and the antiproliferative activity are strongly correlated, as almost all the compounds with TPI IC_{50} values lower than 5 μM show antiproliferative activity at sub-micromolar concentrations, thus indicating that interference with tubulin polymerization is their mechanism of action. However, there is not a strict correlation between the two values, with compounds with highly potent TPI in the sub-micromolar range (e.g. **18**, **29**, **30**, and **24**) showing significant differences in anti-proliferative potency, and compounds with not so high TPI potencies (i.e. **25** or **31**) amongst the more potent inhibitors of cell proliferation. This discrepancy has been

previously noted and justified by the fact that antiproliferative activity is dependent on the inhibition of polymerization dynamics at low (nanomolar) compound concentrations and not so much to polymer mass change at high protein and compound (micromolar) concentration. As a result of these differences, the observed SAR for TPI is slightly different from the anti-proliferative SAR previously discussed.

Concerning the bridge, more differences than in antiproliferative activity are found, with isocombretastatins (1,1-diarylethenes) being more potent than the ketone oximes that are in turn usually more potent than phenstatins (ketones) (e.g. compare **9** *vs* **11** *vs* **13**, **10** *vs* **12** *vs* **14**, **16** *vs* **18** *vs* **22**, **17** *vs* **19** *vs* **23**), with combretastatin **43** showing TPI activity. Similarly, more differences are observed for the B rings in TPI activity than in anti-proliferative activity, with the indolic analogs showing higher potencies than compounds with 4-methoxyphenyl or 4-dimethylaminophenyl moieties (e.g. compare **10** *vs* **17** *vs* **33**, **11** *vs* **18**, **12** *vs* **19** *vs* **34**, and **14** *vs* **23** *vs* **35**). On the other hand, less differences are observed between 2-chloro-6-methylsulfanylpyridines and bis(methylsulfanyl)pyridines (e.g. compare **9** *vs* **10**, **11** *vs* **12**, **13** *vs* **14**, , **16** *vs* **17**, and **18** *vs* **19**, but **22** *vs* **23**), especially in the case of compounds carrying 3-substituted indoles (e.g. compare **20** *vs* **21**, **25** *vs* **26**, **27** *vs* **28**, **29** *vs* **30**, and **31** *vs* **32**).

Replacement of the trimethoxyphenyl A ring with 2-chloro-6-methylsulfanylpyridines or 2,6-bis(methylsulfanyl)pyridines results in highly potent inhibitors of tubulin polymerization for isocombretastatins or ketone oximes with 3-formyl-, 3-carbamoyl- or 3-cyanoindoles as B rings, even more potent than combretastatin A-4.

2.2.3. Effects on cellular microtubules

To confirm that the actions of the compounds in cells are based on their effects on tubulin, we have studied the effect of representative compounds on the microtubule network in HeLa cells. To this end, we have selected compounds **24** and **25**, which showed the lowest anti-proliferative IC_{50} values and were highly potent inhibitors of tubulin polymerization *in vitro*.

Immunofluorescence confocal microscopy studies with the labeling of α-tubulin and nuclei showed that treatment with **24** and **25** promoted a drastic and severe disruption of the microtubule network (Figure 2) as assessed by immunofluorescence confocal microscopy (Figure 2), thus supporting that the above disrupting effects on microtube network were due to interaction of compounds **24** and **25** with tubulin.

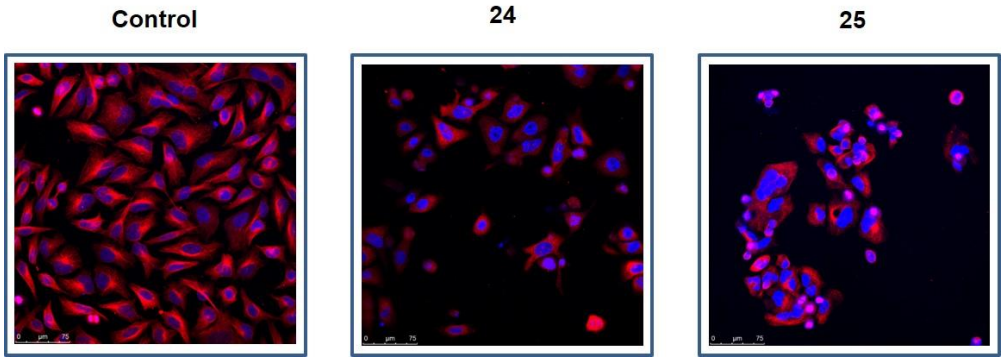

Figure 2. Effects of the treatment with compounds **24** and **25** on the microtubule network in HeLa cells. Cells were incubated in the absence (Control) or the presence of 1 µM of compounds **24** and **25** for 24 h, and then fixed and processed to analyze microtubules (red fluorescence) and nuclei (blue fluorescence) by confocal microscopy as described in the Experimental Section. Bar: 75 µm. The photomicrographs are representative of three independent experiments.

2.2.4 Effects on the cell cycle and induction of apoptosis

The effect of the most potent antiproliferative compounds (Table 2), **24** and **25**, on the cell cycle at different concentrations and times post-treatment was assessed by flow cytometry. Treatment of HeLa cells with **24** or **25** led to cell cycle arrest at G_2/M followed by the induction of apoptosis, as assessed by the appearance of cells with sub-G_0/G_1 DNA content (Figure 3). Treatment of HT-29 cells with **24** led also to a potent cell cycle arrest at G2/M, similar to the response observed in HeLa cells, albeit with a lower apoptotic response (Figure 3). However, compound **25** failed to promote a potent cell cycle arrest in HT-29 cells after 24 h treatment, and the overall response was lower than in HeLa cells (Figure 3). This is in agreement with our previous

observation that HL-60 and HeLa cells were more sensitive than HT-29 to compound **25** (Table 2).

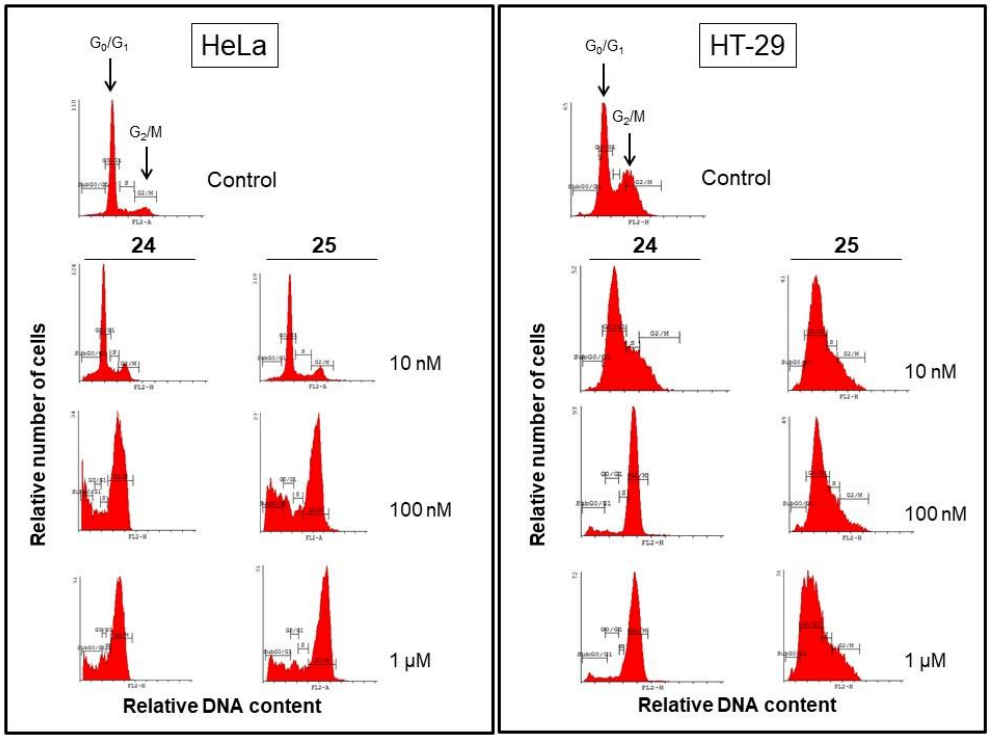

Figure 3. Dose-response of the effects of compounds **24** and **25** on cell cycle in HeLa and HT-29 cells. Cells were incubated with different concentrations of **24** and **25** for 24 h, and their DNA content was analyzed by fluorescence flow cytometry. The positions of the G_0/G_1 and G_2/M peaks are indicated by arrows, and the proportion of cells in each phase of the cell cycle was quantified by flow cytometry. The cell population in the sub-G_0/G_1 region represents cells with hypodiploid DNA content, an indicator of apoptosis. Untreated control cells were run in parallel. Data shown are representative of three independent experiments.

Next, we carried out a dose-response (at concentrations of 1 nM, 10 nM, 100 nM, 1 µM, and 10 µM) and time-course (at 24, 48, and 72 h post-treatment) analyses of the effects on the cell cycle of **24** and **25** in HL-60, HeLa and HT-29 cells (Figure 4).

At a concentration of 1 nM of **24** and **25**, the populations of cells at the different phases of the cell cycle (sub-G_0/G_1, G_0/G_1, S, and G_2/M) for the three cell lines at the three time points did not show differences with the untreated controls (data not shown) and can be used as references.

Incubation with compound **24** at only 100 nM (Figures 3 and 4) arrested most of the HL-60 and HT-29 cells at the G_2/M phase after 24 h (77.4% for HL-60 and 84.4% for HT-29). At the same time point and concentration, 73.2% of HeLa cells were arrested at the G_2/M phase and significant apoptosis induction was evidenced by a substantial number of cells at the sub-G_0/G_1 region (15.7%), with the sum of sub-G_0/G_1 and G_2/M accounting for a total of 88.9%. At later time points (48 h and 72 h), the percentage of cells at the sub-G_0/G_1 region progressively increased (22.7% at 48 h and 33.1% at 72 h for HL-60, 35.9% at 48 h and 83.3% at 72 h for HeLa, and 28.1% at 48h and 64.7% at 72 h for HT-29 cells) at the expense of the cells arrested at G_2/M phase (39.7% at 48 h and 23.3% at 72 h for HL-60, 46.9% at 48 h and 4.6% at 72 h for HeLa, and 54.9% at 48 h and 4.7% at 72 h for HT-29 cells), with the accumulated total of the two phases remaining roughly constant (62.4% at 48 h and 56.3% at 72 h for HL-60, 88.9% at 48 h and 82.8% at 72 h for HeLa, and 82.9% at 48h and 69.4% at 72 h for HT-29 cells). Interestingly, compound **24** at the low 10 nM concentration showed delayed apoptosis after 48h and 72 h in the more resistant HT-29 cell line. At micromolar concentrations (1 µM and 10 µM), the onset of apoptosis in HL-60 and HeLa cells occurs earlier, being already patent at 24 h, but the pattern of cell cycle phases distribution remains. For HT-29 the earlier apoptosis onset is not so apparent, and a significant reduction of the sum of the sub-G_0/G_1 and G_2/M populations is evident at 72 h (the sum equals 91.1% at 1 µM and 92.1% at 10 µM for the 48 h time point and 39.1 at 1 µM and 40.7% at 10 µM for the 72 h time point), as a result of a significative reduction in the G_2/M population.

Incubation with compound **25** at 100 nM (Figure 4) arrested most of the HL-60 cells at the G_2/M phase after 24 h (80.1%). At the same time point and concentration, 56.9% of HeLa cells were arrested at the G_2/M phase and significant apoptosis induction was evidenced by a substantial number of cells (25.2%) at the sub-G_0/G_1 region, with the sum of sub-G_0/G_1 and G_2/M accounting for a total of 82.0%. Under these conditions, HT-29 cells did not show effects on the distribution of the cell cycle phases. At later time points (48 h and 72 h), the percentage of HL-60 and HeLa cells at the sub-G_0/G_1 region progressively increased (20.9% at 48 h and 32.6% at 72 h for HL-60 and 47.6% at 48 h and 59.1% at 72 h for HeLa cells) at the expense of the cells arrested at G_2/M phase (40.5% at 48 h and 22.0% at 72 h for HL-60 and 30.4% at 48 h and 7.9% at 72 h for HeLa cells), with the accumulated total of the two phases remaining roughly constant (61.4% at 48 h and 54.6% at 72 h for HL-60 and 82.0% at 48 h and 78.0% at 72 h for HeLa cells). Under these experimental conditions (100 nM, 48 h, and 72 h incubation), HT-29 cells started to show increasing delayed apoptotic response (11.8% at 48 h and 15.1% at 72 h) in the absence of apparent G_2/M arrest. At higher drug concentrations (Figure 4), HL-60 and HeLa cells show cell cycle distribution patterns like those observed at 100 nM, and HT-29 cells showed augmented sub-G_0/G_1 regions.

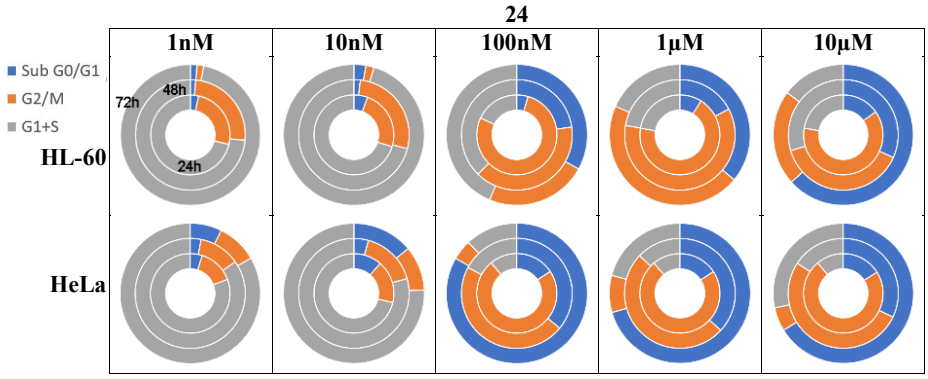

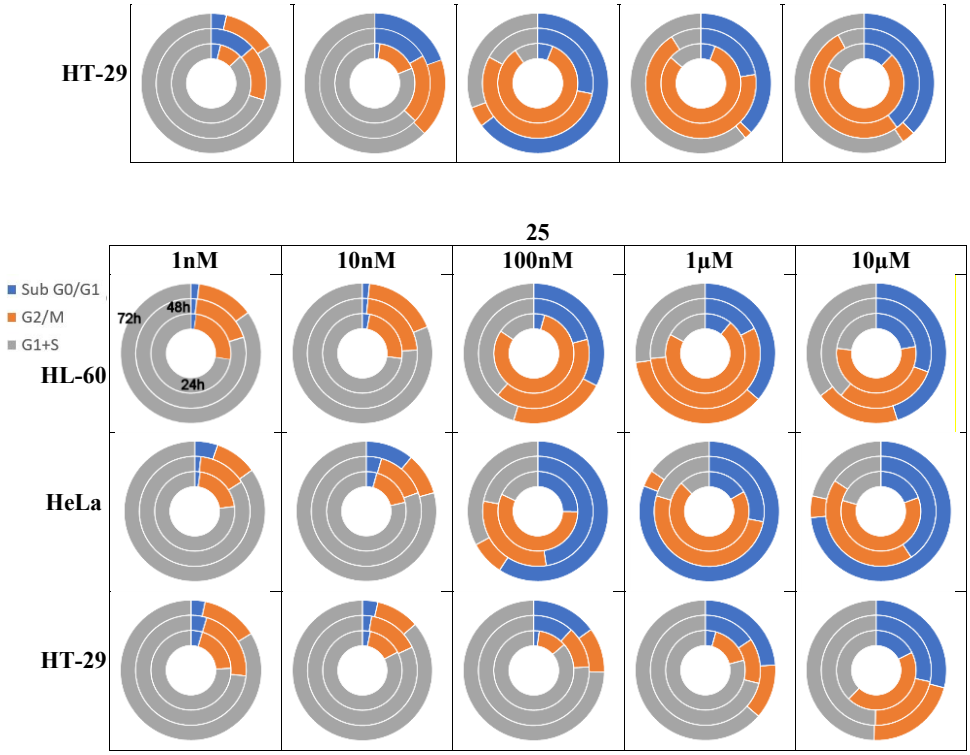

Figure 4. Time course of the effect of compounds **24** and **25** on the sub-G_0/G_1 and G_2/M cell cycle phases in HL-60, HeLa, and HT-29 cells. Compounds were incubated for 24, 48, and 72 h, and then their DNA content was analyzed by flow cytometry as described in the Experimental Section. The different cell cycle phases were quantified and represented in concentric hollow circles (24h inner, 48h center, and 72h outer) to easily visualize the evolution in time of the G_2/M arrest (■) and apoptotic responses (■ sub-G_0/G_1). Untreated control cells were run in parallel, and the percentage of untreated cells in the sub-G_0/G_1 region was less than 3% in all the cell lines assayed. Data shown are representative of at least three independent experiments.

The cell cycle distribution patterns for HL-60 and HeLa cells after treatment with **24** and **25** are very similar to each other, with mitotic arrest followed by an apoptotic response. These data suggest that the disruption of microtubule polymerization by **24** and **25** induce a potent mitotic arrest that eventually triggers an apoptotic response, thus rendering a substantial cell demise in the drug-treated population. On the other hand, HT-29 cells display quite a different cell cycle distribution profiles in response to the two compounds. With **24**, the observed pattern is like

those of HL-60 and HeLa cells, with arrest in the G_2/M arrest followed by the accumulation of apoptotic cells in the sub-G_0/G_1 region. However, after treatment with **25**, HT-29 cells undergo apoptotic response in the absence of patent G_2/M arrest. This different behavior is in accord with the observed difference in tubulin polymerization inhibitory potency of the two compounds (Table 2). Similar experiments on the non – tumorigenic embryonic kidney cell line HEK-293 show a similar mitotic arrest, but no apoptotic induction was observed after 24 h treatment (Supplementary Figure 2), thus suggesting a potential selectivity to induce apoptosis in human tumor cells.

In order to further support the above effects of compounds **24** and **25** on cell cycle arrest and apoptosis induction, we analyzed the expression of proteins related to these processes. Thus, we used the anti-mitotic proteins antibody MPM-2 that recognizes a phosphorylated epitope (S/T)P found in several phosphoproteins that result phosphorylated at the onset of mitosis. Our Western blot results shown in Figure 5 indicate a significant increase in the number of phosphoproteins recognized by MPM-2, simultaneously to the mitotic arrest observed at 24 h in the above cell cycle distribution studies. The lower intensity of the bands after 48 h treatment might likely be due to the onset of apoptosis. In this regard, we analyzed the cleavage of PARP (poly (ADP-ribose) polymerase), a typical caspase-3 substrate, as an early marker of apoptosis. The anti-PARP C2.10 monoclonal antibody detected the full length 116 kDa intact form as well as the 89 kDa cleaved form of PARP. Alongside with the observed sequential increase in the sub-G_0/G_1 population, we found an increase in the levels of cleaved PARP after treatment with 24 and 25, in good agreement with an apoptotic response induced by the sustained mitotic arrest.

Taken together, flow cytometry and biochemical evidences strongly indicate that compounds **24** and **25** behaved as anti-mitotic agents leading to M arrest and subsequent induction of apoptosis.

Formatted: Not Highlight

Formatted: Not Highlight

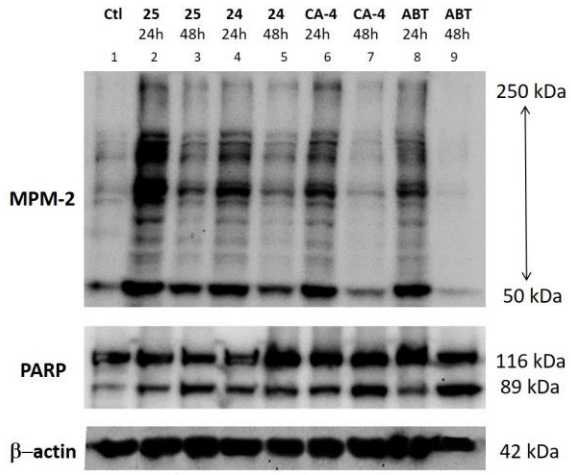

Figure 5. Effect of compounds **24** and **25**, and the reference compounds combretastatin A-4 (CA-4) and ABT-751 (ABT) on MPM-2 expression and PARP cleavage in HeLa cells after 24 and 48 h treatment. Lane 1: untreated HeLa (control Ctl). Lane 2: HeLa treated for 24h with 1 µM **25**. Lane 3: HeLa treated for 48h with 1 µM **25**. Lane 4: HeLa treated for 24 h with 1 µM **24**. Lane 5: HeLa treated for 48h with 1 µM **24**. Lane 6: HeLa treated for 24 h with 1 µM combretastatin A-4. Lane 7: HeLa treated for 48h with 1 µM combretastatin A-4. Lane 8: HeLa treated for 24 h with 1 µM ABT-751. Lane 9: HeLa treated for 48h with 1 µM ABT-751. β-Actin was used as a loading control. The migration positions of full-length PARP (p116) and its cleavage product p89 are indicated. Molecular weights areindicated in kDa. Western blot images are representative of three independent experiments.

2.3. Computational studies

Flexible docking studies of compounds **9** - **44** on the colchicine site of tubulin were carried out to establish the ligands' binding modes (Figure 7). The protein conformational space was sampled by using protein structures with 54 different pocket dispositions. 49 came from available X-ray crystal structures of complexes of tubulin with different colchicine site ligands.[46] 5 additional structures came from a molecular dynamics simulation of tubulin in complex with a 3-substituted indole containing ligand, as previously described.[35, 54] The docking poses were generated and scored by PLANTS[55] and AutoDock 4.2[56], two frequently used docking

Formatted: Not Highlight

programs with very different scoring functions. The docking scores of the two programs were combined to select the binding mode for each ligand (Table S1 of the supplementary material). The assignment of the occupancy of the ligands to zones of the colchicine domain (zones A, B, C, as previously described, and a deeper extension in β tubulin of zone C called zone D) of the binding site was performed in a fully automated way. The most favorable binding poses for all the compounds occupy zones A and B of the colchicine domain (corresponding to the pockets for the trimethoxyphenyl ring and the 3-hydroxy-4-methoxyphenyl ring of combretastatin A-4, respectively), probably reflecting a good steric fit of the bent diaryls to these pockets.[54, 57] In all instances, the substituted pyridines occupy the A zone and the other aromatic ring the zone B. This arrangement places the pyridine nitrogen in contact distance with the sulfur atom of Cys241β (Figure 7), a polar interaction deemed important for the binding of colchicine site ligands, while the rest of the moiety is contacting the hydrophobic sidechains of Leu239β, Leu245β, Ala247β, Leu252β, Ala315β, Lys352β, and Ala354β conforming the A site. The other aromatic ring stacks between the polar sidechain of Asn255β on helix H8 and those of Ala316β of sheet S8 and Lys352β of sheet S9 forming the floor of the site, and Met259β, Thr314β, and Val181α, also conforming zone B.

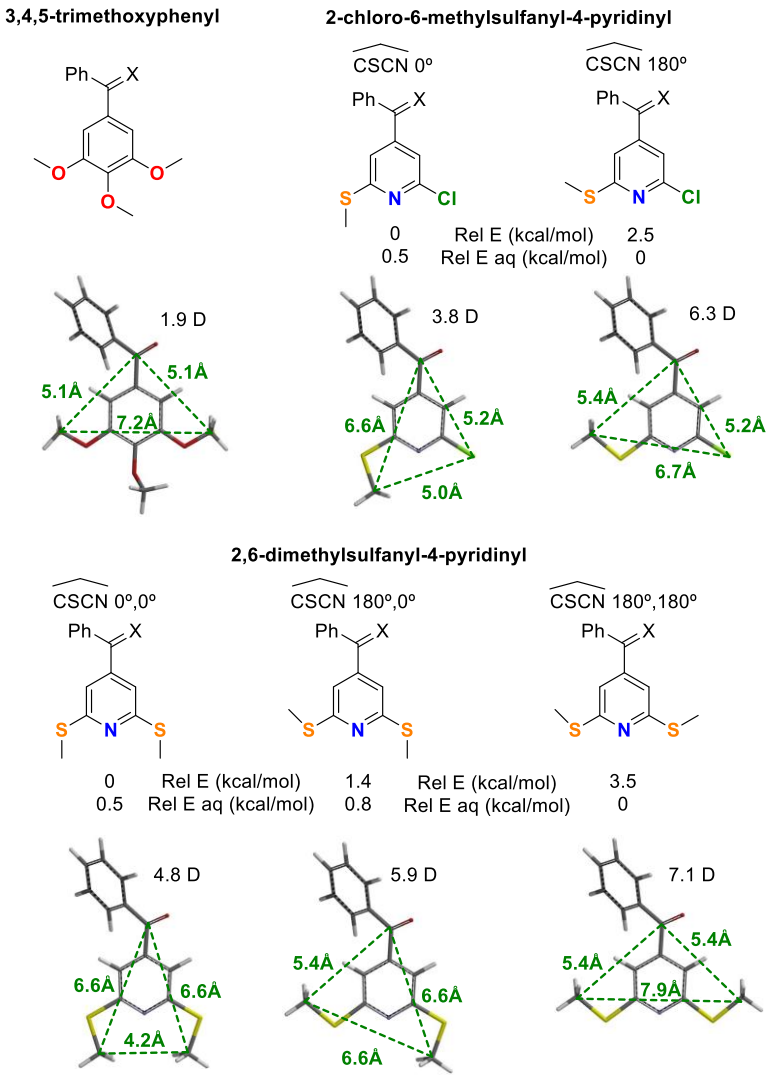

Figure 6. Comparison of the geometries of the trimethoxyphenyl ring taken as a reference A ring and the different conformers found for the 2-chloro-6-methylsulfanyl-4-pyridines and the 2,6-dimethylsulfanyl-4-pyridines. The results shown here are for the benzophenones, but similar results were obtained for oximes and isocombretastatins. The substituents on the pyridine are depicted in the 2D representation in the same dispositions as the 3D structures underneath. The green triangles indicate the dimensions of the A rings. The relative energies are in kcal/mol above the most stable, indicated as 0 kcal/mol. The calculated dipole moments for every conformer are also indicated.

The binding of the methylsulfanylpyridines to the A site always occurs with a rotation of the methylsulfanyl to place one of the sulfur lone pairs side by side to the pyridine nitrogen lone pair (CSCN dihedral angle of 180º, Figures 6 and 7). We have previously shown that this rotation is less unfavorable in methylsulfanyl than in methoxy groups.[46] We have performed DFT calculations to evaluate the energy penalty if any, of rotating the methylsulfanyl group to the observed rotamer in the docking studies (Figure 6) and the geometrical effects of such rotations. In water, the most favorable conformation places the pyridine and the sulfur lone pairs in the same direction (CSCN dihedral angle of 180º, Figure 6), thus increasing the molecule polarity and favoring interactions with water molecules. This should result in more favorable solvation, although solubility is not as high as expected (Table 1). In apolar media, represented by vacuum, the preferred rotamers place the methyl group of the methylsulfanyl close to the pyridine lone pair (CSCN dihedral angle of 0º, Figure 6). This would result in a larger size along the pyridine 1-4 axis and a masking of the nitrogen lone pair (Figure 6), but binding to the A zone as observed in the docking studies (Figure 7) requires a rotation to the polar conformer to reduce the steric demand along the pyridine long axis and to allow a polar interaction between the pyridine lone pair and the thiol group of Cys241β. Two identical methylsulfanyl groups provide an entropic advantage for the rotation, whereas the presence of one methylsulfanyl and one chlorine atom reduces the steric congestion in the long axis of the pyridine (Figure 6).

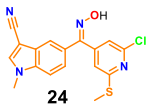

24

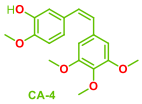

CA-4

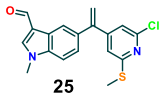

25

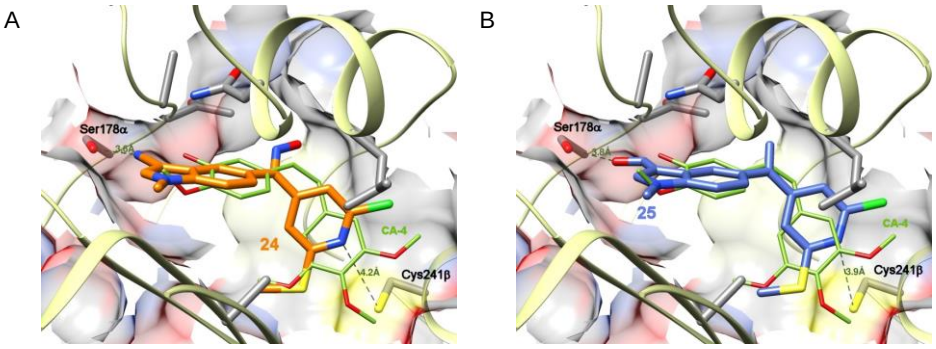

Figure 7. 2D structures of the compounds depicted in A and B. Proposed binding modes for compound **24** (carbons in orange) and **25** (carbons in aegean), superposed onto the X-ray structure of combretastatin A-4 (carbons in green) in their complexes with tubulin. The colchicine binding domain is depicted in lime (pdb ID 5LYJ), and the distances of the pyridine nitrogen to the sulfur atom of the sidechain of Cys241β and of the indole 3-substituent acceptor atom to the hydroxyl group of the sidechain of Ser178α is indicated in green.

The substituents at the 3 position of the indole ring enhance the antiproliferative potency of the 2-chloro-6-methylsulfanylpyridine derivatives. The docking models show that these polar groups hydrogen bond to the hydroxyl group of the sidechain of Ser178a (Figure 7), thus explaining the observed potency improvement. The preference of 2-chloro- versus 2-methylsulfanyl in the isocombretastatin and ketoxime series can be accounted for by the disposition of the methyl group towards the pyridine nitrogen (data not shown) due to conformational preferences and to a need of reducing the transversal size at the A zone (Figure 6) caused by steric hindrance of the site's walls, thus blocking the favorable polar interaction with the thiol group of Cys241β, which is maintained in the chloro derivatives. The unfavorable effect of the same substitution in the ketone (phenstatin) series is due to the higher conjugation of the bridge with the aromatic rings that results in flatter structures that collide with the site's walls when extended by substituents.[35] The combination of conformational and docking studies, therefore, provide a good rationale for the observed SAR of these new family of pyridine-based colchicine site ligands.

3. CONCLUSIONS

The successful replacement of the 3,4,5-trimethoxyphenyl ring by methylsulfanyl substituted pyridine rings in colchicine site ligands is reported. 2-Chloro-6-methylsulfanyl-4-pyridine and 2,6-dimethylsulfanyl-4-pyridines are polar entities that moderately improve the aqueous solubility to the compounds bearing them with respect to the trimethoxyphenyl analogues. The combination of methylsulfanyl substituted pyridine moieties with indole B rings gives diheteroaryl isocombretastatins, phenstatins, and ketone oximes which are potent inhibitors of tubulin polymerization and cytotoxic agents against several human cancer cell lines. The substitution of the indole at the 3 position with amides, nitriles, or formyl groups in the 2-chloro-6-methylsulfanyl-4-pyridine series further increases the polarity and provides optimal potency in the TPI and cytotoxicity assays. The most potent compound, the 3-cyanoindole 2-chloro-6-methylsulfanyl-4-pyridine oxime **24** disrupted the microtubule network of treated cells and arrested the cell cycle at the G_2/M phase after 24 h, followed by a high apoptosis-like cell response. The 3-formylindole 2-chloro-6-methylsulfanyl-4-pyridine isocombretastatin **25**, showed similar effects as **24** in the more sensitive HeLa and HL60 cells, wheres in the more resistant HT-29 cells a weak apoptotic response in the absence of G_2/M arrest is observed after 24 hours, which suggests that it might activate an additional cell death response to the microtubule effect by unknown mechanisms. Binding at the colchicine site is supported by docking studies that allocate the pyridine ring at the sub-pocket of the trimethoxyphenyl rings in the colchicine domain. Docking results combined with conformational studies suggest that binding to the thiol group of Cys241b is more favorable in 2-chloro-6-methylsulfanyl-4-pyridines than in 2,6-dimethylsulfanyl-4-pyridines, thus providing a rationale for their better activity profile. The synthesized compounds have improved aqueous solubility and good anti-mitotic potency and therefore the structural modifications here described could be applied in the design of new colchicine site ligands.

4. EXPERIMENTAL SECTION

4.1. Chemistry

4.1.1. General chemical techniques

Reagents were used as purchased without further purification. Solvents (THF, DMF, dichloromethane, and toluene) were dried and freshly distilled before use according to procedures described in the literature. TLC was performed on pre-coated silica gel polyester plates (0.25 mm thickness) with a UV fluorescence indicator 254 (Polychrome SI F254). Chromatographic separations were performed on silica gel columns by flash (Kieselgel 40, 0.040-0.063; Merck) or gravity (Kieselgel 60, 0.063-0.200 mm; Merck) chromatography. Melting points were determined on a Büchi 510 apparatus and are uncorrected. ^{1}H NMR and ^{13}C NMR spectra were recorded in $CDCl_3$ on a Bruker WP 200-SY spectrometer at 200/50 MHz or on a Bruker SY spectrometer at 400/100 MHz. Chemical shifts (δ) are given in ppm downfield from tetramethylsilane and coupling constants (*J* values) are in Hertz. IR spectra were run on a Nicolet Impact 410 Spectrophotometer. For FABHRMS analyses, a VG-TS250 apparatus (70 eV) was used. HPLCs were run on Waters X-Terra® MS C_{18} (5 mm, 4.6x150 mm) or C_8 (5 mm, 4.6x150 mm) with acetonitrile/water solvent gradients. All the compounds described here were obtained with at least 95% of purity by quantitative HPLC and/or elemental analysis, unless otherwise stated.

4.1.2. Chemical synthesis

General synthetic procedure for the preparation of diarylketones (Procedure 1)

1 equivalent of *n*BuLi (1.6 M in hexane) was added at -40 ºC onto a solution of the aromatic bromoderivative in dry THF. One hour later, 0.4 equivalents of the carboxylic acid in dry THF was added and the mixture was allowed to reach room temperature. After 24 h, the reaction was

poured onto ethyl formate, and then ethyl acetate and water were added. The mixture was partially evaporated, washed with brine, dried over anhydrous Na_2SO_4, filtered, and evaporated to dryness. The products obtained were purified by flash chromatography.

General synthetic procedure for the preparation of isocombretastatins (Procedure 2)

0.67 equivalents of *n*BuLi (1.6 M in hexane) were added to a slurry of the phosphonium salt in dry THF at -40 ºC and, after one-hour stirring, 0.33 equivalents of the diaryl ketone in dry THF was added and then the mixture was allowed to warm to room temperature and react for 24 hours. The mixture was poured onto a 5% solution of NH_4Cl at 0 ºC, ethyl acetate was added and the mixture was partially evaporated under vacuum. The organic layers were washed with brine, dried over anhydrous Na_2SO_4, filtered, and evaporated to dryness. The products were purified by flash chromatography.

General synthetic procedure for the preparation of oximes (Procedure 3)

A solution of the carbonyl compound in methanol, 10 equivalents of hydroxylamine hydrochloride, and 4 drops of pyridine were refluxed for 24 h. The crude was evaporated to dryness, dissolved in dichloromethane, and washed with brine. The organic phases were dried over anhydrous Na_2SO_4, filtered, and evaporated. The products were purified by flash chromatography giving a mixture of oximes (*E* and *Z*). Oximes were obtained as roughly 1:1 mixtures of the two isomers (proportions can significantly change depending on solvent composition), which readily interconvert in solution. Crystallization of one of the isomers is sometimes possible, but it readily regenerates the mixture in solution.

Formatted: Not Highlight

General indole formylation procedure (Procedure 4)

6 mmol of phosphorus oxychloride per mmol of indole derivative were added at 0 ºC onto dry DMF and stirred for 30 minutes. Then, the indole derivative was added and heated to 60 ºC for 2-24 h for benzophenones or kept 2 hours at room temperature for 1,1-diarylethenes. The solution was poured onto a large volume of ice water saturated with sodium acetate. After 24 h at 4 ºC, the precipitate was filtered, dissolved in dichloromethane, dried over anhydrous Na_2SO_4, filtered, and evaporated to dryness. The products were purified by flash chromatography

General synthetic procedure for the preparation of carbonitriles (Procedure 5)

A solution of the aldehyde in methanol and 4 drops of pyridine, and 10 equivalents of hydroxylamine hydrochloride was refluxed for 24 hours. The solvent was removed, and the product was dissolved in dichloromethane. The organic layer was washed with 2N HCl, brine until neutral pH, dried over anhydrous Na_2SO_4, filtered, and concentrated under vacuum. The crude was dissolved in pyridine and an excess of acetic anhydride and stirred for 24-48 hours at 130 ºC. The reaction was poured onto ice and extracted with dichloromethane, washed with 2N HCl, 5% $NaHCO_3$, brine until neutral pH, dried over anhydrous Na_2SO_4, filtered, and evaporated to dryness. The products were purified by flash chromatography.

2,6-Dichloropyridine-4-carboxylic acid (1)

45.1 g of citrazinic acid (291 mmol) and 31 g of tetramethylammonium chloride (282.8 mmol) in $POCl_3$ (80 mL) was heated to 90 °C until complete dissolution. Then, the temperature was gradually increased to 140 ºC. After 24 h, the mixture was cooled to room temperature and poured onto ice. The precipitate was filtered, washed with water and dried under vacuum. The solid was suspended in ethyl acetate, stirred for 15 min, and filtered to remove insoluble citrazinic acid. The filtrate was dried over anhydrous Na_2SO_4 and evaporated to obtain 42 g (218.8 mmol, 75.2%) of a brown solid corresponding to **1.** M.p. 203-204 ºC. IR (KBr): 2600-3300, 1724, 1596, 1547 cm^{-1}. ^1H NMR (200 MHz, DMSO-D_6): 7.83 (2H, s). ^{13}C NMR (50 MHz, CD_3OD): 124.0 (2) (CH), 145.4 (C), 152.2 (2) (C), 165.0 (C).

2-Chloro-6-methylsulfanylpyridine-4-carboxylic acid (2)

3.84 g (54.8 mmol) of sodium methanethiolate in 50 mL of dry DMF and 4 g of KOH were added onto a solution of 7 g (36.5 mmol) of 2,6-dichloropyridine-4-carboxylic acid (**1**) in 100 mL of dry DMF and the mixture was refluxed for 24 h. The reaction was cooled to room temperature, poured onto brine, and extracted with ethyl acetate. The organic phase was washed with 2N HCl and brine until neutral pH, dried over anhydrous Na_2SO_4, filtered and evaporated, obtaining 6.71 g (32.9 mmol, 90.1%) of 2-chloro-6-methylsulfanylpyridine-4-carboxylic acid (**2**). IR (film): 3100, 1706, 1588, 1545 cm^{-1}. ^1H NMR (200 MHz, CD_3OD): 2.46 (3H, s), 7.40 (1H, *d*, *J* = 1), 7.54 (1H, *d*, *J* = 1). ^{13}C NMR (50 MHz, CD_3OD): 13.7 (CH_3), 119.4 (CH), 120.3 (CH), 142.2 (C), 152.6 (C), 163.7 (C), 166.2 (C).

2,6-bis(methylsulfanyl)pyridine-4-carboxylic acid (3)

390 mg (1.92 mmol) of 2-chloro-6-methylsulfanylpyridine-4-carboxylic acid (**2**) and a 10 mol excess of sodium methanethiolate in 5 mL of dry DMF was refluxed for 72 h under N_2 atmosphere. The reaction was cooled down to room temperature, poured onto 2N HCl, and extracted with ethyl acetate. The organic phase was washed with brine until neutral pH, dried over anhydrous Na_2SO_4, filtered and evaporated, obtaining 216 mg (1.01 mmol, 53%) of 2,6-bis(methylsulfanyl)pyridine-4-carboxylic acid (**3**). ^{1}H NMR (200 MHz, CD_3OD): 2.48 (6H, *s*), 7.25 (2H, *s*). ^{13}C NMR (50 MHz, CD_3OD): 13.4 (2) (CH_3), 116.5 (2) (CH), 139.5 (C), 162.2 (2) (C), 167.5 (C).

(2,6-bis(methylsulfanyl)pyridin-4-yl)methanol (4)

290 mg (7.64 mmol) of LAH were slowly added to a cooled solution of 1.098 g (5.10 mmol) of 2,6-bis(methylsulfanyl)pyridine-4-carboxylic acid (**3**) in dry THF. After 1h, the mixture was poured onto cooled ethyl acetate. The organic phase was dried over anhydrous Na_2SO_4, filtered, and chromatographed using Hexane/Ethyl acetate 9/1 to yield 590 mg (2.9 mmol; 58%) of (2,6-bis(methylsulfanyl)pyridin-4-yl)methanol (**4**). ^{1}H NMR (200 MHz, $CDCl_3$): 2.57 (6H, *s*); 4.58 (2H, *s*); 6.84 (2H, *s*). ^{13}C NMR (50 MHz, $CDCl_3$): 13.4 (2) (CH_3), 63.0 (CH_2), 113.8 (2) (CH), 150.3 (C), 159.5 (2) (C). IR (film): 1539, 1581, 3351 cm^{-1}.

4-(bromomethyl)-2,6-bis(methylsulfanyl)pyridine (5)

361 mg (1.8 mmol) of (2,6-bis(methylsulfanyl)pyridin-4-yl)methanol (**4**) were dissolved in 5 mL of a 32% solution of HBr in acetic acid at 0 ºC and stirred for 6h. The reaction was poured onto ice and extracted with EtOAc. The organic layer was washed with 5% $NaHCO_3$ and brine, dried over anhydrous Na_2SO_4, filtered an evaporated to yield 405 mg (1.5 mmol; 86%) of 4-(bromomethyl)-2,6-bis(methylsulfanyl)pyridine (**5**). ^{1}H NMR (200 MHz, $CDCl_3$): 2.59 (6H, *s*), 4.24 (2H, *s*); 6.87 (2H, *s*). ^{13}C NMR (50 MHz, $CDCl_3$): 13.2 (2) (CH_3), 30.5 (CH_2), 116.4 (2) (CH), 146.0 (C), 156.0 (2) (C). IR (film): 1431, 1540, 1581, 1742 cm^{-1}.

((2,6-bis(methylsulfanyl)pyridin-4-yl)methyl)triphenylphosphonium bromide (6)

408 mg (1.6 mmol) of triphenylphosphine was added to a solution of 355 mg (1.34 mmol) of 4-(bromomethyl)-2,6-bis(methylsulfanyl)pyridine (**5**) in toluene. After 24 hours the White solid

formed was filtered to yield 323 mg (0.6 mmol; 46%) of ((2,6-bis(methylsulfanyl)pyridin-4-yl)methyl)triphenylphosphonium bromide (**6**). ^{1}H NMR (200 MHz, $CDCl_3$): 2.39 (6H, *s*), 5.65 (2H, *s*), 6.72 (2H, *s*), 7.80 (15H, *m*). IR (film): 1435, 1535, 1574 cm^{-1}.

1-Methyl-1*H*-indole-5-carbaldehyde (8)

1.04 g (26 mmol) of NaOH and 20 mg of *n*-Bu_4NHSO_4 were added to a stirred solution of 1*H*-indole-5-carbaldehyde (2.0 g, 13.8 mmol) in 40 mL of dry dichloromethane. After 1 h at room temperature 3 mL (40.2 mmol) of methyl iodide were added and the reaction was heated at 50 ºC. After 48 h, the reaction mixture was concentrated, re-dissolved in dichloromethane, washed with brine, dried over anhydrous Na_2SO_4, filtered and concentrated in vacuum to obtain 1.10 g (50.1%) of 1-methyl-1*H*-indole-5-carbaldehyde (**11**): M.p. 85-86 ºC (diethylether). ^{1}H NMR (200 MHz, $CDCl_3$): 3.76 (3H, *s*), 6.55 (1H, *d*, *J* = 3.3), 7.10 (1H, *d*, *J* = 3.3), 7.41(1H, *d*, *J* = 8.8), 7.80 (1H, *dd*, *J* = 8.8 and 1.9), 8.05 (1H, *d*, *J* = 1.9), 9.92 (1H, *s*). ^{13}C NMR (50 MHz, $CDCl_3$): 32.6 (CH_3), 103.1 (CH), 109.8 (CH), 121.4 (CH), 126.1 (CH), 128.2(C), 129.1 (C), 130.9 (CH), 139.8 (C), 192.3 (CH).

(2-chloro-6-(methylsulfanyl)pyridin-4-yl)(4-methoxyphenyl)methanone (**9**)

Following procedure 1, 11.5 ml (18.4 mmol) of *n*BuLi 1.6 M in hexanes were slowly added at -40 ºC to a solution of 2.33 ml (18.4 mmol) of 4-bromoanisole in 40 mL of dry THF. After 45 minutes, 1.5 g (7.37 mmol) of 2-chloro-6-methylsulfanylpyridine-4-carboxylic acid (**2**) dissolved in 15 mL of dry THF was added. Flash chromatography using Hexane/AcOEt (95/5) yielded 509 mg (1.73 mmol; 24%) of (2-chloro-6-(methylsulfanyl)pyridin-4-yl)(4-methoxyphenyl)methanone (**9**) and 864 mg (2.35 mmol; 32%) of ethyl 3-(2-chloro-6-(methylsulfanyl)pyridin-4-yl)-3-hydroxy-3-(4-methoxyphenyl)propanoate (**9a**).

(2-Chloro-6-(methylsulfanyl)pyridin-4-yl)(4-methoxyphenyl)methanone (**9**): ^{1}H NMR (200 MHz, $CDCl_3$): 2.55 (3H, *s*), 3.88 (3H, *s*), 6.95 (2H, *d*, *J* = 8.9), 7.16 (1H, *d*, *J* = 0.7), 7.26 (1H, *d*, *J* = 0.7), 7.77 (2H, *d*, *J* = 8.6). ^{13}C NMR (50 MHz, $CDCl_3$): 13.6 (CH_3), 55.7 (CH_3), 114.1 (2) (CH), 118.2 (CH), 119.0 (CH), 128.1 (C), 132.7 (2) (CH), 147.9 (C), 151.3 (C), 161.9 (C), 164.3 (C), 191.9 (C). IR (film): 1420, 1459, 1528, 1577, 1597, 1660 cm^{-1}. HRMS ($C_{14}H_{13}ClNO_2S$): calculated ($M+H^+$) 294.0350, found 294.0335.

Ethyl 3-(2-chloro-6-(methylsulfanyl)pyridin-4-yl)-3-hydroxy-3-(4-methoxyphenyl)propanoate (**9a**). ^{1}H NMR (200 MHz, $CDCl_3$): 1.20 (3H, *t*, *J* = 7.1), 2.54 (3H, *s*), 3.09 (1H, *d*, *J* = 16.5), 3.12 (1H, *dd*, *J* = 16.4), 3.77 (3H, s), 4.12 (2H, *c*, *J* = 7.1), 6.85 (2H, *d*, *J* = 8.9), 7.03 (1H, *d*, *J* = 1.4), 7.17 (1H, *d*, *J* = 1.4), 7.30 (2H, *d*, *J* = 8.9). ^{13}C NMR (50 MHz, $CDCl_3$): 13.5 (CH_3), 14.0 (CH_3), 44.6 (CH_2), 55.3 (CH_3), 61.4 (CH_2), 75.3 (C), 114.0 (2) (CH), 116.5 (CH), 116.7 (CH), 126.7 (2) (CH), 135.9 (C), 151.2 (C), 158.1 (C), 159.1 (C), 161.1 (C), 172.3 (C). IR (film): 1514, 1533, 1582, 1606, 1714, 3450 cm^{-1}. HRMS ($C_{18}H_{20}ClNO_4S$): calculated ($M+H^+$) 382.0874, found 382.0888.

(2,6-bis(methylsulfanyl)pyridin-4-yl)(4-methoxyphenyl)methanone (**10**)

Following procedure 1, 7.2 ml (11.6 mmol) of *n*BuLi 1.6 M in hexanes were slowly added at -40 ºC to a solution of 1.45 ml (11.6 mmol) of 4-bromoanisole in 40 mL of dry THF. After 45 minutes, 1g (4.6 mmol) of 2,6-bis(methylsulfanyl)pyridine-4-carboxylic acid (**3**) dissolved in 15 mL of dry THF was added. Flash chromatography using Hexane/AcOEt (95/5) yielded 626 mg (2.1 mmol; 45.7%) of (2,6-bis(methylsulfanyl)pyridin-4-yl)(4-methoxyphenyl)methanone (**10**). M.p. (Hex/CH_2Cl_2): 103 ºC. ^{1}H NMR (200 MHz, $CDCl_3$): 2.61 (6H, *s*), 3.89 (3H, *s*), 6.96 (2H, *d*, *J* = 8.8), 7.05 (2H, *s*), 7.80 (2H, *d*, *J* = 8.8). ^{13}C NMR (50 MHz, $CDCl_3$): 13.4 (2) (CH_3), 55.6 (CH_3), 113.9 (2) (CH), 115.6 (2) (CH), 128.6 (C), 132.6 (2) (CH), 145.3 (C), 160.2 (2) (C), 164.0 (C), 193,2 (C). IR (KBr): 1544, 1592, 1655 cm^{-1}. HRMS ($C_{15}H_{16}NO_2S_2$): calculated ($M+H^+$) 306.0617, found 306.0612.

2-chloro-4-(1-(4-methoxyphenyl)vinyl)-6-(methylsulfanyl)pyridine (11)

Following procedure 2, 0.8 ml (1.3 mmol) of *n*BuLi 1.6 M in hexanes were slowly added at -40 ºC to a solution of 790 mg (1.96 mmol) of methyltriphenylphosphonium iodide in 10 mL of dry THF. After 1 hour, 192 mg (0.65 mmol) of (2-chloro-6-(methylsulfanyl)pyridin-4-yl)(4-methoxyphenyl)methanone (**9**) dissolved in 10 mL of dry THF was added. Flash chromatography using Hexane/EtOAc (99/1) yielded 65 mg (0.22 mmol; 34%) of 2-chloro-4-(1-(4-methoxyphenyl)vinyl)-6-(methylsulfanyl)pyridine (**11**). ^{1}H NMR (200 MHz, $CDCl_3$): 2.56 (3H, *s*), 3.84 (3H, *s*), 5.47 (1H, *s*), 5.53 (1H, *s*), 6.88 (2H, *d*, *J* = 8.6), 6.95 (1H, *s*), 7.03 (1H, *s*), 7.20 (2H, *d*, *J* = 8.6). ^{13}C NMR (50 MHz, $CDCl_3$): 13.6 (CH_3), 55.4 (CH_3), 114.0 (2) (CH), 116.4 (CH_2), 118.6 (CH), 119.1 (CH), 129.3 (2) (CH), 113. 6 (C), 146.3 (C), 151.1 (C), 152.1 (C), 159.9 (C),

160.9 (C). IR (film): 1417, 1457, 1518, 1602 cm^{-1}. HRMS ($C_{15}H_{14}ClNOS$): Calculated ($M+H^+$) 292.0557 found 292.0572.

4-(1-(4-methoxyphenyl)vinyl)-2,6-bis(methylsulfanyl)pyridine (12)

Following procedure 2, 1.4 ml (2.2 mmol) of *n*BuLi 1.6 M in hexanes were slowly added at -40 ºC to a solution of 1.32 g (3.27 mmol) of methyltriphenylphosphonium iodide in 10 mL of dry THF. After 1 hour, 333 mg (1.09 mmol) of (2,6-bis(methylsulfanyl)pyridin-4-yl)(4-methoxyphenyl)methanone (**10**) dissolved in 10 mL of dry THF was added. Flash chromatography using Hexane/EtOAc (97/3) yielded 309 mg (1.02 mmol; 94 %) of 4-(1-(4-methoxyphenyl)vinyl)-2,6-bis(methylsulfanyl)pyridine (**12**). ^{1}H NMR (200 MHz, $CDCl_3$): 2.59 (6H, *s*), 3.83 (3H, *s*), 5.42 (1H, *d*, *J* = 1.1), 5.47 (1H, *d*, *J* = 1.1), 6.82 (2H, *s*), 6.86 (2H, *d*, *J* = 8.6), 7.21 (2H, *d*, *J* = 8.6). ^{13}C NMR (50 MHz, $CDCl_3$): 13.3 (2) (CH_3), 55.4 (CH_3), 113.8 (2) (CH), 115.4 (CH_2), 116.3 (2) (CH), 129.3 (2) (CH), 132.1 (C), 147.1 (C), 149.4 (C), 159.3 (2) (C), 159.7 (C). IR (película): 1523, 1593, 1654 cm^{-1}. HRMS ($C_{16}H_{17}NOS_2$): calculated ($M+H^+$) 304.0824, found 304.0835.

(*E*/*Z*)-(2-chloro-6-(methylsulfanyl)pyridin-4-yl)(4-methoxyphenyl)methanone oxime (13)

Following procedure 3, 229 mg (3.30 mmol) of hydroxylamine hydrochloride was added to a solution of 97 mg (0.33 mmol) of (2-chloro-6-(methylsulfanyl)pyridin-4-yl)(4-methoxyphenyl)methanone (**9**) in 15 mL of MeOH to yield 91 mg (0.29 mmol, 89%). The oximes crystalize in hexane/CH_2Cl_2 as a mixture of the oximes (E/Z)-(2-chloro-6-(methylsulfanyl)pyridin-4-yl)(4-methoxyphenyl)methanone oxime (**13**). M.p. (Hex/CH_2Cl_2): 100-105 ºC. ^{1}H NMR (200 MHz, $CDCl_3$): 2.55 (3H, *s*), 2.58 (3H, *s*), 3.83 (3H, *s*), 3.87 (3H, *s*), 6.87 (2H, *d*, *J* = 8.9), 6.98 (1H, *d*, *J* = 1.1), 6.99 (2H, *d*, *J* = 8.9), 7.05 (1H, *d*, *J* = 1.1), 7.09 (1H, *d*, *J* = 1.2), 7.14 (1H, *d*, *J* = 1.2), 7.33 (2H, *d*, *J* = 8.9), 7.37 (2H, *d*, *J* = 8.9). ^{13}C NMR (50 MHz, $CDCl_3$): 13.5 (CH_3), 55.3 (CH_3), 113.9 (CH), 114.0 (2) (CH), 118.9 (CH), 119.6 (CH), 126.5 (C), 128.8 (2) (CH), 130.8 (CH), 143.4 (C), 151.2 (C), 154.4 (C), 160.5 (C), 161.2 (C), 161.4 (C). IR (KBr): 1412, 1446, 1524, 1573, 1603, 3177 cm^{-1}. HRMS ($C_{14}H_{13}ClN_2O_2S$): Calculated ($M+H^+$) 309.0459, found 309.0438.

(*E*/*Z*)-(2,6-bis(methylthio)pyridin-4-yl)(4-methoxyphenyl)methanone oxime (14)

Following procedure 3, 403 mg (5.8 mmol) of hydroxylamine hydrochloride was added to a solution of 177 mg (0.58 mmol) of (2,6-bis(methylsulfanyl)pyridin-4-yl)(4-methoxyphenyl)methanone (**10**) in 15 mL of MeOH. The resulting product was chromatographed with hexane/EtOAc (9:1) to give 13 mg (0.04 mmol; 7%) of one oxime, and 141,2 mg (0,44 mmol; 76%) of the mixture of the two oximes (*E*/*Z*)-(2,6-bis(methylthio)pyridin-4-yl)(4-methoxyphenyl)methanone oxime (**14**), that crystalize in Hex/CH_2Cl_2. M.p. (Hex/CH_2Cl_2): 125 – 127 ºC. ^{1}H NMR (200 MHz, $CDCl_3$): 2.56 (6H, *s*), 3.86 (3H, *s*), 6.93 (2H, *s*), 6.98 (2H, *d*, *J* = 8.9), 7.36 (2H, *d*, *J* = 8.9). ^{1}H NMR (200 MHz, $CDCl_3$): 2.60 (6H, s), 3.81 (3H, s), 6.85 (2H, d, J = 8.9), 6.85 (2H, s), 7.36 (2H, d, J=8.9). ^{13}C NMR (50 MHz, $CDCl_3$): 13.4 (2) (CH_3), 55.4 (CH_3), 113.8 (2) (CH), 115.5 (2) (CH), 122.8 (C), 131.2 (2) (CH), 144.1 (C), 155.6 (C), 159.9 (2) (C), 160.6 (C). ^{13}C NMR (50 MHz, $CDCl_3$): 13.4 (2) (CH_3), 55.4 (CH_3), 114.1 (2) (CH), 116.3 (2) (CH), 126.7 (C), 129.0 (2) (CH), 140.9 (C), 155.3 (C), 159.9 (2) (C), 161.2 (C). IR (KBr): 1417, 1456, 1518, 1573, 1605, 3434 cm^{-1}. HRMS ($C_{15}H_{16}N_2O_2S_2$): calculated ($M+Na^+$) 343.0545, found 343.0562.

4-(1-(4-methoxyphenyl)ethyl)-2,6-bis(methylsulfanyl)pyridine (15)

16 mg (0.05 mmol) of 4-(1-(4-methoxyphenyl)vinyl)-2,6-bis(methylsulfanyl)pyridine **(12)** in 10 ml of AcOEt/EtOH (95/5) was vigorously stirred under H_2 atmosphere with Pd(C) catalysis for 24h. The reaction was filtered through celite©, evaporated and chromatographed by preparative thin layer chromatography with Hexane/EtOAc (98/2) to yield 7 mg (0.02 mmol; 45%) of 4-(1-(4-methoxyphenyl)ethyl)-2,6-bis(methylsulfanyl)pyridine **(15)**. ^{1}H NMR (200 MHz, $CDCl_3$): 1.55 (3H, *d*, *J* = 7.2), 2.56 (6H, *s*), 3.79 (3H, *s*), 3.90 (1H, *c*, *J* = 7.2), 6.71 (2H, *s*), 6,83 (2H, *d*, *J* = 8.8), 7,06 (2H, *d*, *J* = 8.8). ^{13}C NMR (50 MHz, $CDCl_3$): 13.3 (2) (CH_3), 21.2 (CH_3), 43.3 (CH), 55.4 (CH_3), 113.9 (2) (CH), 114.0 (C), 116.3 (2) (CH), 128.6 (2) (CH), 136.3 (2) (C), 155.5 (C), 159.0 (C). IR (film): 1456, 1513, 1533, 1575, 1610 cm^{-1}. HRMS ($C_{16}H_{19}NOS_2$): calculated ($M+H^+$) 306.0981, found 306.0987.

(2-Chloro-6-(methylsulfanyl)pyridin-4-yl)(1-methyl-1H-indol-5-yl)methanone (16)

Following procedure 1, 15.4 ml (24.6 mmol) of *n*BuLi 1.6 M in hexanes was slowly added to a solution of 5.16 g (24.6 mmol) of 5-bromo-*N*-methyl-1*H*-indol (**7**) in dry THF at -40 ºC. After 45 minutes, 2 g (9.8 mmol) of 2-chloro-6-methylsulfanylpyridine-4-carboxylic acid (**2**) in 10 mL of dry THF was added. The reaction product was flash chromatographed using Hexane/EtOAc (9/1) toyield 1.09 g (3.44 mmol, 35%) of (2-chloro-6-(methylsulfanyl)pyridin-4-yl)(1-methyl-1*H*-indol-5-yl)methanone (**16**) as white needles. M.p. (Hex/AcOEt): 116-123 ºC. ^{1}H NMR (200 MHz, $CDCl_3$): 2.60 (3H, *s*), 3.86 (3H, *s*), 6.63 (1H, *d*, *J* = 2.8), 7,16 (1H, *d*, *J* = 2.8), 7.25 (1H, *s*), 7.33 (1H, *s*), 7.40 (1H, *bd*, *J* = 8.9), 7.79 (1H, *bd*, *J* = 8,6), 8.06 (1H, *s*). ^{13}C NMR (50 MHz, $CDCl_3$): 13.7 (CH_3), 33.2 (CH_3), 103.5 (CH), 109.7 (CH), 118.5 (CH), 119.2 (CH), 123.4 (CH), 125.9 (CH), 127.3 (C), 127.9 (C), 131.0 (CH), 139.6 (C), 149.0 (C), 151.3 (C), 161.8 (C), 193.8 (C). IR (KBr): 1446, 1530, 1565, 1601, 1645 cm^{-1}. HRMS ($C_{16}H_{13}ClN_2OS$): calculated ($M+Na^+$) 339.0329, found 339.0316.

(2,6-Bis(methylsulfanyl)pyridin-4-yl)(1-methyl-1*H*-indol-5-yl)methanone (17)

Following procedure 1, 7.2 ml (11.5 mmol) of *n*BuLi 1.6 M in hexanes was slowly added to a solution of 2.44 g (11.5 mmol) of 5-bromo-*N*-methyl-1*H*-indol (**7**) in dry THF at -40 ºC. After 45 minutes, 1 g (4.6 mmol) of 2,6-bis(methylsulfanyl)pyridine-4-carboxylic acid (**3**) in 10 mL of dry THF was added. The reaction product was flash chromatographed using Hexane/EtOAc (9/1) to yield 412 mg (1.25 mmol; 27%) of (2,6-bis(methylsulfanyl)pyridin-4-yl)(1-methyl-1*H*-indol-5-yl)methanone (**17**). ^{1}H NMR (200 MHz, $CDCl_3$): 2.62 (6H, *s*), 3.85 (3H, *s*), 6.60 (1H, *d*, *J* = 3.2), 7.10 (2H, *s*), 7.15 (1H, *d*, *J* = 3.2), 7.38 (1H, *bd*, *J* = 8.8), 7.80 (1H, *dd*, *J* = 1.8, *J* = 8.8), 8.07 (1H, *d*, *J* = 1.8). ^{13}C NMR (50 MHz, $CDCl_3$): 13.5 (2) (CH_3), 33.2 (CH_3), 103.4 (CH), 109.6 (CH), 115.9 (2) (CH), 123.5 (CH), 125.8 (CH), 127.7 (C), 127.9 (C), 130.9 (CH), 139.5 (C), 146.4 (C), 160.1 (2) (C), 195.1 (C). IR (KBr): 1526, 1565, 1603, 1652 cm^{-1}. HRMS ($C_{17}H_{16}N_2OS_2$): calculated ($M+H^+$) 329.0777, found 329.0761.

5-(1-(2-Chloro-6-(methylsulfanyl)pyridin-4-yl)vinyl)-1-methyl-1*H*-indole (18)

Following procedure 2, 3.4 ml (5.4 mmol) of *n*BuLi 1.6 M in hexanes was slowly added to a stirred suspension of 3.251 g (8.07 mmol) of methyltriphenylphosphonium iodide in 50 mL of dry THF at -40 ºC. After 45 minutes, 852 mg (2.69 mmol) of (2-chloro-6-(methylsulfanyl)pyridin-4-yl)(1-methyl-1*H*-indol-5-yl)methanone (**16**) was added. Flash chromatography with

Hexane/EtOAc (98/2) yielded 194 mg (0.62 mmol; 23 %) of 5-(1-(2-chloro-6-(methylsulfanyl)pyridin-4-yl)vinyl)-1-methyl-1*H*-indole (**18**). ^{1}H NMR (200 MHz, $CDCl_3$): 2.60 (3H, *s*), 3.82 (3H, *s*), 5.53 (1H, *s*), 5.61 (1H, *s*), 6.50 (1H, *s*), 7.01 (1H, *s*), 7.10 (2H, *s*), 7.14 (1H, *bd*, *J* = 8,6), 7.33 (1H, *bd*, *J* = 8.6), 7.54 (1H, *s*). ^{13}C NMR (50 MHz, $CDCl_3$): 13.7 (CH_3), 33.0 (CH_3), 101.6 (CH), 109.4 (CH), 116.4 (CH_2), 118.9 (CH), 119.3 (CH), 120.9 (CH), 122.0 (CH), 128.5 (C), 129.9 (CH), 130.7 (C), 136.7 (C), 147.9 (C), 151.1 (C), 153.0 (C), 160.8 (C). IR (film): 1422, 1442, 1492, 1519, 1576 cm^{-1}. HRMS ($C_{17}H_{15}ClN_2S$): calculated ($M+H^+$) 315.0717, found 315.0723.

5-(1-(2,6-Bis(methylsulfanyl)pyridin-4-yl)vinyl)-1-methyl-1*H*-indole (19)

Following procedure 2, 1.1 ml (1.76 mmol) of *n*BuLi 1.6 M in hexanes was slowly added to a stirred suspension of 1.07 g (2.65 mmol) of methyltriphenylphosphonium iodide in 50 mL of dry THF at -40 ºC. After 45 minutes, 290 mg (0.88 mmol) of (2,6-bis(methylsulfanyl)pyridin-4-yl)(1-methyl-1*H*-indol-5-yl)methanone (**17**) was added. Flash chromatography with 95/5 Hexane/EtOAc yielded 134 mg (0.41 mmol; 47 %) of 5-(1-(2,6-bis(methylsulfanyl)pyridin-4-yl)vinyl)-1-methyl-1*H*-indole (**19**). ^{1}H NMR (200 MHz, $CDCl_3$): 2.63 (6H, *s*), 3.81 (3H, *s*), 5.51 (1H, *d*, *J* = 1.1), 5.59 (1H, *d*, *J* = 1.1), 6.50 (1H, *d*, *J* = 3.2), 6.94 (2H, *s*), 7.09 (1H, *d*, *J* = 3.2), 7.20 (1H, *dd*, *J* = 1.8, *J* = 8.8), 7.31 (1H, *bd*, *J* = 8.8), 7.58 (1H, *d*, *J* = 1.8). ^{13}C NMR (50 MHz, $CDCl_3$): 13.4 (2) (CH_3), 33.0 (CH_3), 101.5 (CH), 109.2 (CH), 115.4 (CH_2), 116.5 (2) (CH), 120.9 (CH), 122.1 (CH), 128.4 (C), 129.7 (CH), 131.2 (C), 136.6 (C), 148.7 (C), 150.3 (C), 159.2 (2) (C). IR (film): 1517, 1571, 1607 cm^{-1}. HRMS ($C_{18}H_{18}N_2S_2$): Calculated ($M+H_+$) 327.0984, found 329.1031.

5-(2-Chloro-6-(methylsulfanyl)isonicotinoyl)-1-methyl-1*H*-indole-3-carbaldehyde (20)

Following procedure 4, 0.35 ml (3.7 mmol) of $POCl_3$ was added to 2 mL of dry DMF at 0 ºC. After 30 minutes, 200 mg (0.63 mmol) of (2-chloro-6-(methylsulfanyl)pyridin-4-yl)(1-methyl-1*H*-indol-5-yl)methanone (**16**) was added and the mixture heated to 60 ºC. After precipitation, the filtrate was flash chromatographed with Hexane/EtOAc (1/1) to yield 140 mg (0.41 mmol, 64%) of 5-(2-chloro-6-(methylsulfanyl)isonicotinoyl)-1-methyl-1*H*-indole-3-carbaldehyde (**20**). ^{1}H NMR (200 MHz, $CDCl_3$): 2.59 (3H, *s*), 3.95 (3H, *s*), 7.22 (1H, *s*), 7.31 (1H, *s*), 7.46 (1H, *d*, *J* = 8.6), 7.81 (1H, *s*), 7.85 (1H, *dd*, *J* = 8.6; *J* = 1.4), 8.66 (1H, *s*), 9.99 (1H, *s*). ^{13}C NMR (50 MHz,

$CDCl_3$): 13.7 (CH_3), 34.1 (CH_3), 110.5 (CH), 118.4 (CH), 119.1 (CH), 122.4 (C), 124.8 (C), 125.7 (CH), 125.9 (CH), 130.5 (C), 140.7 (CH), 148.0 (C), 151.4 (C), 162.1 (C), 184.2 (CH), 193.6 (C). IR (film): 1466, 1530, 1607, 1658 cm^{-1}. HRMS ($C_{17}H_{13}ClN_2O_2S$): calculated ($M+H^+$) 345.0459, found 345.0444.

5-(2,6-bis(methylsulfanyl)isonicotinoyl)-1-methyl-1*H*-indole-3-carbaldehyde (21)

Following procedure 4, 0.15 ml (1.6 mmol) of $POCl_3$ was added to 2 mL of dry DMF at 0 ºC. After 30 minutes, 96 mg (0.29 mmol) of (2,6-bis(methylsulfanyl)pyridin-4-yl)(1-methyl-1*H*-indol-5-yl)methanone (**17**) was added and the mixture heated to 60 ºC for 2 hours. After precipitation, the filtrate was flash chromatographed with 1/1 Hexane/EtOAc to yield 45 mg (0.13 mmol; 44%) of 5-(2,6-bis(methylsulfanyl)isonicotinoyl)-1-methyl-1*H*-indole-3-carbaldehyde (**21**). ^{1}H NMR (200 MHz, $CDCl_3$): 2.62 (6H, *s*), 3.94 (3H, *s*), 7.10 (2H, *s*), 7.44 (1H, *bd*, *J* = 8.4), 7.79 (1H, *s*), 7.88 (1H, *dd*, *J* = 1.8, *J* = 8.4), 8.69 (1H, *d*, *J* = 1.8), 10.02 (1H, *s*). ^{13}C NMR (50 MHz, $CDCl_3$): 13.4 (2) (CH_3), 33.9 (CH_3), 110.2 (CH), 115.8 (2) (CH), 119.1 (C), 124.7 (C), 125.6 (CH), 125.7 (CH), 130.9 (C), 140.2 (CH), 145.3 (C), 160.3 (2) (C), 184.1 (CH), 194.9 (C). IR: (film): 1457, 1529, 1568, 1610, 1658 cm^{-1}. HRMS ($C_{18}H_{15}N_2NaO_2S_2$): calculated ($M+H^+$) 357.0731, found 357.0742.

(2-Chloro-6-(methylsulfanyl)pyridin-4-yl)(1-methyl-1*H*-indol-5-yl)methanone oxime (22)

Following procedure 3, 305 mg (4.39 mmol) of hydroxylamine hydrochloride was added onto a solution of 139 mg (0.43 mmol) of (2-chloro-6-(methylsulfanyl)pyridin-4-yl)(1-methyl-1*H*-indol-5-yl)methanone (**16**) in 20 mL of MeOH. 105 mg (0.32 mmol, 74%) of the mixture of oximes was crystalized in Hexane/CH_2Cl_2 from the reaction. (*E*/*Z*)-(2-chloro-6-(methylsulfanyl)pyridin-4-yl)(1-methyl-1*H*-indol-5-yl)methanone oxime (**22**). ^{1}H NMR (200 MHz, $CDCl_3$): 2.55 (3H, *s*), 2.60 (3H, *s*), 3.79 (3H, *s*), 3.83 (3H, *s*), 6.48 (1H, *d*, *J* = 3.0), 6.56 (1H, *d*, *J* = 3.0), 7.00 – 7.59 (2H, *m*), 7.71 (1H, *s*). ^{13}C NMR (50 MHz, $CDCl_3$): 13.7 (CH_3), 33.1 (CH3), 102.0 (CH), 102.1 (CH), 109.4 (CH), 109.8 (CH), 118.1 (CH), 118.7 (CH), 119.4 (CH), 119.9 (CH), 120.6 (CH), 121.5 (CH), 122.6 (CH), 124.3 (C), 125.5 (C), 128.2 (CH), 130.1 (CH), 137.1 (C), 137.6 (C), 144.5 (C), 147.7 (C), 151.2 (C), 155.8 (C), 156.2 (C), 161.3 (C), 161.5 (C). IR (film): 1441, 1524, 1577 cm^{-1}. HRMS ($C_{16}H_{14}N_3OSCl$): calculated ($M+H^+$) 332.0619, found 332.0610.

(E/Z)-(2,6-bis(methylsulfanyl)pyridin-4-yl)(1-methyl-1*H*-indol-5-yl)methanone oxime (23)

Following procedure 3, 284 mg (4.08 mmol) of hydroxylamine hydrochloride was added onto a solution of 134 mg (0.41 mmol) of (2,6-bis(methylsulfanyl)pyridin-4-yl)(1-methyl-1*H*-indol-5-yl)methanone (**17**) in 20 mL of MeOH. The mixture of oximes was chromatographed with 9/1 Hexane/EtOAc to yield 48 mg (0.14 mmol; 34%) of one isomer, 21 mg (0.06 mmol; 15%) of the other, and 52 mg (0.15 mmol; 37%) of the mixture of (*E*/*Z*)-(2,6-bis(methylsulfanyl)pyridin-4-yl)(1-methyl-1*H*-indol-5-yl)methanone oximes (**23**). ^{1}H NMR (200 MHz, $CDCl_3$), major isomer: 2.56 (6H, s), 3.84 (3H, *s*), 6.54 (1H, *d*, *J* = 3.2), 6.98 (2H, *s*), 7.12 (1H, *d*, *J* = 3.2), 7.24 (1H, *dd*, *J* = 1.8, *J* = 8.6), 7.40 (1H, *bd*, *J* = 8.6), 7.68 (1H, *d*, *J* = 1.8). ^{1}H NMR (200 MHz, $CDCl_3$), minor isomer: 2.61 (6H, *s*), 3.80 (3H, *s*), 6.46 (1H, *d*, *J* = 3.2), 6.90 (2H, *s*), 7.06 (1H, *d*, *J* = 3.2), 7.29 (1H, *bd*, *J* = 8.6), 7.47 (1H, *d*, *J* = 1.8), 7.51 (1H, *dd*, *J* = 1.8, *J* = 8.6). ^{13}C NMR (50 MHz, $CDCl_3$): 13.3 (2) (CH_3), 32.9 (CH_3), 102.0 (CH), 109.4 (CH), 116.5 (2) (CH), 120.6 (CH), 121.6 (CH), 125.5 (C), 128.1 (C), 129.8 (CH), 137.5 (C), 141.5 (C), 156.9 (C), 159.7 (2) (C). IR: (film): 1435, 1517, 1571, 3214 cm^{-1}. HRMS ($C_{17}H_{17}N_3OS_2$): calculated ($M+H^+$) 344.0886, found 344.0870.

(*E/Z*)-5-((2-chloro-6-(methylsulfanyl)pyridin-4-yl)(hydroxyimino)methyl)-1-methyl-1*H*-indole-3-carbonitrile (24)

Following procedure 3, 282 mg (4.06 mmol) of hydroxylamine hydrochloride was added onto a solution of 140 mg (0.41 mmol) of 5-(2-chloro-6-(methylsulfanyl)isonicotinoyl)-1-methyl-1*H*-indole-3-carbaldehyde (**20**) in 20 mL of MeOH, yielding 129 mg (0.34 mmol; 84%) of a mixture of oximes. The oximes were dissolved in 1 mL of pyridine and 0.5 mL of acetic anhydride, following procedure 5 to yield 103 mg (0.26 mmol; 76%) of (*E/Z*)-5-((2-chloro-6-(methylsulfanyl)pyridin-4-yl)(acetoxyimino)methyl)-1-methyl-1*H*-indole-3-carbonitrile, that was dissolved in 3 mL of MeOH and 1 mL of 10% NaOH and stirred for 72 hours at room temperature. The mixture was poured onto CH_2Cl_2 and the organic layer was washed with brine until neutral pH, dried over anhydrous Na_2SO_4, filtered and evaporated to dryness, yielding 89 mg. Column chromatography using 95/5 CH_2Cl_2/EtOAc gave 45 mg (0.13 mmol; 50%) of (*E/Z*)-5-((2-chloro-6-(methylsulfanyl)pyridin-4-yl)(hydroxyimino)methyl)-1-methyl-1*H*-indole-3-carbonitrile (**24**) as light yellow needles (CH_2Cl_2/Hexane). ^{1}H NMR (200 MHz, $CDCl_3$): 2.46 (3H, *s*), 2.52 (3H, *s*), 3.80 (3H, *s*), 3.84 (3H, *s*), 6.93 (1H, *s*), 6.99 (1H, *s*), 7.01 (1H, *s*), 7.04 (1H, *s*), 7.18 (1H, *d*, *J* = 1,6), 7.22 (1H, *d*, *J* = 8.6), 7.30 (1H, *d*, *J* = 8.6), 7.43 (1H, *d*, *J* = 8.6), 7.53 (1H, *s*), 7.58 (1H, *s*), 7.63 (1H, *s*), 7.71 (1H, *s*). ^{13}C NMR (50 MHz, $CDCl_3$): 13.5 (CH_3), 33.8 (CH_3),

110.7 (CH), 115.3 (C), 117.4 (CH), 118.3 (CH), 119.0 (C), 119.7 (CH), 121.0 (CH), 123.1 (C), 124.5 (CH), 127.6 (C), 136.2 (C), 136.7 (CH), 146.6 (C), 151.2 (C), 155.1 (C), 161.6 (C), 175.8 (C). IR (film): 1428, 1448, 1527, 1574, 2219, 3316, 3338 cm^{-1}. HRMS ($C_{17}H_{13}ClN_4OS$): calculated ($M+Na^+$) 379.0391, found 379.0389.

5-(1-(2-chloro-6-(methylsulfanyl)pyridin-4-yl)vinyl)-1-methyl-1*H*-indole-3-carbaldehyde (25)

Following procedure 4, 0.16 ml (1.7 mmol) of $POCl_3$ was added to 2 mL of dry DMF at 0 ºC. After 30 minutes, 89 mg (0.28 mmol) of 5-(1-(2-chloro-6-(methylsulfanyl)pyridin-4-yl)vinyl)-1-methyl-1*H*-indole (**18**) was added stirred for 2 hours at room temperature. After precipitation, the filtrate was flash chromatographed with Hexane/EtOAc (4/6) to yield 67 mg (0.20 mmol; 70%) of 5-(1-(2-chloro-6-(methylsulfanyl)pyridin-4-yl)vinyl)-1-methyl-1*H*-indole-3-carbaldehyde (**25**). ^{1}H NMR (200 MHz, $CDCl_3$): 2.56 (3H, *s*), 3.92 (3H, *s*), 5.62 (1H, *s*), 5.65 (1H, *s*), 6.94 (1H, *d*, *J* = 1.4), 7.03 (1H, *d*, *J* = 1.4), 7.17 (1H, *dd*, *J* = 1.8; *J* = 8.2), 7.34 (1H, *bd*, *J* = 8.2), 7.73 (1H, *s*), 8.29 (1H, *d*, *J* = 1.8), 10.0 (1H, *s*). ^{13}C NMR (50 MHz, $CDCl_3$): 13.6 (CH_3), 33.9 (CH_3), 110.0 (CH), 118.0 (CH_2), 118.3 (C), 118.5 (CH), 119.0 (CH), 121.8 (CH), 124.5 (CH), 125.4 (C), 134.5 (C), 137.8 (C), 140.2 (CH), 147.2 (C), 151.1 (C), 152.3 (C), 160.9 (C), 184.4 (CHO). IR (film): 1528, 1577, 1657 cm^{-1}. HRMS ($C_{18}H_{15}ClN_2OS$): calculated ($M+H^+$) 343.0666, found 343.0666.

5-(1-(2,6-bis(methylsulfanyl)pyridin-4-yl)vinyl)-1-methyl-1*H*-indole-3-carbaldehyde (26)

Following procedure 4, 309 µl (3.38 mmol) of $POCl_3$ was added to 2 mL of dry DMF at 0 ºC. After 30 minutes, 184 mg (0.56 mmol) of 5-(1-(2,6-bis(methylsulfanyl)pyridin-4-yl)vinyl)-1-methyl-1*H*-indole (**19**) was added and the mixture stirred for 2 hours at room temperature. After precipitation, the filtrate was flash chromatographed with 6/4 Hexane/EtOAc to yield 183 mg (0.51 mmol; 92%) of 5-(1-(2,6-bis(methylsulfanyl)pyridin-4-yl)vinyl)-1-methyl-1*H*-indole-3-carbaldehyde (**26**) ^{1}H NMR (200 MHz, $CDCl_3$): 2.57 (6H, *s*), 3.88 (3H, *s*), 5.56 (1H, *s*), 5.60 (1H, *s*), 6.82 (2H, *s*), 7.17 (1H, *bd*, *J* = 8.6), 7.32 (1H, *bd*, *J* = 8.6), 7.70 (1H, *s*), 8.29 (1H, *s*), 9.98 (1H, *s*). ^{13}C NMR (50 MHz, $CDCl_3$): 13.3 (2) (CH_3), 33.8 (CH_3), 109.9 (CH), 116.1 (2) (CH), 116.9 (CH_2), 118.2 (C), 121.6 (CH), 124.5 (CH), 125.3 (C), 134.9 (C), 137.7 (C), 140.2 (CH), 148.0 (C), 149.5 (C), 159.3 (2) (C), 184.3 (CH). IR (film): 1456, 1481, 1524, 1572, 1652, 2918 cm^{-1}. HRMS ($C_{19}H_{18}N_2OS_2$): calculated ($M+H^+$) 355.0933, found 355.0939.

5-(1-(2-Chloro-6-(methylsulfanyl)pyridin-4-yl)vinyl)-1-methyl-1*H*-indole-3-carboxylic acid (27)

393 µl (0.74 mmol) of phosgene was added to a solution of 85 mg (0.27 mmol) of 5-(1-(2-chloro-6-(methylsulfanyl)pyridin-4-yl)vinyl)-1-methyl-1*H*-indole-3-carbaldehyde (**25**) in 20 mL of dry CH_2Cl_2 at 0 ºC. After stirring 72 hours at room temperature the reaction is poured onto iced water and extracted with EtOAc. The organic layer were washed with 4% NaOH and brine until neutral pH, dried over anhydrous Na_2SO_4, filtered and evaporated to dryness, yielding 66 mg (0.19 mmol; 71%) of 5-(2-chloro-6-(methylsulfanyl)isonicotinoyl)-1-methyl-1*H*-indole-3-carbaldehyde (**20**). The basic waters were acidified with 2N HCl and extracted with EtOAc. The organic layer was washed with brine until neutral pH, dried over anhydrous Na_2SO_4, filtered and evaporated to dryness, yielding 13 mg (0.04 mmol; 13%) of 5-(1-(2-chloro-6-(methylsulfanyl)pyridin-4-yl)vinyl)-1-methyl-1*H*-indole-3-carboxylic acid (**27**). ^{1}H NMR (200 MHz, $CDCl_3$): 2.48 (3H, *s*), 3.81 (3H, *s*), 5.55 (1H, *s*), 5.58 (1H, *s*), 6.89 (1H, *d*, *J* = 1.1), 6.97 (1H, *d*, *J* = 1.1), 7.05 (1H, *bd*, *J* = 8.5), 7.26 (1H, *bd*, *J* = 8.5), 7.83 (1H, *s*), 8.12 (1H, *s*). IR (film): 1465, 1532, 1577, 1610, 1662 cm^{-1}. HRMS ($C_{18}H_{15}ClN_2O_2S$): calculated (M+Na$^+$) 381.0435, found 381.0453.

5-(1-(2,6-Bis(methylsulfanyl)pyridin-4-yl)vinyl)-1-methyl-1*H*-indole-3-carboxylic acid (28)

125 µl (0.24 mol) of phosgene was added to a solution of 79 mg (0.24 mmol) of 5-(1-(2,6-bis(methylsulfanyl)pyridin-4-yl)vinyl)-1-methyl-1*H*-indole (**19**) in 20 mL of dry CH_2Cl_2 at 0 ºC. After stirring 72 hours at room temperature the reaction is poured onto iced water, basified with 4% NaOH and extracted with CH_2Cl_2. The basic aqueous layer was acidified with HCl 2N and extracted with CH_2Cl_2. The organic layer was washed with and brine until neutral pH, dried over anhydrous Na_2SO_4, filtered and evaporated to dryness, yielding 22 mg (0.06 mmol; 25%) of 5-(1-(2,6-bis(methylsulfanyl)pyridin-4-yl)vinyl)-1-methyl-1*H*-indole-3-carboxylic acid (**28**). ^{1}H NMR (200 MHz, $CDCl_3$): 2.58 (6H, *s*), 3.88 (3H, *s*), 5.58 (1H, *s*), 5.61 (1H, *s*), 6.84 (2H, *s*), 7.12 (1H, *bd*, *J* = 8.9), 7.31 (1H, *bd*, *J* = 8.9), 7.90 (1H, *s*), 8.22 (1H, *s*). ^{13}C NMR (50 MHz, DMSO-D_6): 12.7 (2) (CH_3), 33.1 (CH_3), 106.5 (C), 110.9 (CH), 115.3 (2) (CH), 117.1 (CH_2), 120.2 (CH), 122.4 (CH), 126.4 (C), 132.7 (C), 136.9 (CH), 147.4 (C), 149.6 (C), 159.2 (2) (C), 165.5 (C). IR (KBr): 1422, 1482, 1523, 1573, 1615, 1656 cm^{-1}. HRMS ($C_{19}H_{18}N_2O_2S_2$): calculated (M+H$^+$) 371.0882, found 371.0886.

5-(1-(2-Chloro-6-(methylsulfanyl)pyridin-4-yl)vinyl)-1-methyl-1*H*-indole-3-carbonitrile (29)

Following procedure 3, 324 mg (4.67 mmol) of hydroxylamine hydrochloride was added onto a solution of 160 mg (0.46 mmol) of 5-(1-(2-chloro-6-(methylsulfanyl)pyridin-4-yl)vinyl)-1-methyl-1*H*-indole-3-carbaldehyde (**25**) in 20 mL of MeOH, yielding 149 mg (0.42 mmol; 90%) of a mixture of oximes. The oximes were dissolved in 1 mL of pyridine and 0.5 mL of acetic anhydride, following procedure 5. Column chromatography using 7/3 Hexane/EtOAc gave 106 mg (0.31 mmol; 74%) of 5-(1-(2-chloro-6-(methylsulfanyl)pyridin-4-yl)vinyl)-1-methyl-1*H*-indole-3-carbonitrile (**29**). ^{1}H NMR (200 MHz, $CDCl_3$): 2.56 (3H, *s*), 3.88 (3H, *s*), 5.62 (1H, *s*), 5.63 (1H, *s*), 6.93 (1H, *s*, *J* = 1.2), 7.02 (1H, *s*, *J* = 1.2), 7.20 (1H, *dd*, *J* = 1.6, *J* = 8.6), 7.37 (1H, *bd*, *J* = 8.6), 7.61 (1H, *s*), 7.70 (1H, *s*). ^{13}C NMR (50 MHz, $CDCl_3$) 13.5 (CH_3), 33.8 (CH_3), 110.4 (CH), 115.6 (C), 117.9 (CH_2), 118.4 (CH), 119.0 (CH), 119.5 (CH), 124.3 (CH), 127.9 (C), 133.8 (C), 135.9 (C), 136.3 (CH), 146.8 (C), 151.1 (C), 151.9 (C), 161.0 (C). IR (film): 1526, 1576, 2218 cm^{-1}. HRMS (C18H14ClN3S): calculated (M+H+) 340.0670, found 340.0673.

5-(1-(2,6-bis(methylsulfanyl)pyridin-4-yl)vinyl)-1-methyl-1*H*-indole-3-carbonitrile (30)

Following procedure 3, 271 mg (3.89 mmol) of hydroxylamine hydrochloride was added onto a solution of 138 mg (0.39 mmol) of 5-(1-(2,6-bis(methylsulfanyl)pyridin-4-yl)vinyl)-1-methyl-1*H*-indole-3-carbaldehyde (**26**) in 20 mL of MeOH, yielding 138 mg (0.37 mmol; 95%) of 5-(1-(2,6-bis(methylthio)pyridin-4-yl)vinyl)-1-methyl-1*H*-indole-3-carbaldehyde oxime. The oximes were dissolved in 1 mL of pyridine and 0.5 mL of acetic anhydride, following procedure 5. Column chromatography using 3/1 Hexane/EtOAc gave 51 mg (0.15 mmol; 39%) of 5-(1-(2,6-bis(methylsulfanyl)pyridin-4-yl)vinyl)-1-methyl-1*H*-indole-3-carbonitrile (**30**). ^{1}H NMR (200 MHz, $CDCl_3$): 2.55 (6H, *s*), 3.77 (3H, *s*), 5.48 (1H, *s*), 5.49 (1H, *s*), 6.72 (2H, *s*), 7.13 (1H, *bd*, *J* = 8.8), 7.26 (1H, *bd*, *J* = 8.8), 7.50 (1H, *s*), 7.60 (1H, *s*). ^{13}C NMR (50 MHz, $CDCl_3$): 13.6 (2) (CH_3), 34.2 (CH_3), 110.7 (CH), 116.1 (C), 116.5 (2) (CH), 117.3 (CH_2), 119.8 (CH), 124.8 (CH), 128.2 (C), 134.7 (C), 136.2 (C), 136.6 (CH), 148.0 (C), 159.6 (C), 159.7 (2) (C). IR (film): 1484, 1527, 1573, 1714, 2218 cm^{-1}. HRMS ($C_{19}H_{17}N_3S_2$): calculated ($M+H^+$) 352.0937, found 352.0939.

5-(1-(2-chloro-6-(methylsulfanyl)pyridin-4-yl)vinyl)-1-methyl-1*H*-indole-3-carboxamide (31)

12 ul (0.14 mmol) of chlorosulfonylisocyanide was added to a solution of 29 mg (0.09 mmol) of 5-(1-(2-chloro-6-(methylsulfanyl)pyridin-4-yl)vinyl)-1-methyl-1*H*-indole (**18**) in 2 mL of 1,2-dichloroethane and the mixture stirred 24 hours at room temperature under N_2. The mixture was poured onto ice and extracted with CH_2Cl_2. The organic layer was washed with brine until neutral pH, dried over anhydrous Na_2SO_4, filtered, evaporated to dryness, and subjected to preparative thin layer chromatography, yielding 12 mg (0.03 mmol; 31%) of 5-(1-(2-chloro-6-(methylsulfanyl)pyridin-4-yl)vinyl)-1-methyl-1*H*-indole-3-carboxylic acid (**27**) and 10 mg (0.03 mmol; 31%) of 5-(1-(2-chloro-6-(methylsulfanyl)pyridin-4-yl)vinyl)-1-methyl-1*H*-indole-3-carboxamide (**31**). ^{1}H NMR (200 MHz, $CDCl_3$): 2.55 (3H, *s*); 3.86 (3H, *s*); 5.56 (2H, *s*); 5.60 (1H, *s*); 5.62 (1H, *s*); 6.95 (1H, *d*, *J* = 1.2); 7.03 (1H, *d*, *J* = 1.2); 7.13 (1H, *dd*, *J* = 1.7; *J* = 8.6); 7.33 (1H, *bd*, *J* = 8.6); 7.68 (1H, *s*); 7.95 (1H, *d*, *J* = 1.7). ^{13}C NMR (50 MHz, $CDCl_3$): 13.5 (CH_3), 33.5 (CH_3), 110.0 (CH), 110.2 (C), 117.6 (CH), 118.5 (CH), 119.0 (CH), 120.4 (CH_2), 123.3 (CH), 125.9 (C), 133.3 (CH), 137.1 (C), 147.4 (C), 151.1 (C), 152.3 (C), 159.5 (C), 166.6 (C). IR: (film): 1519, 1574, 1651, 2925, 3342 cm^{-1}. HRMS ($C_{18}H_{16}ClN_3OS$): calculated (M+H$^+$) 358.0775, found 358.0780.

5-(1-(2,6-bis(methylsulfanyl)pyridin-4-yl)vinyl)-1-methyl-1*H*-indole-3-carboxamide (32)

29 ul (0.32 mmol) of chlorosulfonylisocyanide was added to a solution of 70 mg (0.21 mmol) of 5-(1-(2,6-bis(methylsulfanyl)pyridin-4-yl)vinyl)-1-methyl-1*H*-indole (**19**) in 2 mL of 1,2-dichloroethane and the mixture stirred 24 hours at room temperature under N_2. The mixture was poured onto ice and extracted with CH_2Cl_2. The organic layer was washed with brine until neutral pH, dried over anhydrous Na_2SO_4, filtered, evaporated to dryness, and chromatographed with 99:1 CH_2Cl_2/MeOH to yield 24 mg (0.06 mmol; 31%) of 5-(1-(2,6-bis(methylsulfanyl)pyridin-4-yl)vinyl)-1-methyl-1*H*-indole-3-carboxamide (**32**). ^{1}H NMR (200 MHz, $CDCl_3$): 2.51 (6H, *s*), 3.78 (3H, *s*), 5.50 (1H, *s*), 5.51 (1H, *s*), 5.66 (2H, *s*), 6.76 (2H, *s*), 7.08 (1H, *dd*, *J* = 1.6, *J* = 8.6), 7.24 (1H, *bd*, *J* = 8.6), 7.63 (1H, *s*), 7.86 (1H, *d*, *J* = 1.6). ^{13}C NMR (50 MHz, $CDCl_3$): 13.3 (2) (CH_3), 33.5 (CH_3), 110.0 (CH), 110.1 (C), 116.2 (2) (CH), 120.1 (CH_2), 123.4 (CH), 125.6 (CH), 133.6 (C), 133.8 (CH), 137.1 (C), 148.1 (C), 149.5 (C), 159.2 (2) (C), 166.7 (C). IR (film): 1462, 1519, 1573, 1651, 2924, 3341cm^{-1}. HRMS ($C_{19}H_{19}N_3OS_2$): calculated (M+H$^+$) 370.1042, found 370.1051.

(2,6-bis(methylsulfanyl)pyridin-4-yl)(4-(dimethylamino)phenyl)methanone (33)

Following procedure 1, 7.3 ml (11.6 mmol) of *n*BuLi 1.6 M in hexanes was slowly added to a solution of 2.32 g (11.6 mmol) of 4-bromo-*N,N*-dimethylaniline in dry THF at -40 ºC. After 45 minutes, 1 g (4.6 mmol) of 2,6-bis(methylsulfanyl)pyridine-4-carboxylic acid (**3**) in 10 mL of dry THF was added. The reaction product was flash chromatographed using 98/2 Hexane/EtOAc to yield 81 mg (0.18 mmol; 4%) of (2,6-bis(methylsulfanyl)pyridin-4-yl)bis(4-(dimethylamino)phenyl)methanol and 669 mg (2.1 mmol; 46%) of (2,6-bis(methylsulfanyl)pyridin-4-yl)(4-(dimethylamino)phenyl)methanone (**33**). M.p. (Hex/EtOAc): 103 - 105 ºC. ^{1}H NMR (200 MHz, $CDCl_3$): 2.61 (6H, *s*), 3.09 (6H, *s*), 6.67 (2H, *d*, *J* = 9.2), 7.04 (2H, *s*), 7.75 (2H, *d*, *J* = 9.2). ^{13}C NMR (50 MHz, $CDCl_3$): 13.3 (2) (CH_3), 40.1 (2) (CH_3), 110.7 (2) (CH), 115.6 (2) (CH), 123.4 (C), 132.6 (2) (CH), 146.5 (C), 153.7 (C), 159.8 (2) (C), 192.6 (C). IR (KBr): 1435, 1523, 1591, 1639 cm^{-1}. HRMS ($C_{16}H_{18}N_2OS_2$): calculated ($M+H^+$) 319.0933, found 319.1221. (2,6-bis(methylsulfanyl)pyridin-4-yl)bis(4-(dimethylamino)phenyl)methanol: ^{1}H NMR (200 MHz, $CDCl_3$): 2.55 (6H, *s*), 2.94 (12H, *s*), 6.66 (4H, *d*, *J* = 8.8), 6.91 (2H, *s*), 7.09 (4H, *d*, *J* = 8.8). ^{13}C NMR (50 MHz, $CDCl_3$): 13.2 (2) (CH_3), 40.4 (4) (CH_3), 80.7 (C), 111.7 (4) (CH), 115.9 (2) (CH), 128.6 (4) (CH), 133.6 (2) (C), 149.7 (2) (C), 156.5 (C), 158.6 (2) (C). IR (KBr): 1522, 1576, 1608, 2921, 3432 cm^{-1}. HRMS ($C_{24}H_{29}N_3OS_2$): calculated ($M+H^+$) 440.1825, found 440.1838.

4-(1-(2,6-bis(methylsulfanyl)pyridin-4-yl)vinyl)-*N*,*N*-dimethylaniline (34)

Following procedure 2, 1.5 ml (2.4 mmol) of *n*BuLi 1.6 M in hexanes was slowly added to a stirred suspension of 1.33 g (3.3 mmol) of methyltriphenylphosphonium iodide in 50 mL of dry THF at -40 ºC. After 45 minutes, 302 mg (0.95 mmol) of (2,6-bis(methylsulfanyl)pyridin-4-yl)(4-(dimethylamino)phenyl)methanone (**33**) was added. Flash chromatography with 97/3 Hexane/EtOAc yielded 118 mg (0.37 mmol; 39 %) of 4-(1-(2,6-bis(methylsulfanyl)pyridin-4-yl)vinyl)-*N*,*N*-dimethylaniline (**34**). ^{1}H NMR (200 MHz, $CDCl_3$): 2.59 (6H, *s*); 2.99 (6H, *s*); 5.31 (1H, *d*, *J* = 1.0); 5.45 (1H, *d*, *J* = 1.0); 6.69 (2H, *d*, *J* = 9.2); 6.86 (2H, *s*); 7.18 (2H, *d*, *J* = 9.2). ^{13}C NMR (50 MHz, $CDCl_3$): 13.2 (2) (CH_3), 40.4 (2) (CH_3), 111.7 (2) (CH), 113.5 (CH_2), 116.4 (2) (CH), 127.5 (C), 128.8 (2) (CH), 147.3 (C), 149.9 (C), 150.3 (C), 159.0 (2) (C). IR (film): 1519, 1572, 1606 cm^{-1}. HRMS ($C_{17}H_{20}N_2S_2$): calculated ($M+H^+$) 317.1141, found 317.1142.

(E/Z)-(2,6-bis(methylthio)pyridin-4-yl)(4-(dimethylamino)phenyl)methanone oximes (35).

Following procedure 3, 432 mg (6.22 mmol) of hydroxylamine hydrochloride was added onto a solution of 198 mg (0.62 mmol) of (2,6-bis(methylsulfanyl)pyridin-4-yl)(4-(dimethylamino)phenyl)methanone (**33**) in 20 mL of MeOH. The mixture of oximes was chromatographed with 9/1 Hexane/EtOAc to yield 141 mg (0.42 mmol; 69%) of the mixture of (E/Z)-(2,6-bis(methylthio)pyridin-4-yl)(4-(dimethylamino)phenyl)methanone oximes (**35**). Major isomer: ^{1}H NMR (200 MHz, $CDCl_3$): 2.59 (6H, *s*), 2.99 (6H, *s*), 6.62 (2H, *d*, *J* = 9.0), 6.83 (2H, *s*), 7.30 (2H, *d*, *J* = 9.0). ^{13}C NMR (50 MHz, $CDCl_3$): 13.2 (2) (CH_3), 40.2 (2) (CH_3), 111.7 (2) (CH), 116.4 (2) (CH), 128.4 (C), 128.4 (2) (CH), 137.8 (C), 151.3 (C), 155.7 (C), 159.6 (2) (C). IR (KBr): 1524, 1574, 1605, 3246, 3273 cm^{-1}. HRMS ($C_{16}H_{20}N_3OS_2$): calculated ($M+Na^+$) 356.0867, found 356.1157. Minor isomer: ^{1}H NMR (200 MHz, $CDCl_3$): 2.57 (6H, *s*), 3.02 (6H, *s*), 6.72 (2H, *d*, *J* = 8.9), 6.96 (2H, *s*), 7.36 (2H, *d*, *J* = 8.9). ^{13}C NMR (50 MHz, $CDCl_3$): 13.3 (2) (CH_3), 40.1 (2) (CH_3), 111.2 (2) (CH), 115.9 (2) (CH), 118.0 (C), 121.7 (C), 131.1 (2) (CH), 150.9 (C), 155.6 (C), 159.5 (2) (C).

(2,6-bis(methylsulfanyl)pyridin-4-yl)(3-(dimethylamino)phenyl)methanone (36)

Following procedure 1, 7.3 ml (11.6 mmol) of *n*BuLi 1.6 M in hexanes was slowly added to a solution of 1.29 ml (8.75 mmol) of 3-bromo-*N,N*-dimethylaniline in dry THF at -40 ºC. After 45 minutes, 754 mg (3.5 mmol) of 2,6-bis(methylsulfanyl)pyridine-4-carboxylic acid (**3**) in 10 mL of dry THF was added. The reaction product was flash chromatographed using 95/5 Hexane/EtOAc to yield 590 mg (1.85 mmol; 53%) of (2,6-bis(methylsulfanyl)pyridin-4-yl)(3-(dimethylamino)phenyl)methanone (**36**). M.p. (Hex/CH_2Cl_2): 114 – 116 ºC. ^{1}H NMR (200 MHz, $CDCl_3$): 2.61 (6H, *s*), 3.00 (6H, *s*), 6.96 (1H, *dd*, *J* = 1.7, *J* = 8.6), 7.02 (1H, *dd*, *J* = 7.6), 7.15 (2H, *s*), 7.16 (1H, *d*, *J* = 1.7), 7.31(1H, *t*, *J* = 7.9). ^{13}C NMR (50 MHz, $CDCl_3$): 13.3 (2) (CH_3), 40.5 (2) (CH_3), 112.6 (CH), 115.4 (2) (CH), 117.3 (CH), 118.7 (CH), 129.0 (CH), 136.6 (C), 144.9 (C), 150.4 (C), 160.1 (2) (C), 195.5 (C). IR (KBr): 1525, 1568, 1596, 1656 cm^{-1}. HRMS ($C_{16}H_{18}N_2OS_2$): calculated (M+H) 319.0939, found 319.0938.

3-(1-(2,6-bis(methylsulfanyl)pyridin-4-yl)vinyl)-*N*,*N*-dimethylaniline (37)

Following procedure 2, 1.22 ml (1.95 mmol) of *n*BuLi 1.6 M in hexanes was slowly added to a stirred suspension of 1.18 g (2.93 mmol) of methyltriphenylphosphonium iodide in 50 mL of dry THF at -40 ºC. After 45 minutes, 312 mg (0.98 mmol) of (2,6-bis(methylsulfanyl)pyridin-4-yl)(3-

(dimethylamino)phenyl)methanone (**36**) was added. Flash chromatography with 97/3 Hexane/EtOAc yielded 118 mg (0.37 mmol; 39 %) of 112 mg (0.35 mmol; 36 %) of 3-(1-(2,6-bis(methylsulfanyl)pyridin-4-yl)vinyl)-*N*,*N*-dimethylaniline (**37**). ^{1}H NMR (200 MHz, $CDCl_3$): 2.59 (6H, *s*), 2.94 (6H, *s*), 5.52 (1H, *d*, *J* = 1.2), 5.54 (1H, *d*, *J* = 1.2), 6.62 (1H, *dd*, *J* = 6.7), 6.64 (1H, *s*), 6.73 (1H, *dd*, *J* = 6.7), 6.85 (2H, *s*), 7.21 (1H, *t*, *J* = 8.1). ^{13}C NMR (50 MHz, $CDCl_3$): 13.4 (2) (CH_3), 40.7 (2) (CH_3), 112.4 (CH), 112.5 (CH), 116.3 (2) (CH), 116.5 (CH_2), 116.8 (CH), 129.1 (CH), 140.6 (C), 148.4 (C), 149.2 (C), 150.5 (C), 159.2 (2) (C). IR (film): 1517, 1571, 1596 cm^{-1}. HRMS ($C_{17}H_{20}N_2S_2$): calculated ($M+Na^+$) 339.0960, found 339.0959.

(*E/Z*)-(2,6-bis(methylsulfanyl)pyridin-4-yl)(3-(dimethylamino)phenyl)methanone oxime (38)

Following procedure 3, 465 mg (6.69 mmol) of hydroxylamine hydrochloride was added onto a solution of 213 mg (0.67 mmol) of (2,6-bis(methylsulfanyl)pyridin-4-yl)(3-(dimethylamino)phenyl)methanone (**36**) in 20 mL of MeOH. The mixture of oximes was chromatographed with 9/1 Hexane/EtOAc to yield 182 mg (0.55 mmol; 82%) of the mixture of (*E/Z*)-(2,6-bis(methylsulfanyl)pyridin-4-yl)(3-(dimethylamino)phenyl)methanone oximes (**38**). Major isomer: ^{1}H NMR (200 MHz, $CDCl_3$): 2.57 (6H, *s*), 2.96 (6H, *s*), 6.59 (1H, *m*), 6.61 (1H, *bd*, *J* = 8.2), 6.80 (1H, *bd*, *J* = 8.2), 6.98 (2H, *s*), 7.33 (1H, *t*, *J* = 8.2). ^{13}C NMR (50 MHz, $CDCl_3$): 13.4 (2) (CH_3), 40.5 (2) (CH_3), 112.3 (CH), 113.5 (CH), 115.1 (2) (CH), 116.6 (CH), 129.3 (CH), 131.7 (C), 143.7 (C), 150.4 (C), 156.9 (C), 159.6 (2) (C). IR (film): 1521, 1572, 1597, 2921, 3265 cm^{-1}. HRMS ($C_{16}H_{19}N_3OS_2$): calculated ($M+H^+$) 334.1042, found 334.1042. Minor isomer: ^{1}H NMR (200 MHz, $CDCl_3$): 2.59 (6H, *s*), 2.92 (6H, *s*), 6.61 (1H, *d*, *J* = 7.9), 6.63 (1H, *m*), 6.78 (1H, *bd*, *J* = 7.9), 6.87 (2H, *s*), 7.18 (1H, *t*, *J* = 7.9). ^{13}C NMR (50 MHz, $CDCl_3$): 13.4 (2) (CH_3), 40.7 (2) (CH_3), 111.2 (CH), 112.6 (CH), 114.5 (CH), 116.5 (2) (CH), 129.3 (CH), 135.2 (C), 141.0 (C), 150.5 (C), 156.2 (C), 159.7 (2) (C).

(2,6-bis(methylsulfanyl)pyridin-4-yl)(6-(dimethylamino)pyridin-3-yl)methanone (39)

7.3 ml (11.6 mmol) of *n*BuLi 1.6 M in hexanes was slowly added to a solution of 1.167 g (5.80 mmol) of 5-bromo-*N*,*N*-dimethylpyridin-2-amine in dry THF at -40 ºC and stirred for 1 hour. 215 mg (8,96 mmol) of NaH was added to a solution of 1 g (4.6 mmol) of 2,6-bis(methylsulfanyl)pyridine-4-carboxylic acid (**3**) in 10 mL of dry THF and stirred for 1 hour at 0

ºC. The first solution was slowly added onto the second and stirred for 24 hours. 2 mL of ethyl formate was added and the miture was poured onto 5% NH_4Cl and EtOAc. The mixture was partially evaporated and the organic layer was washed with 2N HCl, 5% $NaHCO_3$, and brine, dried over anhydrous Na_2SO_4, filtered and evaporated. The reaction product was flash chromatographed using 8/2 Hexane/EtOAc to yield 71 mg (0.16 mmol; 3%) of (2,6-bis(methylsulfanyl)pyridin-4-yl)bis(6-(dimethylamino)pyridin-3-yl)methanol and 97 mg (0.30 mmol; 5%) of (2,6-bis(methylsulfanyl)pyridin-4-yl)(6-(dimethylamino)pyridin-3-yl)methanone (**39**). ^{1}H NMR (200 MHz, $CDCl_3$): 2.61 (6H, *s*), 3.21 (6H, *s*), 6.55 (1H, *bd*, *J* = 9.2), 7.04 (2H, *s*), 7.98 (1H, *dd*, *J* = 2.2, *J* = 9.2), 8.57 (1H, *d*, *J* = 2.2). ^{13}C NMR (50 MHz, $CDCl_3$): 13.4 (2) (CH_3), 38.1 (2) (CH_3), 105.3 (CH), 115.5 (2) (CH), 119.9 (C), 138.3 (CH), 145.5 (C), 153.1 (CH), 160.2 (2) (C), 160.7 (C), 191.8 (C). IR (KBr): 1524, 1593, 1645 cm^{-1}. HRMS ($C_{15}H_{17}N_3OS_2$): calculated ($M+H^+$) 320.0886, found 320.0901. (2,6-bis(methylsulfanyl)pyridin-4-yl)bis(6-(dimethylamino)pyridin-3-yl)methanol: M.p. (Hex/CH_2Cl_2): 175 – 177 ºC. ^{1}H NMR (200 MHz, $CDCl_3$): 2.55 (6H, *s*), 3.09 (12H, *s*), 6.45 (2H, *bd*, *J* = 8.8), 6.86 (2H, *s*), 7.36 (2H, *dd*, *J* = 2.4, *J* = 8.8), 7,95 (2H, *d*, *J* = 2.4). ^{13}C NMR (50 MHz, $CDCl_3$): 13.3 (2) (CH_3), 38.2 (4) (CH_3), 78.2 (C), 105.5 (2) (CH), 115.6 (2) (CH), 128.1 (2) (C), 137.2 (2) (CH), 146.9 (2) (CH), 155.3 (C), 158.4 (2) (C), 159.2 (2) (C). IR (KBr): 1515, 1568, 1605, 2924 cm^{-1}. HRMS ($C_{22}H_{27}N_5OS_2$): calculated ($M+H^+$) 442.1730, found 442.1722.

(2,6-bis(methylsulfanyl)pyridin-4-yl)(naphthalen-2-yl)methanone (40)

Following procedure 1, 7.2 ml (11.5 mmol) of *n*BuLi 1.6 M in hexanes was slowly added to a solution of 2.41 g (11.5 mmol) of 2-bromonaphthalene in dry THF at -40 ºC. After 45 minutes, 1 g (4.6 mmol) of 2,6-bis(methylsulfanyl)pyridine-4-carboxylic acid (**3**) in 10 mL of dry THF was added. The reaction product was flash chromatographed using 95/5 Hexane/EtOAc to yield 709 mg (2.18 mmol; 47%) of (2,6-bis(methylsulfanyl)pyridin-4-yl)(naphthalen-2-yl)methanone (**40**). ^{1}H NMR (200 MHz, $CDCl_3$): 2.61 (6H, *s*), 7.17 (2H, *s*), 7.4 - 8.3 (7H, *m*). ^{13}C NMR (50 MHz, $CDCl_3$): 13.5 (2) (CH_3), 116.2 (2) (CH), 124.3 (CH), 125.5 (CH), 126.8 (CH), 128.0 (CH), 128.6 (CH), 129.5 (CH), 132.9 (CH), 130.8 (C), 133.8 (C), 134.1 (C), 145.1 (C), 160.8 (2) (C), 196.4 (C). IR (film): 1529, 1570, 1665 cm^{-1}.

2,6-bis(methylsulfanyl)-4-(1-(naphthalen-2-yl)vinyl)pyridine (41)

Following procedure 2, 1.91 ml (3.06 mmol) of *n*BuLi 1.6 M in hexanes was slowly added to a stirred suspension of 1.85 g (5.49 mmol) of methyltriphenylphosphonium iodide in 50 mL of dry THF at -40 ºC. After 45 minutes, 497 mg (1.53 mmol) of (2,6-bis(methylsulfanyl)pyridin-4-yl)(naphthalen-2-yl)methanone (**40**) was added. Flash chromatography with 97/3 Hexane/EtOAc yielded 118 mg (0.37 mmol; 39 %) of 293 mg (0.91 mmol; 59 %) of 2,6-bis(methylsulfanyl)-4-(1-(naphthalen-2-yl)vinyl)pyridine (**41**). ^{1}H NMR (200 MHz, $CDCl_3$): 2.56 (6H, s), 5.53 (1H, d, J = 1.1), 6.08 (1H, d, J = 1.1), 6.81 (2H, s), 7.2 – 7.7 (7H, *m*). ^{13}C NMR (50 MHz, $CDCl_3$): 13.4 (2) (CH_3), 114.7 (2) (CH), 120.0 (CH_2), 125.5 (CH), 126.1 (2) (CH), 126.4 (CH), 127.6 (CH), 128.5 (CH), 128.7 (CH), 131.6 (C), 133.8 (C), 138.0 (C), 146.2 (C), 148.5 (C), 159.6 (2) (C). IR (film): 1519, 1570 cm^{-1}. HRMS ($C_{19}H_{17}NS_2$): calculated ($M+H^+$) 324.0875, found 324.0893.

(*E/Z*)-(2,6-bis(methylsulfanyl)pyridin-4-yl)(naphthalen-2-yl)methanone oxime (42)

Following procedure 3, 199 mg (0.29 mmol) of hydroxylamine hydrochloride was added onto a solution of 93 mg (0.29 mmol) of (2,6-bis(methylsulfanyl)pyridin-4-yl)(naphthalen-2-yl)methanone (**40**) in 20 mL of MeOH. The mixture of oximes was chromatographed with 9/1 Hexane/EtOAc to yield 188 mg (0.26 mmol; 89%) of the mixture of (*E/Z*)-(2,6-bis(methylsulfanyl)pyridin-4-yl)(naphthalen-2-yl)methanone oxime (**43**). Major isomer: ^{1}H NMR (200 MHz, $CDCl_3$): 2.53 (6H, *s*), 6.95 (2H, *s*), 7.2 - 8.0 (7H, *m*). ^{13}C NMR (50 MHz, $CDCl_3$): 13.4 (2) (CH_3), 114.4 (2) (CH), 125.4 (2) (CH), 126.3 (CH), 126.5 (CH), 127.0 (CH), 127.3 (C),128.7 (CH), 129.8 (CH), 130.2 (C), 133.6 (C), 143.3 (C), 155.6 (C), 159.9 (2) (C). IR: (película): 1435, 1522, 1571, 3271, 3295 cm^{-1}. HRMS ($C_{18}H_{16}N_2OS_2$): calculated ($M+H^+$) 341.0777, found 341.0792. Minor isomer: ^{1}H NMR (200 MHz, $CDCl_3$): 2.55 (6H, *s*), 7.01 (2H, *s*), 7.4 – 8.0 (7H, *m*). ^{13}C NMR (50 MHz, $CDCl_3$): 13.4 (2) (CH_3), 114.4 (CH), 116.8 (CH), 125.4 (2) (CH), 126.5 (CH), 127.0 (CH), 128.5 (CH), 129.7 (CH), 130.2 (CH), 131.5 (C), 133.9 (C), 140.6 (C), 143.4 (C), 154.8 (C), 155.5 (C), 159.8 (2) (C).

(*Z*)-4-(4-methoxystyryl)-2,6-bis(methylsulfanyl)pyridine (43)

Following procedure 2, 0.25 ml (0.40 mmol) of *n*BuLi 1.6 M in hexanes was slowly added to a stirred suspension of 189 mg (0.36 mmol) of ((2,6-bis(methylthio)pyridin-4-yl)methyl)triphenylphosphonium bromide (**6**) in 50 mL of dry THF at -40 ºC. After 45 minutes, a

solution of 0.13 ml (1.10 mmol) of 4-methoxybenzaldehyde in 5 mL of dry THF was added over 30 minutes. Flash chromatography with 97/3 Hexane/EtOAc yielded 118 mg (0.37 mmol; 39 %) of 59 mg (0.19 mmol; 54%) of (*E*)-4-(4-methoxystyryl)-2,6-bis(methylsulfanyl)pyridine (**43*E***) and 19 mg (0.06 mmol; 17%) of (*Z*)-4-(4-methoxystyryl)-2,6-bis(methylsulfanyl)pyridine (**43**). ^{1}H NMR (200 MHz, $CDCl_3$): 2.49 (6H, *s*), 3.79 (3H, *s*), 6.25 (1H, *d*, *J* = 12), 6.65 (1H, *d*, *J* = 12), 6.73 (2H, *s*), 6.78 (2H, *d*, *J* = 8.2), 7.16 (2H, *d*, *J* = 8.2). ^{13}C NMR (50 MHz, $CDCl_3$): 13.3 (2) (CH_3), 55.3 (CH_3), 113.8 (2) (CH), 116.3 (2) (CH), 125.5 (CH), 128.4 (C), 130.3 (2) (CH), 132.8 (C), 133.6 (CH), 145.5 (C), 159.4 (2) (C). IR (KBr): 1512, 1566, 1604 cm^{-1}. HRMS ($C_{16}H_{17}NOS_2$): calculated ($M+H^+$) 304.0824, found 304.0823. (*E*)-4-(4-methoxystyryl)-2,6-bis(methylsulfanyl)pyridine (**43*E***): ^{1}H NMR (200 MHz, $CDCl_3$): 2.61 (6H, *s*), 3.84 (3H, *s*), 6.73 (1H, *d*, *J* = 16), 6.91 (2H, *d*, *J* = 8.6), 6.94 (2H, *s*), 7.18 (1H, *d*, *J* = 16), 7.45 (2H, *d*, *J* = 8.6). ^{13}C NMR (50 MHz, $CDCl_3$): 13.4 (2) (CH_3), 55.4 (CH_3), 114.0 (2) (CH), 114.3 (2) (CH), 123.3 (CH), 128.4 (2) (CH), 128.9 (C), 132.8 (C), 132.9 (CH), 159.4 (2) (C). Falta un C. IR (KBr): 1517, 1571, 1604, 1635 cm^{-1}. HRMS ($C_{16}H_{18}NOS_2$): calculated ($M+H^+$) 304.0830, found 304.0823.

(*Z*)-5-(2-(2,6-bis(methylsulfanyl)pyridin-4-yl)vinyl)-1-methyl-1*H*-indole (44)

Following procedure 2, 0.4 ml (0.64 mmol) of *n*BuLi 1.6 M in hexanes was slowly added to a stirred suspension of 139 mg (0.26 mmol) of ((2,6-bis(methylthio)pyridin-4-yl)methyl)triphenylphosphonium bromide (**6**) in 50 mL of dry THF at -40 ºC. After 45 minutes, a solution of 252 mg (1.58 mmol) of *N*-methyl-1*H*-indole-5-carbaldehyde in 5 mL of dry THF was added over 30 minutes. Flash chromatography with 98/2 Hexane/EtOAc yielded 22 mg (0.07 mmol; 26%) of (*E*)-5-(2-(2,6-bis(methylsulfanyl)pyridin-4-yl)vinyl)-1-methyl-1*H*-indole (**44*E***) and 12 mg (0.04 mmol; 14%) of (*Z*)-5-(2-(2,6-bis(methylsulfanyl)pyridin-4-yl)vinyl)-1-methyl-1*H*-indole (**44**). ^{1}H NMR (200 MHz, $CDCl_3$): 2.45 (6H, *s*), 3.77 (3H, *s*), 6.26 (1H, *d*, *J* = 12), 6.43 (1H, *d*, *J* = 3.2), 6.78 (2H, *s*), 6.86 (1H, *d*, *J* = 12), 7.03 (1H, *d*, *J* = 3.2), 7.12 (1H, *bd*, *J* = 8.6), 7.12 (1H, *bd*, *J* = 8.6), 7.52 (1H, *s*). ^{13}C NMR (50 MHz, $CDCl_3$): 13.4 (2) (CH_3),33.1 (CH_3), 101.7 (CH), 109.7 (CH), 114.0 (2) (CH), 120.5 (CH), 120.8 (CH), 122.5 (CH), 124.7 (C), 127.8 (C), 128.8 (C), 129.8 (CH), 134.9 (CH), 145.5 (C), 159.3 (2) (C). IR (film): 1521, 1571, 1608, 1626 cm^{-1}. HRMS ($C_{18}H_{18}N_2S_2$): calculated ($M+H^+$) 327.0984, found 327.1001.

4.1.3. Determination of Aqueous Solubility.

The aqueous solubility was determined by the shaking-flask method. Roughly 2 mg of the compound was shaken in 0.3 mL of pH 7.0 phosphate buffer for 72 h at room temperature. The saturated supernatant was passed through a 45 µm filter and the absorbance of the filtrate measured at the maximum UV absorbance wavelength for every compound in a Helios Alfa Spectrophotometer. The aqueous solubility was calculated by comparison with a calibration curve.

4.2. Biology

4.2.1. Inhibition of tubulin polymerization.

Bovine brain tubulin was isolated as previously described.[35] Tubulin polymerization assays were carried out with 1.5 mg/mL protein at pH 6.7 in assay buffer containing 0.1 M MES buffer, 1.5 mM GTP, 1 mM EGTA, 1 mM β-ME, 1 mM $MgCl_2$, and the required ligand concentration. Samples were incubated 30 min at 20 °C, followed by cooling on ice for 10 min. Tubulin polymerization was assessed by the UV absorbance increase at 450 nm due to the turbidity caused by a temperature shift from 4 ºC to 37 ºC. When a stable plateau was reached and maintained for at least 20 minutes, the temperature was switched back to 4 ºC to ascertain the return to the initial absorption values, to confirm the reversibility of the process. The degree of tubulin assembly for each experiment was calculated as the difference in amplitude between the stable plateau and the initial baseline of the curves. Control experiments in identical conditions but the absence of ligand were taken as 100% tubulin polymerization. In a first screening, all the compounds were assayed at 5 µM in at least two independent measurements. For those compounds with TPI values higher than 40% on average, the IC_{50} values of tubulin polymerization were determined by measuring the tubulin polymerization inhibitory activity at different ligand concentrations. The obtained values of the mole ratio of total ligand to total tubulin in solution were fitted to mono-exponential curves and the IC_{50} values of tubulin polymerization inhibition calculated from the best-fitting curves.

4.2.2. Cell culture.

HL-60 (human acute myeloid leukemia) and HT-29 (human colon carcinoma) cell lines were grown at 37 °C in humidified 95% air and 5% CO_2 in RPMI-1640 culture medium containing 10% (v/v) heat-inactivated fetal bovine serum (FBS), 100 U/mL penicillin, 100 µg/mL streptomycin, and 2 mM L-glutamine. HeLa (human cervical carcinoma) cell line was grown at 37 °C in humidified 95% air and 5% CO_2 in DMEM culture medium containing 10% (v/v) heat-inactivated fetal bovine serum (FBS), 2 mM L-glutamine, 100 U/mL penicillin, and 100 µg/mL streptomycin. Cells were periodically tested for *Mycoplasma* infection and found to be negative.

4.2.3. Cell Growth Inhibition Assay.

The effect of the compounds on the proliferation of human tumor cell lines (cytostatic activity) was determined using the XTT (sodium 3′-[1-(phenylaminocarbonyl)-3,4-tetrazolium]-bis(4-methoxy-6-nitro)-benzenesulfonic acid hydrate) cell proliferation kit (Roche Molecular Biochemicals, Mannheim, Germany) according to the manufacturer's instructions as previously described.[51] Cells (5×10^3 HL-60, 1.5×10^3 HeLa, or 3×10^3 HT-29 in 100 µL) were incubated for 72 h in 96-well flat-bottomed microtiter plates at 37 °C in a humidified atmosphere of air/CO_2 (19/1) in culture medium containing 10% heat-inactivated FBS in the absence (control) and the presence of the indicated compounds at concentrations ranging from 10^{-5} to 10^{-13} M. After incubation, the XTT assay was performed. Each experiment was repeated three times and measurements were performed in triplicate. The IC_{50} (50% inhibitory concentration) value, defined as the drug concentration required to cause 50% inhibition in cellular proliferation with respect to the untreated controls, was determined for each compound by nonlinear curve fitting of the experimental data.

4.2.4. Cell Cycle Analysis.

For cell cycle analyses, untreated and drug-treated cells ($2-4 \times 10^5$) were centrifuged and fixed overnight in 70% ethanol at 4 °C. Then cells were washed three times with PBS, incubated for 1 h with 1 mg/mL RNase A and 20 µg/mL propidium iodide at room temperature, and analyzed with a Becton Dickinson fluorescence-activated cell sorter (FACSCalibur) flow cytometer (San Jose, CA) as previously described.[58, 59] Quantification of apoptotic cells was calculated as the percentage of cells in the sub-G_0/G_1 region in cell cycle analysis.[58, 59]

4.2.5. Confocal Microscopy.

HeLa cells were grown on 0.01% poly-L-lysine coated coverslips, and after drug treatment, the coverslips were washed three times with HPEM buffer (25 mM HEPES, 60 mM PIPES, 10 mM EGTA, 3 mM $MgCl_2$, pH 6.6), fixed with 4% formaldehyde in HPEM buffer for 20 min, and permeabilized with 0.5% Triton X-100 as previously described.[53] Coverslips were incubated with a specific Ab-1 anti-α-tubulin mouse monoclonal antibody (diluted 1:150 in PBS) (Calbiochem, San Diego, CA) for 1 h, washed four times with PBS, and then incubated with CY3-conjugated sheep anti-mouse IgG (diluted 1:100 in PBS) (Jackson ImmunoResearch, West Grove, PA) for 1 h at 4 °C. After four washes with PBS, a drop of SlowFade light antifading reagent (Molecular Probes, Eugene, OR), with DAPI (Sigma, St. Louis, MO) to stain cell nuclei, was added to preserve fluorescence. The samples were analyzed by confocal microscopy using a ZeissLSM 310 laser scan confocal microscope. Negative controls, lacking the primary antibody or using an irrelevant antibody, showed no staining.

4.2.6.Western Blot Analysis.

About 5×10^6 cells were pelleted by centrifugation, washed with PBS, lysed, and subjected to Western blot analysis as described previously.[58] Proteins (15 µg) were separated through 8% sodium dodecyl sulfate-polyacrylamide gels under reducing conditions, transferred to nitrocellulose filters, blocked with 5% nonfat dry milk, and incubated overnight with the

corresponding antibodies (anti-mitotic proteins mouse monoclonal antibody MPM-2, Abcam; C2.10 anti-PARP mouse monoclonal antibody, Cell Signaling). Signals were developed using an enhanced chemiluminescence (ECL) detection kit (Amersham). Immunoblotting with the mouse monoclonal anti-β-actin antibody AC15 (Sigma) was used as an internal loading control, revealing equivalent amounts of protein in each lane of the gel.

4.3. Computational studies

4.3.1. Chemical Structure.

Calculations were performed consecutively using the Spartan 08 software package at the molecular mechanics (MMFF94s), semiempirical (AM1), and B3LYP 6-31+G* DFT levels. Conformational analyses were performed by systematically rotating the bonds between the rings in 18° steps with AM1 and the substituents on the pyridine ring were subjected to final unrestrained energy minimization until convergence at the B3LYP/6-31+G* DFT level of theory.

4.3.2. Docking Experiments.

The coordinates of the tubulin – colchicine site ligands complexes available were retrieved from the pdb [60] and chains C−E were removed. Five representative structures selected from previous studies of energy minimization and molecular dynamics simulations at 300 K on 1SA1.pdb using AMBER14[61], initially with a restrained backbone and later 200 ns unrestrained were also used.[54] The ligands were built with Spartan 08[62] and prepared with AutodockTools. Docking experiments were run with PLANTS[55] using default settings and 10 runs per ligand and AutoDock 4.2 [56, 63], by running the Lamarckian genetic algorithm (LGA) 100−300 times with a maximum of 2.5×10^6 energy evaluations, 150 individuals in the population, and a maximum of 27000 generations. The occupancy of the colchicine site sub-pockets by the obtained binding poses was automatically determined, and the results tabulated using in-house KNIME pipelines. The binding energies were converted to *z*-scores and used for

comparison across programs. The results were analyzed with Chimera,[64] AutoDockTools,[56, 63] Marvin,[65] OpenEye[66] and with JADOPPT.[67] The selection of the docking poses was done by searching for automatically determined similar docking poses coming from the two docking programs and scored in the two first quartiles and by comparing them to the alternative binding modes based on the combined *z* scoring.

ACKNOWLEDGMENTS

We thank the people at Frigoríficos Salamanca S.A. slaughterhouse for providing us with the calf brains and “Servicio General de NMR” and “Servicio General de Espectrometría de Masas” of the Universidad de Salamanca for equipment. L.A. acknowledges a predoctoral fellowship from the Junta de Castilla y León. A.V.B acknowledges a predoctoral fellowship from the Spanish Ministerio de Educación, Cultura y Deporte (FPU15/02457).

FUNDING SOURCES

This work was supported by the Consejería de Educación de la Junta de Castilla y León (SA030U16 and SA262P18), co-funded by the EU's European Regional Development Fund-FEDER, and the Spanish Ministry of Science, Innovation, and Universities (RTI2018-099474-B-I00 and SAF2017-89672-R).

REFERENCES

[1] C. Dumontet, M.A. Jordan, Microtubule-binding agents: a dynamic field of cancer therapeutics, Nature reviews. Drug discovery, 9 (2010) 790-803. D.O.I.:10.1038/nrd3253

[2] A. Vicente-Blazquez, M. Gonzalez, R. Alvarez, S. Del Mazo, M. Medarde, R. Pelaez, Antitubulin sulfonamides: The successful combination of an established drug class and a multifaceted target, Medicinal research reviews, (2018). D.O.I.:10.1002/med.21541

[3] R. Gaspari, A.E. Prota, K. Bargsten, A. Cavalli, M.O. Steinmetz, Structural Basis of cis- and trans-Combretastatin Binding to Tubulin, Chem, 2 (2017) 102-113. D.O.I.:https://doi.org/10.1016/j.chempr.2016.12.005

[4] F. Mollinedo, C. Gajate, Microtubules, microtubule-interfering agents and apoptosis, Apoptosis : an international journal on programmed cell death, 8 (2003) 413-450.

[5] M.J. Perez-Perez, E.M. Priego, O. Bueno, M.S. Martins, M.D. Canela, S. Liekens, Blocking Blood Flow to Solid Tumors by Destabilizing Tubulin: An Approach to Targeting Tumor Growth, Journal of medicinal chemistry, 59 (2016) 8685-8711. D.O.I.:10.1021/acs.jmedchem.6b00463
[6] E.M. Agency, European Medicines Agency, in, 2020.
[7] W. Liang, Y. Ni, F. Chen, Tumor resistance to vascular disrupting agents: mechanisms, imaging, and solutions, Oncotarget, 7 (2016) 15444-15459. D.O.I.:10.18632/oncotarget.6999
[8] G.M. Tozer, C. Kanthou, G. Lewis, V.E. Prise, B. Vojnovic, S.A. Hill, Tumour vascular disrupting agents: combating treatment resistance, The British journal of radiology, 81 Spec No 1 (2008) S12-20. D.O.I.:10.1259/bjr/36205483
[9] L.M. Greene, M.J. Meegan, D.M. Zisterer, Combretastatins: more than just vascular targeting agents?, The Journal of pharmacology and experimental therapeutics, 355 (2015) 212-227. D.O.I.:10.1124/jpet.115.226225
[10] R. Kaur, G. Kaur, R.K. Gill, R. Soni, J. Bariwal, Recent developments in tubulin polymerization inhibitors: An overview, European journal of medicinal chemistry, 87 (2014) 89-124. D.O.I.:10.1016/j.ejmech.2014.09.051
[11] Y. Lu, J. Chen, M. Xiao, W. Li, D.D. Miller, An overview of tubulin inhibitors that interact with the colchicine binding site, Pharmaceutical research, 29 (2012) 2943-2971. D.O.I.:10.1007/s11095-012-0828-z
[12] L.M. Greene, N.M. O'Boyle, D.P. Nolan, M.J. Meegan, D.M. Zisterer, The vascular targeting agent Combretastatin-A4 directly induces autophagy in adenocarcinoma-derived colon cancer cells, Biochemical pharmacology, 84 (2012) 612-624. D.O.I.:10.1016/j.bcp.2012.06.005
[13] M.A. Soussi, S. Aprile, S. Messaoudi, O. Provot, E. Del Grosso, J. Bignon, J. Dubois, J.D. Brion, G. Grosa, M. Alami, The metabolic fate of isocombretastatin A-4 in human liver microsomes: identification, synthesis and biological evaluation of metabolites, ChemMedChem, 6 (2011) 1781-1788. D.O.I.:10.1002/cmdc.201100193
[14] S. Aprile, E. Del Grosso, G.C. Tron, G. Grosa, In vitro metabolism study of combretastatin A-4 in rat and human liver microsomes, Drug metabolism and disposition: the biological fate of chemicals, 35 (2007) 2252-2261. D.O.I.:10.1124/dmd.107.016998
[15] G.C. Tron, T. Pirali, G. Sorba, F. Pagliai, S. Busacca, A.A. Genazzani, Medicinal chemistry of combretastatin A4: present and future directions, Journal of medicinal chemistry, 49 (2006) 3033-3044. D.O.I.:10.1021/jm0512903
[16] Z.S. Seddigi, M.S. Malik, A.P. Saraswati, S.A. Ahmed, A.O. Babalghith, H.A. Lamfon, A. Kamal, Recent advances in combretastatin based derivatives and prodrugs as antimitotic agents, MedChemComm, 8 (2017) 1592-1603. D.O.I.:10.1039/c7md00227k
[17] A.M. Malebari, L.M. Greene, S.M. Nathwani, D. Fayne, N.M. O'Boyle, S. Wang, B. Twamley, D.M. Zisterer, M.J. Meegan, beta-Lactam analogues of combretastatin A-4 prevent metabolic inactivation by glucuronidation in chemoresistant HT-29 colon cancer cells, European journal of medicinal chemistry, 130 (2017) 261-285. D.O.I.:10.1016/j.ejmech.2017.02.049
[18] D. Simoni, G. Grisolia, G. Giannini, M. Roberti, R. Rondanin, L. Piccagli, R. Baruchello, M. Rossi, R. Romagnoli, F.P. Invidiata, S. Grimaudo, M.K. Jung, E. Hamel, N. Gebbia, L. Crosta, V. Abbadessa, A. Di Cristina, L. Dusonchet, M. Meli, M. Tolomeo, Heterocyclic and phenyl double-bond-locked combretastatin analogues possessing potent apoptosis-inducing activity in HL60 and in MDR cell lines, Journal of medicinal chemistry, 48 (2005) 723-736. D.O.I.:10.1021/jm049622b
[19] W. Li, H. Sun, S. Xu, Z. Zhu, J. Xu, Tubulin inhibitors targeting the colchicine binding site: a perspective of privileged structures, Future medicinal chemistry, 9 (2017) 1765-1794. D.O.I.:10.4155/fmc-2017-0100
[20] A. Vicente-Blazquez, M. Gonzalez, R. Alvarez, S. Del Mazo, M. Medarde, R. Pelaez, Antitubulin sulfonamides: The successful combination of an established drug class and a multifaceted target, Medicinal research reviews, 39 (2019) 775-830. D.O.I.:10.1002/med.21541
[21] M. Borowiak, W. Nahaboo, M. Reynders, K. Nekolla, P. Jalinot, J. Hasserodt, M. Rehberg, M. Delattre, S. Zahler, A. Vollmar, D. Trauner, O. Thorn-Seshold, Photoswitchable Inhibitors of Microtubule

Dynamics Optically Control Mitosis and Cell Death, Cell, 162 (2015) 403-411. D.O.I.:10.1016/j.cell.2015.06.049
[22] G.R. Pettit, B. Toki, D.L. Herald, P. Verdier-Pinard, M.R. Boyd, E. Hamel, R.K. Pettit, Antineoplastic agents. 379. Synthesis of phenstatin phosphate, Journal of medicinal chemistry, 41 (1998) 1688-1695. D.O.I.:10.1021/jm970644q
[23] C. Alvarez, R. Alvarez, P. Corchete, C. Perez-Melero, R. Pelaez, M. Medarde, Exploring the effect of 2,3,4-trimethoxy-phenyl moiety as a component of indolephenstatins, European journal of medicinal chemistry, 45 (2010) 588-597. D.O.I.:10.1016/j.ejmech.2009.10.047
[24] N. Sirisoma, A. Pervin, H. Zhang, S. Jiang, J.A. Willardsen, M.B. Anderson, G. Mather, C.M. Pleiman, S. Kasibhatla, B. Tseng, J. Drewe, S.X. Cai, Discovery of N-(4-methoxyphenyl)-N,2-dimethylquinazolin-4-amine, a potent apoptosis inducer and efficacious anticancer agent with high blood brain barrier penetration, Journal of medicinal chemistry, 52 (2009) 2341-2351. D.O.I.:10.1021/jm801315b
[25] I. Khelifi, T. Naret, A. Hamze, J. Bignon, H. Levaique, M.C. Garcia Alvarez, J. Dubois, O. Provot, M. Alami, N,N-bis-heteroaryl methylamines: Potent anti-mitotic and highly cytotoxic agents, European journal of medicinal chemistry, 168 (2019) 176-188. D.O.I.:10.1016/j.ejmech.2019.02.038
[26] S. Messaoudi, A. Hamze, O. Provot, B. Treguier, J. Rodrigo De Losada, J. Bignon, J.M. Liu, J. Wdzieczak-Bakala, S. Thoret, J. Dubois, J.D. Brion, M. Alami, Discovery of isoerianin analogues as promising anticancer agents, ChemMedChem, 6 (2011) 488-497. D.O.I.:10.1002/cmdc.201000456
[27] R. Alvarez, C. Alvarez, F. Mollinedo, B.G. Sierra, M. Medarde, R. Pelaez, Isocombretastatins A: 1,1-diarylethenes as potent inhibitors of tubulin polymerization and cytotoxic compounds, Bioorganic & medicinal chemistry, 17 (2009) 6422-6431. D.O.I.:10.1016/j.bmc.2009.07.012
[28] S. Messaoudi, B. Treguier, A. Hamze, O. Provot, J.F. Peyrat, J.R. De Losada, J.M. Liu, J. Bignon, J. Wdzieczak-Bakala, S. Thoret, J. Dubois, J.D. Brion, M. Alami, Isocombretastatins a versus combretastatins a: the forgotten isoCA-4 isomer as a highly promising cytotoxic and antitubulin agent, Journal of medicinal chemistry, 52 (2009) 4538-4542. D.O.I.:10.1021/jm900321u
[29] A. Hamze, M. Alami, O. Provot, Developments of isoCombretastatin A-4 derivatives as highly cytotoxic agents, European journal of medicinal chemistry, 190 (2020) 112110. D.O.I.:10.1016/j.ejmech.2020.112110
[30] L.M. Greene, S. Wang, N.M. O'Boyle, S.A. Bright, J.E. Reid, P. Kelly, M.J. Meegan, D.M. Zisterer, Combretazet-3 a novel synthetic cis-stable combretastatin A-4-azetidinone hybrid with enhanced stability and therapeutic efficacy in colon cancer, Oncology reports, 29 (2013) 2451-2458. D.O.I.:10.3892/or.2013.2379
[31] K. Ohsumi, R. Nakagawa, Y. Fukuda, T. Hatanaka, Y. Morinaga, Y. Nihei, K. Ohishi, Y. Suga, Y. Akiyama, T. Tsuji, Novel combretastatin analogues effective against murine solid tumors: design and structure-activity relationships, Journal of medicinal chemistry, 41 (1998) 3022-3032. D.O.I.:10.1021/jm980101w
[32] M. Gonzalez, Y. Ellahioui, R. Alvarez, L. Gallego-Yerga, E. Caballero, A. Vicente-Blazquez, L. Ramudo, M. Marin, C. Sanz, M. Medarde, R. Pelaez, The Masked Polar Group Incorporation (MPGI) Strategy in Drug Design: Effects of Nitrogen Substitutions on Combretastatin and Isocombretastatin Tubulin Inhibitors, Molecules, 24 (2019). D.O.I.:10.3390/molecules24234319
[33] M. Lawson, A. Hamze, J.F. Peyrat, J. Bignon, J. Dubois, J.D. Brion, M. Alami, An efficient coupling of N-tosylhydrazones with 2-halopyridines: synthesis of 2-alpha-styrylpyridines endowed with antitumor activity, Organic & biomolecular chemistry, 11 (2013) 3664-3673. D.O.I.:10.1039/c3ob40263k
[34] R. Alvarez, C. Gajate, P. Puebla, F. Mollinedo, M. Medarde, R. Pelaez, Substitution at the indole 3 position yields highly potent indolecombretastatins against human tumor cells, European journal of medicinal chemistry, 158 (2018) 167-183. D.O.I.:10.1016/j.ejmech.2018.08.078
[35] R. Alvarez, P. Puebla, J.F. Diaz, A.C. Bento, R. Garcia-Navas, J. de la Iglesia-Vicente, F. Mollinedo, J.M. Andreu, M. Medarde, R. Pelaez, Endowing indole-based tubulin inhibitors with an anchor for derivatization: highly potent 3-substituted indolephenstatins and indoleisocombretastatins, Journal of medicinal chemistry, 56 (2013) 2813-2827. D.O.I.:10.1021/jm3015603

[36] C. Jimenez, Y. Ellahioui, R. Alvarez, L. Aramburu, A. Riesco, M. Gonzalez, A. Vicente, A. Dahdouh, A. Ibn Mansour, C. Jimenez, D. Martin, R.G. Sarmiento, M. Medarde, E. Caballero, R. Pelaez, Exploring the size adaptability of the B ring binding zone of the colchicine site of tubulin with para-nitrogen substituted isocombretastatins, European journal of medicinal chemistry, 100 (2015) 210-222. D.O.I.:10.1016/j.ejmech.2015.05.047
[37] I. Khelifi, T. Naret, D. Renko, A. Hamze, G. Bernadat, J. Bignon, C. Lenoir, J. Dubois, J.D. Brion, O. Provot, M. Alami, Design, synthesis and anticancer properties of IsoCombretaQuinolines as potent tubulin assembly inhibitors, European journal of medicinal chemistry, 127 (2017) 1025-1034. D.O.I.:10.1016/j.ejmech.2016.11.012
[38] W. Li, F. Xu, W. Shuai, H. Sun, H. Yao, C. Ma, S. Xu, H. Yao, Z. Zhu, D.H. Yang, Z.S. Chen, J. Xu, Discovery of Novel Quinoline-Chalcone Derivatives as Potent Antitumor Agents with Microtubule Polymerization Inhibitory Activity, Journal of medicinal chemistry, 62 (2019) 993-1013. D.O.I.:10.1021/acs.jmedchem.8b01755
[39] M.A. Soussi, O. Provot, G. Bernadat, J. Bignon, D. Desravines, J. Dubois, J.D. Brion, S. Messaoudi, M. Alami, IsoCombretaQuinazolines: Potent Cytotoxic Agents with Antitubulin Activity, ChemMedChem, 10 (2015) 1392-1402. D.O.I.:10.1002/cmdc.201500069
[40] T. Naret, I. Khelifi, O. Provot, J. Bignon, H. Levaique, J. Dubois, M. Souce, A. Kasselouri, A. Deroussent, A. Paci, P.F. Varela, B. Gigant, M. Alami, A. Hamze, 1,1-Diheterocyclic Ethylenes Derived from Quinaldine and Carbazole as New Tubulin-Polymerization Inhibitors: Synthesis, Metabolism, and Biological Evaluation, Journal of medicinal chemistry, 62 (2019) 1902-1916. D.O.I.:10.1021/acs.jmedchem.8b01386
[41] S. Banerjee, K.E. Arnst, Y. Wang, G. Kumar, S. Deng, L. Yang, G.B. Li, J. Yang, S.W. White, W. Li, D.D. Miller, Heterocyclic-Fused Pyrimidines as Novel Tubulin Polymerization Inhibitors Targeting the Colchicine Binding Site: Structural Basis and Antitumor Efficacy, Journal of medicinal chemistry, 61 (2018) 1704-1718. D.O.I.:10.1021/acs.jmedchem.7b01858
[42] T.J. Ritchie, S.J. Macdonald, R.J. Young, S.D. Pickett, The impact of aromatic ring count on compound developability: further insights by examining carbo- and hetero-aromatic and -aliphatic ring types, Drug discovery today, 16 (2011) 164-171. D.O.I.:10.1016/j.drudis.2010.11.014
[43] T.J. Ritchie, S.J. Macdonald, The impact of aromatic ring count on compound developability--are too many aromatic rings a liability in drug design?, Drug discovery today, 14 (2009) 1011-1020. D.O.I.:10.1016/j.drudis.2009.07.014
[44] F. Xu, W. Li, W. Shuai, L. Yang, Y. Bi, C. Ma, H. Yao, S. Xu, Z. Zhu, J. Xu, Design, synthesis and biological evaluation of pyridine-chalcone derivatives as novel microtubule-destabilizing agents, European journal of medicinal chemistry, 173 (2019) 1-14. D.O.I.:10.1016/j.ejmech.2019.04.008
[45] W. Shuai, X. Li, W. Li, F. Xu, L. Lu, H. Yao, L. Yang, H. Zhu, S. Xu, Z. Zhu, J. Xu, Design, synthesis and anticancer properties of isocombretapyridines as potent colchicine binding site inhibitors, European journal of medicinal chemistry, 197 (2020) 112308. D.O.I.:10.1016/j.ejmech.2020.112308
[46] R. Alvarez, L. Aramburu, C. Gajate, A. Vicente-Blazquez, F. Mollinedo, M. Medarde, R. Pelaez, Potent colchicine-site ligands with improved intrinsic solubility by replacement of the 3,4,5-trimethoxyphenyl ring with a 2-methylsulfanyl-6-methoxypyridine ring, Bioorganic chemistry, 98 (2020) 103755. D.O.I.:10.1016/j.bioorg.2020.103755
[47] R. Schobert, K. Effenberger-Neidnicht, B. Biersack, Stable combretastatin A-4 analogues with sub-nanomolar efficacy against chemoresistant HT-29 cells, International journal of clinical pharmacology and therapeutics, 49 (2011) 71-72.
[48] K.E. Henegar, S.W. Ashford, T.A. Baughman, J.C. Sih, R.-L. Gu, Practical Asymmetric Synthesis of (S)-4-Ethyl-7,8-dihydro-4-hydroxy-1H-pyrano[3,4-f]indolizine- 3,6,10(4H)-trione, a Key Intermediate for the Synthesis of Irinotecan and Other Camptothecin Analogs, The Journal of organic chemistry, 62 (1997) 6588-6597. D.O.I.:10.1021/jo970173f
[49] J. Fernandes, C.R. Gattass, Topological polar surface area defines substrate transport by multidrug resistance associated protein 1 (MRP1/ABCC1), Journal of medicinal chemistry, 52 (2009) 1214-1218. D.O.I.:10.1021/jm801389m

[50] J. Chen, Z. Wang, C.M. Li, Y. Lu, P.K. Vaddady, B. Meibohm, J.T. Dalton, D.D. Miller, W. Li, Discovery of novel 2-aryl-4-benzoyl-imidazoles targeting the colchicines binding site in tubulin as potential anticancer agents, Journal of medicinal chemistry, 53 (2010) 7414-7427. D.O.I.:10.1021/jm100884b
[51] M.H. David-Cordonnier, C. Gajate, O. Olmea, W. Laine, J. de la Iglesia-Vicente, C. Perez, C. Cuevas, G. Otero, I. Manzanares, C. Bailly, F. Mollinedo, DNA and non-DNA targets in the mechanism of action of the antitumor drug trabectedin, Chemistry & biology, 12 (2005) 1201-1210. D.O.I.:10.1016/j.chembiol.2005.08.009
[52] C. Alvarez, R. Alvarez, P. Corchete, J.L. Lopez, C. Perez-Melero, R. Pelaez, M. Medarde, Diarylmethyloxime and hydrazone derivatives with 5-indolyl moieties as potent inhibitors of tubulin polymerization, Bioorganic & medicinal chemistry, 16 (2008) 5952-5961. D.O.I.:10.1016/j.bmc.2008.04.054
[53] A.B. Maya, C. Perez-Melero, C. Mateo, D. Alonso, J.L. Fernandez, C. Gajate, F. Mollinedo, R. Pelaez, E. Caballero, M. Medarde, Further naphthylcombretastatins. An investigation on the role of the naphthalene moiety, Journal of medicinal chemistry, 48 (2005) 556-568. D.O.I.:10.1021/jm0310737
[54] R. Alvarez, M. Medarde, R. Pelaez, New ligands of the tubulin colchicine site based on X-ray structures, Current topics in medicinal chemistry, 14 (2014) 2231-2252.
[55] O. Korb, T. Stutzle, T.E. Exner, Empirical scoring functions for advanced protein-ligand docking with PLANTS, Journal of chemical information and modeling, 49 (2009) 84-96. D.O.I.:10.1021/ci800298z
[56] S. Forli, R. Huey, M.E. Pique, M.F. Sanner, D.S. Goodsell, A.J. Olson, Computational protein-ligand docking and virtual drug screening with the AutoDock suite, Nature protocols, 11 (2016) 905-919. D.O.I.:10.1038/nprot.2016.051
[57] A. Massarotti, A. Coluccia, R. Silvestri, G. Sorba, A. Brancale, The tubulin colchicine domain: a molecular modeling perspective, ChemMedChem, 7 (2012) 33-42. D.O.I.:10.1002/cmdc.201100361
[58] C. Gajate, A.M. Santos-Beneit, A. Macho, M. Lazaro, A. Hernandez-De Rojas, M. Modolell, E. Munoz, F. Mollinedo, Involvement of mitochondria and caspase-3 in ET-18-OCH(3)-induced apoptosis of human leukemic cells, International journal of cancer, 86 (2000) 208-218.
[59] C. Gajate, I. Barasoain, J.M. Andreu, F. Mollinedo, Induction of apoptosis in leukemic cells by the reversible microtubule-disrupting agent 2-methoxy-5-(2',3',4'-trimethoxyphenyl)-2,4,6-cycloheptatrien-1-one: protection by Bcl-2 and Bcl-X(L) and cell cycle arrest, Cancer research, 60 (2000) 2651-2659.
[60] S. Aprile, E. Del Grosso, G. Grosa, Identification of the human UDP-glucuronosyltransferases involved in the glucuronidation of combretastatin A-4, Drug metabolism and disposition: the biological fate of chemicals, 38 (2010) 1141-1146. D.O.I.:10.1124/dmd.109.031435
[61] D.A. Case, T.E. Cheatham, 3rd, T. Darden, H. Gohlke, R. Luo, K.M. Merz, Jr., A. Onufriev, C. Simmerling, B. Wang, R.J. Woods, The Amber biomolecular simulation programs, Journal of computational chemistry, 26 (2005) 1668-1688. D.O.I.:10.1002/jcc.20290
[62] I. WAVEFUNCTION, Spartan08, in, 2008.
[63] G.M. Morris, R. Huey, W. Lindstrom, M.F. Sanner, R.K. Belew, D.S. Goodsell, A.J. Olson, AutoDock4 and AutoDockTools4: Automated docking with selective receptor flexibility, Journal of computational chemistry, 30 (2009) 2785-2791. D.O.I.:10.1002/jcc.21256
[64] E.F. Pettersen, T.D. Goddard, C.C. Huang, G.S. Couch, D.M. Greenblatt, E.C. Meng, T.E. Ferrin, UCSF Chimera--a visualization system for exploratory research and analysis, Journal of computational chemistry, 25 (2004) 1605-1612. D.O.I.:10.1002/jcc.20084
[65] Marvin 17.8 in, ChemAxon (http://www.chemaxon.com), 2017.
[66] W. Li, Y. Yin, W. Shuai, F. Xu, H. Yao, J. Liu, K. Cheng, J. Xu, Z. Zhu, S. Xu, Discovery of novel quinazolines as potential anti-tubulin agents occupying three zones of colchicine domain, Bioorganic chemistry, 83 (2019) 380-390. D.O.I.:10.1016/j.bioorg.2018.10.027
[67] C. Garcia-Perez, R. Pelaez, R. Theron, J. Luis Lopez-Perez, JADOPPT: java based AutoDock preparing and processing tool, Bioinformatics, 33 (2017) 583-585. D.O.I.:10.1093/bioinformatics/btw677